Proteomic Profiling of hiPSC-CMs Harbouring Hypertrophic Cardiomyopathy-Troponin T Variants

by

Farah Jayousi

B.Sc. (Hons.), Birzeit University, 2020

Thesis Submitted in Partial Fulfillment of the
Requirements for the Degree of
Master of Science

in the
Department of Biomedical Physiology and Kinesiology
Faculty of Science

SIMON FRASER UNIVERSITY
Spring 2023

Declaration of Committee

Name: **Farah Jayousi**

Degree: **Master of Science (Biomedical Physiology and Kinesiology)**

Title: **Proteomic Profiling of hiPSC-CMs Harbouring Hypertrophic Cardiomyopathy Troponin T variants**

Committee:

Chair: **Dawn Mackey**
Associate Professor, Biomedical Physiology and Kinesiology

Glen F Tibbits
Supervisor
Professor, Biomedical Physiology and Kinesiology

Thomas Claydon
Committee Member
Professor, Biomedical Physiology and Kinesiology

Philipp Lange
Committee Member
Assistant Professor, Pathology
University of British Columbia

R John Solaro
Examiner
Professor, Physiology & Biophysics
University of Illinois at Chicago

Abstract

Hypertrophic cardiomyopathy (HCM) is a genetic heart disease which typically results in asymmetric hypertrophy, myofibrillar disarray, hypercontractility, and impaired relaxation. It is inherited in an autosomal dominant pattern and is the most common heritable heart disease. HCM often results in an increased incidence of arrhythmogenesis which can lead to sudden cardiac arrest (SCA) and death. Its prevalence in the general population is about one in five hundred, making it the leading known cause for SCA in youth and young athletes. This study focuses on HCM inducing variants in the cardiac-troponin T protein, encoded by the *TNNT2* gene, which account for five percent of total HCM cases. The two HCM-associated *TNNT2* variants that were investigated are: I79N$^{+/-}$ and R278C$^{+/-}$. The mechanisms underlying pathogenesis of these variants at the proteomic level remain poorly understood. There is a crucial need to utilize a model that represents human cardiac physiology better than animal models. Human-induced Pluripotent Stem Cell-derived Cardiomyocytes (hiPSC-CMs) have been increasingly used in cardiac research due to their ability to reflect disease manifestation on many different cellular levels, including but not limited to proteomic deviations. The effects of the *TNNT2* variants on the thin-filament proteome quantity and quality in multiple hiPSC-CM lines were studied using bottom-up Mass Spectrometry (MS). Proteomic characterization using MS provided us with a novel perception regarding the intrinsic mechanisms and pathways responsible for the pathogenic cardiac remodelling seen in HCM patients. This presents a future opportunity to identify new therapeutic targets and broad-spectrum treatments for this genetically challenging disease.

Keywords: Hypertrophic Cardiomyopathy; Human-induced Pluripotent Stem Cell-Cardiomyocytes (hiPSC-CMs); Troponin T variants; Mass spectrometry.

Dedication

'To my beloved mother, father and

late grandma for their endless love,

support and encouragement'.

Acknowledgements

I stand here at the end of this academic journey to express my deep gratitude to the people who made this work possible. First and foremost, I would like to express my warmest appreciation to Dr. Glen Tibbits for offering me the great opportunity to carry out my research under his guidance, continuous support, and encouragement. Without his belief in me, I would have never gotten this far in my learning. He was always present to answer questions and provide directions to make this research achievable. Moreover, I am most grateful to Dr. Philipp Lange for providing me with detailed discussions, thoughtful comments, and constructive suggestions. I truly learned a lot from your insights and recommendations. Both Dr. Tibbits and Dr. Lange provided inspiring guidance that helped in maintaining the progress of my work and shaping it in a much better way. Another special acknowledgment goes to Dr. Thomas Claydon for taking a valuable part in my supervisory committee and mentoring me during my first teaching assistant experience. His useful remarks and insights helped in making this thesis possible.

Furthermore, I am truly thankful and honored to have had the chance to work with a group of excellent researchers and colleagues, the Tibbits' lab members. Each and every one of you has left an impact on me and contributed to making this work a reality. I also will never forget the help and support provided by the Lange lab members, Janice, Georgina, and Lorenz, thank you for our mind-expanding discussions, which were an inexhaustible source of inspiration and provided invaluable input for my publications and this thesis.

A special appreciation to the love, care, and support provided by my siblings, Majed, Yousef, Abdallah, and Dana. Thank you for being there for me in my ups and downs through your encouraging calls.

My deepest gratitude goes to my dearest friend, roommate, sister, and support system, Muna. Thank you for providing me with endless emotional and moral support to persevere and finish my thesis, thank you for being my rock, thank you for listening to my problems and helping me solve them, I am forever grateful.

Last, but not least, to you, my dear parents, thank you for all your prayers, for all your motivating calls, for believing in my potential since day one, and for checking up on me at every step of my life. Without the inspiration, drive, and support you gave me, I would have never imagined myself in the position I am in today. No words can ever be strong enough to express my gratitude for your unconditional love and support. To you, mom and dad, I dedicate this work.

Table of Contents

List of Tables

List of Figures

List of Abbreviations and Acronyms

ACTC	Actin
AMPK	Adenosine monophosphate-activated protein kinase
ANOVA	Analysis of variance
Ca^{2+}	Calcium ion
Cav1.2	L-type calcium channel
CICR	Ca2+-induced Ca2+-released
CM	Cardiomyocyte
CRISPR	Clustered regularly interspaced short palindromic repeats
DCM	Dilated cardiomyopathy
DDA	Data-dependent acquisition
EC coupling	Excitation-Contraction coupling
ECM	Extracellular matrix
ELC	Essential light chain
FDR	False discovery rate
FHL	Four and a half LIM domain
HCM	Hypertrophic Cardiomyopathy
HF	Heart Failure
hiPSC-CMs	Human induced pluripotent stem cells- derived Cardiomyocytes
I79N	Isoluecine 79 -> Aspargine substitution
MAPK	Mitogen-activated protein kinase
MM	Maturation media
MQ	MaxQuant
MS	Mass Spectrometry
MTs	Microtubules
MYBPC3	Cardiac myosin binding protein C
MYH	Myosin Heavy Chain
MYL	Myosin Light Chain
NADH	Nicotinamide adenine dinucleotide
NCX	Sodium-calcium exchanger

NEBL	Nebulette
NEXN	Nexilin
NFAT	Nuclear factor of activated T-cells
OBSCN	Obscurin
OXSPHOS	Oxidative Phosphorylation
PCA	Principal component analysis
PCr	Phosphocreatine
PD	Proteome discoverer
PTMs	Post-translational modifications
R278C	Arginine 278 -> Cystine substitution
RLC	Regulatory light chain
ROS	Reactive oxygen species
RPMI	Roswell Park Memorial Institute 1640 basal medium
RYR2	Ryanodine receptor (cardiac)
SCA	Sudden cardiac arrest
Ser	Serine
SERCA2a	Sarcoplasmic reticulum Ca^{2+} ATPase pump
SNPs	Single nucleotide polymorphisms
SP3	Single-pot, solid phase- enhanced sample-preparation
SR	Sarcoplasmic reticulum
TCA cycle	Tricarboxylic acid cycle
TNNC- cTnC	Cardiac Troponin C
TNNI- cTnI	Cardiac Troponin I
TNNT2- cTnT	Cardiac Troponin T
TPM1	Tropomyosin

1 Chapter One: Introduction

1.1 Cardiac Physiology and Molecular Structure

The heterogeneity of the myocardium is due, at least in part, to its composition of different interacting cell types[1]. The four main cellular constituents of the heart are cardiac fibroblasts (CFs), cardiomyocytes (CMs), smooth muscle cells (SMCs), and endothelial cells (ECs)[2]. Cardiomyocytes are the dominant cell type by volume in the heart, making up 70-80% of the organ's total cellular mass[1,2]. CMs are electrically coupled via gap junctions or connexins, allowing the formation of a functional electrical syncytium; an action potential originating from the sinus atrial node that propagates along the surface membrane of the cardiomyocytes to the atrioventricular node and the left and right bundle branches[3]. In response to this electrical stimulation during a cardiac cycle, the CMs generate force and shorten to eject blood into the systemic and pulmonary circulations and subsequently relax, which enables the diastolic filling of the heart[4].

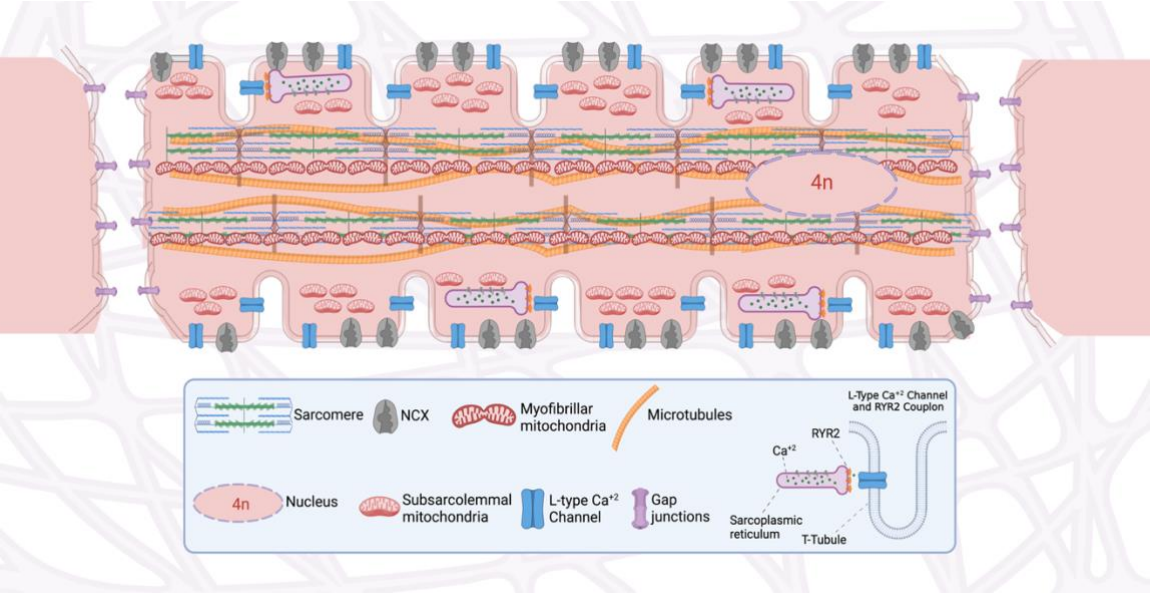

Figure 1.1: Illustration of the structural organization and different components within a single cardiomyocyte (CM). *Created with BioRender.com.*

The timely regulation of contraction and relaxation during the cardiac cycle is attributed to the intricate molecular structure of the cardiomyocytes. Each cardiomyocyte is highly organized with various structural and functional elements that collectively preserve the integrity of the cell[4]. A single cardiomyocyte in the adult human heart is cylindrical in shape and about 100-120 μm long and 10–25 μm in diameter[5]. Figure 1.1 displays the general structural organization of a cardiomyocyte which will be explored in further detail in the following subsections.

1.1.1 The contractile element

A functioning ventricular cardiomyocyte consists of parallel bundles of myofibrils of ~1 μm in diameter. Each myofibril is composed of many sarcomeres connected in series at the Z-discs[6]. The sarcomere consists of a hexagonal lattice that is made of three main filaments[6,7]: A) thin, actin-containing filaments attached to an anchor called the Z-disc. B) thick, myosin-containing filaments (interconnected in the middle via the M-band), and C) titin filaments running from the Z-discs to the M-lines in the middle of the sarcomere (Figure 1.2A). A single sarcomere represents the basic contractile building block of the cardiomyocyte, in which the sliding of thick and thin filaments relative to each other results in muscle contraction and relaxation during the cardiac cycle[7]. To understand how changes in these dynamics underlie dysfunction of the heart during disease, some background will be provided on the proteins of the sarcomere and their role in cardiac muscle cell contraction and regulation.

As seen in Figure 1.2B, the thin filament consists of two strands of globular actin arranged to form a helical structure, filamentous actin, two tropomyosin (TPM) strands, and the three troponin (Tn) subunits Troponin T (TnT), Troponin I (TnI), and Troponin C (TnC), which form the Ca^{+2}-regulatory complex of the thin filament. TnT binds TPM, The troponin complex is positioned at every 7^{th} actin molecule. TnC binds Ca^{2+}, and TnI is the inhibitory subunit that reduces calcium sensitivity of the complex upon its phosphorylation. The thin filament stability, flexibility, and

cooperativity is maintained by the TPM strands which lie within the two grooves of the F actin[8].

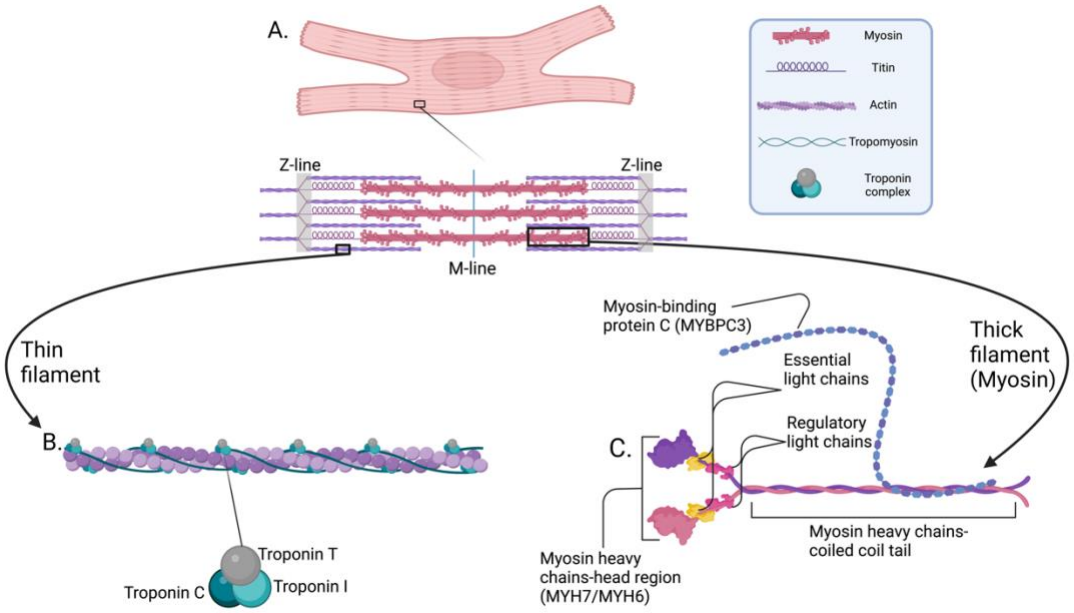

Figure 1.2: A) Visual illustration of a normal sarcomere unit organization in a cardiomyocyte, with a focus on the major structural components of the B) thin filament and C) thick filament. *Created with BioRender.com.*

The thick filament mainly consists of myosin, myosin binding protein C (*MYBPC3*), and titin. The myosin superfamily encodes 18 classes of myosin motors, which are ubiquitous in eukaryotes and participate in many different cellular processes[9]. In cardiomyocytes, the myosin participating in contraction is comprised of two different pairs of myosin light chains (MYLs) and two myosin heavy chains (MYHs) (Figure 1.2C). MYH6 (α-MYH) and MYH7 (β-MYH), are known as the cardiac myosin heavy chain paralogs[10]. Despite their similarity in composition, they still display significantly different functional properties. α-MYH has a higher ATPase activity but generates less force than β-MYH[11]. In the adult human ventricle, the cardiac myosin composition is 95% β-MYH and 5% α-MYH. [9]This ratio may be subject to change due to variable expression of β-MYH in cardiac diseases[12]. The two pairs of MYLs reside on the lever arm (or S1) of the myosin molecule. Each pair is made of one regulatory light chain (RLC) encoded by *MYL2* and one

essential light chain (ELC)[13] encoded by *MYL3*. The RLC regulates muscle contraction by mediating the movement of myosin head molecules for optimal cross-bridge formation. The phosphorylation of RLC at specific amino acid residues promotes the movement of myosin heads towards the actin filaments[13]. The ELC has been shown to interact with the C-terminus of actin and possibly lead to direct alterations in force development during muscle contraction [14,15].

Myosin-binding protein C (MYBPC3), which is associated with both the thick and thin filaments of the sarcomere in cardiac myocytes, is a crucial protein that binds to MYH7 and cardiac actin to regulate the actomyosin interaction. It binds myosin with its N-terminus to reduce its ATPase activity. MYBPC3 undergoes extensive posttranslational modifications (PTMs), particularly phosphorylation by PKA (protein kinase A), PKC (protein kinase C), and other kinases. This phosphorylation results in the removal of its inhibition of crossbridge cycling[16].

At rest or diastole, the low cytosolic calcium [Ca^{+2}] causes myosin-binding sites on the actin filament to be blocked by the TPM–Troponin complex. A subsequent increase in cytosolic free [Ca^{+2}] from ~0.1 μM to up to ~1.6 μM results in increased binding of Ca^{+2} to cardiac TnC, which alters the conformation of the Tm–Tn complex, leading to a position shift of Tm thus exposing the myosin-binding sites on the actin filament. This facilitates cross-bridge formation and force development during the active phase of cardiac contraction (systole). A subsequent release of Ca^{+2} from the myofilaments and removal of Ca^{+2} from the cytosol results in relaxation of muscle cells during the relaxation phase of the heart (diastole)[17]. Nevertheless, the contraction/relaxation cycle of the heart is far more complex than that, it involves other molecular regulatory components, such as Troponin I, which through its phosphorylation state, enhances the Ca^{2+} off rate constant (k_{off}) from troponin C thereby accelerating mechanical relaxation[17–19].

Lastly, the titin filament, which spans the Z-disc to the M-band (half a sarcomere length), is the largest protein in the human body. It is well recognized for its role in

maintaining the elastic recoil and the passive stiffness of the cardiac muscle[20]. Titin is encoded by a single gene that contains 368 exons. Multiple splicing pathways in the massive I-band region give rise to various isoforms with different spring composition[21]. Titin undergoes a gradual isoform switch during cardiac development[22]. The heart first expresses the compliant fetal N2BA isoform that is then replaced after birth by the smaller and stiffer N2BA and the N2B isoforms. A similar switch is seen in the progression of stiffness-inducing cardiac diseases[22,23].

1.1.2 The Cytoskeleton

The non-sarcomeric cytoskeleton is the main component that provides scaffolding for the myofilaments and positioning of the organelles within each cardiac myocyte. The cytoskeleton forms an interconnected lattice throughout the cell, it is well positioned to sense and transmit mechanical signals that enable the heart to regulate gene transcription and adapt to changing demands[24]. Moreover, the main constituents of the cytoskeleton, microtubules (MTs), are distorted during contraction which allows them to directly regulate contractility by mechanically hindering myocyte shortening. The MT network is a dynamic structure whose density is regulated by various enzymes (kinases and phosphatases) and MT-binding proteins that alter the equilibrium between MT filament growth and disassembly[25]. The MTs make up a cytoskeletal network composed of two main tubulin proteins, α-tubulin and β- tubulin heterodimers, both of which have variable expression of different paralogs. Post-translational modifications of these tubulins are heavily involved in modulating contractility[26]. For example, MT terminal detyrosination profoundly regulates mechanotransduction by modifying the mechanical properties of the cytoskeleton, thus making it stiffer[25,26].

1.1.3 The Extracellular matrix (ECM)

The ECM is comprised of many proteins that dynamically interact to maintain the integrity of the cardiomyocyte. Hyaluronan, proteoglycans, collagens, elastin, fibrilin, tenascin, fibronectins, and laminins play a fundamental role during embryonic development through the regulation of a wide array of cellular

processes[27,28]. This extensive extracellular network is involved in cell-cell signaling, cell proliferation, differentiation, and migration. The ECM also creates an initial barrier that influences the exchange of macromolecules between the extracellular space and the myocyte[25].

1.1.4 The Mitochondria

Mitochondria are crucial organelles that provide subcellular compartmentalization for major energy production processes, which mainly include the tricarboxylic acid (TCA) cycle and oxidative phosphorylation (OXPHOS)[29]. A mitochondrion is composed of an outer membrane, an inner membrane, and an intermembrane space[29]. The outer membrane serves as the physical boundary between the cytoplasm and mitochondria. The mitochondria contain several receptors to facilitate communication between the mitochondrion and other organelles. The inner membrane is folded into cristae that bulge into the matrix, thus creating a much larger surface area than the outer membrane. The OXPHOS complexes, (e.g., complexes I to V), are located on the inner membrane and mediate electron transportation over the chain to generate ATP[30]. The mitochondrial matrix refers to the space inside the inner membrane, and contains the mitochondrial DNA (mtDNA), ribosomes, enzymes, and ions. It is also the location of the TCA cycle[29,30].

As implied in Figure 1.1, each CM must contain a massive number of mitochondria to meet the energetic demands of the cell. In fact, since mitochondria produce about ~90% of the CM's ATP, they occupy up to 40% of the adult cardiac cell total volume[29,30]. Consequently, cardiac disorders that affect contractility have been evidently shown to induce metabolic remodeling which is characterized by a decrease in cardiac energy production due to progressive impairments in substrate use and mitochondrial biogenesis and function[31].

1.1.5 The Sarcolemma

The sarcolemma is composed of a lipid bilayer which controls the diffusion of molecules and ions across it. The hydrophobic core of the lipid bilayer causes the sarcolemma to be impermeable to charged molecules. Specialized intercalated disks in the sarcolemma provides strong mechanical and electrical linkages between CMs. These disks include a low resistance path referred to as a gap junction that aids in the rapid conduction of the action potential between CMs, thus resulting in a functional syncytium. The membrane proteins of the sarcolemma include receptors, ion pumps, and ion channels that are responsible for ion influx and efflux through the cell. The T-tubules are invaginations of the sarcolemma that form a permeability barrier between the cytosol and the extracellular space[32]. The t-tubule plays a central role in cellular activation by allowing the uniform spread of the excitation wave across the length of the cardiomyocyte. This role is crucial to sustain the excitation-contraction (EC) coupling phenomenon[32,33].

1.1.6 The Sarcoplasmic reticulum (SR)

The sarcoplasmic reticulum (SR) is a specialized calcium-storing organelle. It has been described as a functionally modified endoplasmic reticulum (ER) found predominantly in muscle cells due to their high demand for calcium to facilitate the unremitting contraction/relaxation cycles[34]. The SR forms a continuous network surrounding the myofilaments with connections across the Z-disks and transverse connections between myofibrils. Moreover, the lumens of the entire SR network and nuclear envelope are interconnected in adult cardiac myocytes, thus facilitating ion diffusion. The SR [Ca^{2+}] content is critical to normal cardiac function and electrophysiology, and its abnormalities contribute to systolic and diastolic dysfunction and arrhythmias[35]. The cardiac ryanodine receptor (RyR2) is embedded in the SR membrane and mediates SR release Ca^{2+}. Figure 1.1 shows how the RyR channels are mainly located in the SR membrane at the junctions with the T tubules, thus creating a coupled structure termed “the dyad”. Each couplon has ~50 to 250 RyR channels on the SR that are directly under a cluster of sarcolemmal L-type Ca^{2+} channels. This proximity allows for a rapid interaction

of the incoming Ca^{2+} ions with the SR-RyR complex, which further enables EC-coupling[35].

1.1.7 Excitation Contraction-coupling and Calcium Handling

The process of excitation–contraction (EC) coupling links the electrical excitation (action potential propagation) of the surface membrane to the contraction event of the cardiac cell. Due to an incoming depolarization current, the L-type Ca^{2+} opens in response to depolarization (Figure 1.3). The resulting influx of a small amount of Ca^{2+} results in a large increase of $[Ca^{2+}]$ into the dyadic space (the region between the t-tubule and the SR). This increase of dyadic $[Ca^{2+}]$ makes the RyR channels open which in turn leads to a much larger amount of Ca^{2+} released from the SR in a process called calcium-induced calcium release (CICR)[33].

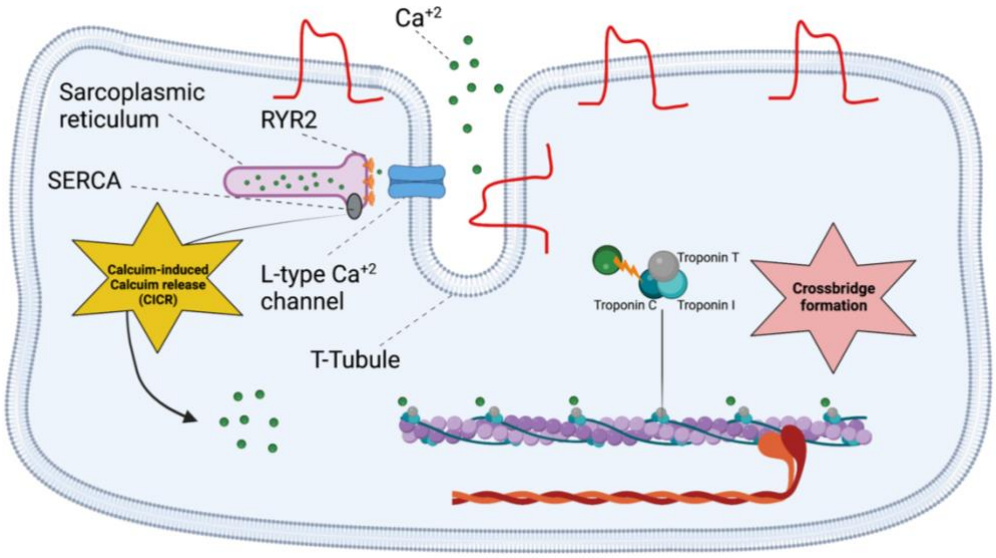

Figure 1.3: Schematic diagram of EC-coupling. Shows the plasma membrane or sarcolemma, transverse tubule, sarcoplasmic reticulum (SR), a dyad, and the various proteins involved in this phenomenon. *Created with BioRender.com.*

For contraction to take place, the increased cytosolic $[Ca^{2+}]$ (100nM → 1μM) resulting in it binding to troponin C resulting in cross bridge formation followed by the sliding of the thick and thin filaments, cell shortening, and thence the development of pressure within the ventricle and ejection of blood. Therefore, force of contraction depends on the amount of Ca^{2+} bound to troponin[35]. This means that

the force is a function of both the magnitude and duration of the rise of the intracellular [Ca^{2+}]. It will also depend on the strength of Ca binding, which relies on the myofilament sensitivity for Ca^{2+}. This sensitivity is controlled by factors such as phosphorylation or the presence of pathogenic variants that may alter the myofilament sensitivity of calcium. This concept further demonstrates that the major factor regulating contraction is the level of intracellular [Ca^{2+}][36]. Nevertheless, contractility does not solely depend on Ca^{2+} binding to TNNC1. The nature of the cooperative calcium-based activation is a much more complex function of interactions among the thin filament regulatory units[19]. For instance, the cTnC-cTnI interaction has been shown to have a profound effect on cross bridge formation and force generation. In recent FRET-based studies, it was evident that Ca^{2+} binding induces exposure of a hydrophobic patch on cTnC that binds to the switch peptide of cTnI, causing release of the inhibitory peptide of cTnI on actin-TPM, thus allowing for proper crossbridge formation[19,37].

For relaxation to occur, Ca^{2+} must be removed from the cytosol to bring it to diastolic levels of ~ 100 nM. This requires that the RyR channels close and then that Ca^{2+} must be (1) pumped back into the SR, through re-uptake by the SERCA2a (SR Ca^{2+} - ATPase) and (2) driven out of the cell, which is mostly done by the sodium–calcium exchanger (NCX1) (Figure 1.3). The activity of SERCA is tightly regulated by Phospholamban (PLN), which acts as an inhibitor until its phosphorylation relieves this inhibition and allows SERCA to accelerate its pumping of Ca^{2+} back into the SR. It is important to note that proper cardiac function requires that cytosolic [Ca^{2+}] drop rapidly to low enough levels such that relaxation is sufficient to allow the heart to refill with blood. Therefore, both diastolic and systolic [Ca^{2+}] must be tightly regulated in a timely manner[35,36].

1.1.8 Contractility and mechanotransduction

Various proteins have been proposed as key mechanosensors and mechanotransducers that can directly sense and respond to mechanical loads in a cardiac cell. These sensors can trigger structural and signaling pathway

alterations associated with various cellular functions. These pathways include regulation of electrophysiology via stretch-sensitive ion channels, contractile function, and an essential downstream outcome of mechanical signaling that affects cardiac hypertrophy and muscle growth. The sarcomere is the molecular mechanical unit of the cardiomyocyte, and forces generated by actin–myosin crossbridges are transmitted in a composite fashion throughout the sarcomere, to the rest of the cytoskeleton, sarcolemma, and eventually through the intercalated disk to the neighboring cells. As forces are transmitted throughout the structural proteins to the sarcomere, several molecules are likely involved with sensing and transducing this mechanical force[38].

Titin and muscle LIM protein (MLP or cysteine-rich protein) are two critical structural proteins heavily involved in force transmission and sensing within the sarcomere. The muscle LIM protein has been shown to be a key component for localization of the Ca^{2+}-regulated phosphatase, calcineurin, at the Z-disc. Due to this activation, calcineurin dephosphorylates the nuclear factor of activated T-cells (NFAT) family of transcription factors, thus leading to NFAT translocation into the nucleus, which in turn activates a pro-hypertrophic/pro-growth gene program. Studies using MLP–deficient mice have shown that mislocalization of calcineurin in response to reduced MLP levels is associated with reduced NFAT signaling, pronounced left ventricular dilatation, and cardiac dysfunction[39,40].

Another protein localized at the Z-disc is Calsarcin-1, which unlike MLP, interacts with and negatively regulates calcineurin activity. This is further shown in Calsarcin-1 knockout mice in which they display enhanced calcineurin/NFAT pathways activation and consequently have enhanced cardiac hypertrophy and an exacerbated cardiomyopathy[41].

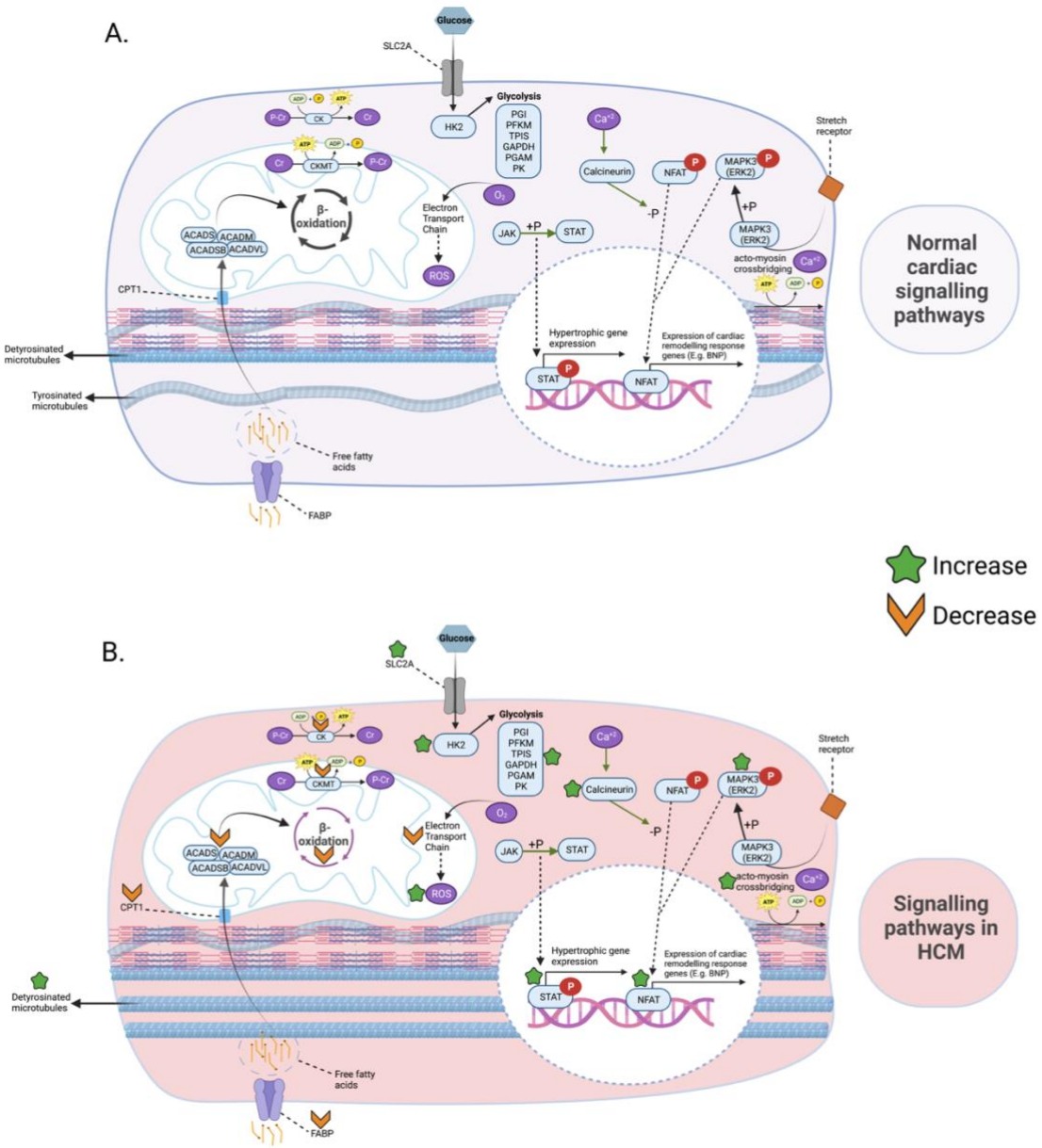

Figure 1. 4: Schematic presentation of the A) normal vs. B) HCM-related signalling pathways. This includes glycolysis, β-oxidation, electron transport chain (ETC), JAK-STAT pathway, and the calcineurin-NFAT pathway. *Created with BioRender.com.*

As described in section 1.1.1, titin is a giant sarcomeric protein that spans the Z-disc to the M-line. In addition to titin's several roles in passive stiffness and elastic recoil, it also functions as a signal transducer in response to mechanical burden[42]. Distinctive regions within titin have been shown to serve as anchoring sites for several cytoskeletal proteins that transfer biomechanical stress responses during cardiac hypertrophy and failure[43]. These proteins include MLP, titin-Cap (TCAP), calsarcin-1, four-and-a half-LIM domain protein-1 (FHL1), and muscle-specific ankyrin repeat protein (MARP)[42]. Many studies have shown that the Z-disc region of titin and its various proteins are heavily involved in strain sensing which causes re-localization of some Z-disc proteins into the nucleus to activate the expression of many growth and hypertrophy related genes[44]. Figure 1.4 summarizes these calcium-mediated signaling pathways which are just a few of the many complex interactions that can be activated through mechanosensitive proteins. Thus, possible modulation of these pathways is a promising therapeutic application for cardiac diseases that involve muscle hypertrophy and failure.

1.1.9 Cardiomyocyte metabolism

In the mitochondrion, the heart utilizes a variety of energy substrates, including carbohydrates, lipids, amino acids, and ketone bodies, for ATP production. As mentioned in section 1.1.4, mitochondria occupy about one third of the cell volume in cardiac myocytes making them the cell type in humans with the highest mitochondrial content. This is reflected by the CMs having the highest oxygen consumption rate per unit weight of all cells in the human body which confirms the robustness of cardiac metabolism. For a human heart, it is well known that fatty acids are the predominant source of energy utilized in the adult myocardium[45].

During development, the heart transitions from a high glycolytic activity in the early phases of development to almost exclusively relying on oxidative metabolism at maturity[46]. *In utero*, the low levels of circulating fatty acids and high levels of lactate contribute to establish the glycolytic upregulation seen in the fetal myocardium. As a result, only ~12-15% of total energy production is derived from the use of fatty

acids in the fetal heart[47]. However, within the first week of life, the newborn heart rapidly switches energy substrate dependence to fatty acids. This elevation is due to an increased AMP Kinase (AMPK) activity, fatty acid binding protein (FABP), acyl-coA dehydrogenases (ACADs), and many other proteins, resulting in increased translocation of activated fatty acid into the mitochondria, subsequently increasing ß-oxidation of fatty acids for energy production[48]. In some cardiomyopathies, a switch back to glycolytic metabolism is a hallmark of pathogenesis and disease progression[49]. A striking change studied in pathological hypertrophy is the shift in fuel metabolism from fatty acid oxidation to increased dependence on glucose and an overall reduced oxidative metabolism and impaired energetics[50]. The current ruling hypothesis is that gene expression in the hypertrophied heart reverts to a fetal program and thus a reappearance of the *In utero* metabolic profile[31,49,50].

Nevertheless, the cardiac metabolic network is highly flexible in utilizing other available substrates if needed. For example, in experiments performed on rat hearts, it was found that cardiac lactate oxidation becomes prevalent during exercise as skeletal muscle lactate production increases resulting in increased plasma lactate levels[51]. Moreover prolonged fasting or practicing a ketogenic diet increases the blood level of ketone bodies, thus resulting in enhanced ketone body-based metabolism by the heart[52]. These various studies, under a variety of physiological conditions, support the concept of metabolic plasticity that confers the importance of adequately supplying ATP for the perpetual cardiac contraction.

1.1.10 Inherited cardiomyopathies

Heritable disorders of the heart that affect or alter the structure and function of the heart are called cardiomyopathies. In the past century, cardiomyopathies have undergone a transformation from being considered idiopathic syndromes of the heart with different clinical phenotypes to being identified as diseases with genetically complex etiologies. The pathophysiology of inherited cardiomyopathies is highly complex and has been under investigation for over 120 years[53]. Table 1

summarizes the different classes of primary cardiomyopathies according to the American Heart Association (AHA)[54].

Different variants within the same gene can underlie different disorders. For instance, variants that affect adjacent amino acids in the β-MYH, can cause either hypertrophic cardiomyopathy (HCM) or dilated cardiomyopathy (DCM). Dilated cardiomyopathy, as the name suggests, is characterized by left ventricular dilatation, systolic dysfunction, myocyte death, and myocardial fibrosis.

Table 1: Summary of the Different Classifications of Primary Cardiomyopathies [54].

Cause	Disease	Prevalence
Genetic	Hypertrophic cardiomyopathy (HCM)	~1:500
	Arrhythmogenic right ventricular cardiomyopathy (ARVC)	~1:5000
	Left ventricular non-compaction cardiomyopathy (LVNC)	~1:2500
	Glycogen storage cardiomyopathy- PRKAG2 variants	~1:100,000
	Conduction defects	N/A
	Mitochondrial cardiomyopathies	~1:5000
Mixed	Dilated cardiomyopathy (DCM)	~1:2500
	Restrictive cardiomyopathies (amyloidosis)	~1:100,000
Acquired	Inflammatory (myocarditis)	~1:10,000
	Stress-provoked	N/A
	Peripartum	
	Tachycardia-induced cardiomyopathy	

Most of the genes involved in the development of DCM encode structural elements of the cardiomyocytes, particularly dystrophy-associated glycoproteins, or components of the sarcomere. Several of the variants linked to causing the autosomal dominant DCM encode the same contractile sarcomeric proteins that are responsible for causing HCM, these include: α- actin; α-tropomyosin; cardiac troponin T, I and C; β- and α-myosin heavy chain; myosin binding protein C; Z-disc protein-encoding genes, including muscle LIM protein, α- actinin-2, and titin. Even though DCM and HCM share similar genes of origin, disease progression and manifestation are completely different through distinct signaling pathways. Hypertrophic cardiomyopathy is one of the most common heritable heart diseases. It is characterized by left ventricular hypertrophy with preserved or increased ejection fraction. It is commonly asymmetrical with the most severe hypertrophy involving the interventricular septum. At the cellular level, the cardiomyocytes are hypertrophied, disorganized, and parted by areas of interstitial fibrosis[55]. All of the inherited cardiomyopathies are genetically heterogeneous; within each category there are multiple disease-related genes, and various mutations in the same gene that could result in divergent phenotypes with differing levels of pathogenicity[56].

1.2 Hypertrophic Cardiomyopathy (HCM)

As mentioned in section 1.1.10, HCM is one of the major inherited cardiomyopathies. Its prevalence in the general population is about 0.2%- 0.5% (~1:500-1:200 individuals)[55]. It is typically a single gene disorder with an autosomal dominant pattern of inheritance, whereby a single amino acid residue substitution is usually sufficient to cause the disease phenotype, though with variable penetrance and expressivity[57]. HCM often results in an increased incidence of arrhythmogenesis which can lead to sudden cardiac arrest (SCA) and death in young adults and elite athletes[55].

The first genetic cause for HCM was defined in 1990 by the Seidmans as a point variant, R403Q, in the gene encoding β-myosin heavy chain (*MYH7*)[58]. Since that time, >1500 different variants have been defined in at least 12 different sarcomeric

genes. For that reason, HCM has been termed “the disease of the sarcomere”[55,59]. Previous reports stated that mutations in the thick filament; β-myosin heavy chain, the regulatory/essential light chains, and myosin binding protein-C are estimated to be responsible for approximately ~50% of HCM occurrences. Thin filament variants are estimated to cause ~20 to 30% of HCM. It is predicted that in the future, the HCM research field will shift from targeting treatments for general phenotypes such as hypertrophy, fibrosis, and arrhythmias, towards targeting the direct underlying molecular insult. It is hoped that the focus will transition from population- to individual-based approaches, since one treatment cannot be applied to all patients due to the wide variability in disease phenotype presentation[60].

Currently, the main knowledge gaps are related to the signaling pathways involved in HCM manifestation, how they are triggered, and how they lead to altered cellular electrophysiology, contractility, metabolism, and overall structure. Based on that, the focus of this thesis will be to help further our understanding of the molecular basis of HCM disease progression. This might present a future opportunity to identify novel potential markers and therapeutic targets.

1.2.1 Genetic basis of HCM

Each human genome is made of about ≈3.2 billion base pairs, which differ in four to five million nucleotides from the reference genome[61]. This variation is due to the error rate of the DNA replication machinery. Consequently, each genome is introduced to about ≈60 de novo variants (not inherited from parents’ genomes)[61,62]. Variants affecting a single nucleotide, referred to as single-nucleotide polymorphism (SNPs), are the most common type of genomic variation. SNPs in specific coding regions of sarcomeric genes have been shown, with strong evidence, to be the leading cause for HCM[63]. Since the discovery of the MYH7 (R403Q) variant in 1990[58], many reports were published of multiple separate mutations in distinct sarcomeric proteins directly related to HCM manifestation. Over time, this established HCM as a genetically heterogeneous disease. Among the known causal genes, *MYH7* and *MYBPC* are the two most common ones,

followed by variants in *TNNT2* and *TNNI3* [55,63,64]. Table 2 shows a list of the most common reported sarcomeric variants that cause HCM phenotype.

Table 2: Established HCM-causing Variants in Thick and Thin filament Proteins [55,63,65,66].

Causal gene	Symbol	Potential HCM-causing variants	Frequency
β-Myosin heavy chain	*MYH7*	A26V, R54Z, V59I, T124I, R143Q, Y162C, N187K, Q222K, N232S, F244L, K246Q, R249Q, G256E, A259E, I263T, M349T, K383N, R403Q, R403W, R403L, R453C, F513C, G584R, D587V, N602S, V606M, K615N, G716R, R719W, R719Q, R723R, P731L, I736M, G741R, G741W, D778G, S782N, A797T, R870H, L908V, E924K, E930K, and E1205K	~35%
Myosin binding protein C	*MYBPC3*	E258K, E451Q, R495Q, R502Q, E542Q, E654H, and N755K	~25%
Cardiac troponin T	*TNNT2*	I79N, R92Q, F110I, E163K, E244D, and R278C	~5-10%
Cardiac troponin I	*TNNI3*	R145G, R145Q, R162W, G203S, and K206Q	~3-5%
Tropomyosin	*TPM1*	A63V, K70T, D175N, and E180G	~1%
Myozenin 2	*MYOZ2*	S48P and I246M	~0.5%
Essential myosin light chain	*MYL3*	M149V and R154H	Rare
Regulatory myosin light chain	*MYL2*	A13T, F18L, E22K, R58Q, and P95A	Rare
α-actin	*ACTC1*	H88Y, R95C, E99K, Y166C, A230V, S271F, A295S, M305L, and A331P	Rare
Titin	*TTN*	R740L and S3799Y	Rare
Cardiac troponin C	*TNNC1*	A8V, C84Y, E134D, and D145E	Rare
α-Myosin heavy chain	*MYH6*	A1004S and Q1065H	Rare

1.2.2 Disease manifestation pathways in HCM

As discussed in the previous section, HCM manifests as a maladaptive response to certain genetic variants which encode for contractile proteins, most of which are sarcomeric proteins. This triggers alterations in the biophysical dynamics of the thick and thin filaments. As seen in Figure 1.2, it is crucial that each component of the sarcomere is functioning properly to support the complex dynamic machinery behind cardiac contraction. The thin filament particularly is a crucial part of the sarcomere, it contains the regulatory proteins actin, troponin complex (T, I, C), and tropomyosin.

In HCM caused by thin filament variants, depending on which protein is defective and the variant type, cardiac muscle responds with various HCM features such as: progressive hyper-contractility, impaired energetics, maladaptive mechanical signal transduction, and pathogenic muscle remodelling. For example, Troponin T (*TNNT2*) plays a crucial role in the thin filament, it binds tropomyosin and helps position it on actin for optimal cross-bridge formation between the actin and myosin domains[67] (Figure 1.2). Subsequently, any mutation-caused disturbance in this dynamic relationship will result in molecular consequences affecting the myocyte on multiple levels, including: calcium-based contractility regulation, the transcriptome, and the proteome[64,67]. As a consequence of the enhanced contractility, there is an increased initiation of mechano-sensitive signaling pathways via transcriptional activation. This includes expression of trophic and mitotic factors, such as calcineurin, mitogen-activated protein kinases (MAPK), and transforming growth factor beta (TGF β) pathways (figure 1.4B).

Additionally, secondary molecular and intracellular changes occur in response to the changes of sarcomere protein structure and function. Those include epigenetic modifications, such as micro RNAs (miRNAs) which are small noncoding RNAs with ~22 nucleotides, regulating gene expression at the posttranscriptional level, protein posttranslational modifications, and histone modifications[68].

1.2.3 Consequences on contractility and EC-coupling

One critical aspect that has been the focus of many recent studies is the biophysical consequence of HCM-causing variants on calcium-based contractility and regulation and being a trigger for the change in the transcriptome. As described in section 1.1.7, the contraction cascade is initiated by a local calcium influx through the L-type calcium channels (Cav1.2), localized primarily in the t-tubules, followed by the activation of RyR2 on the sarcoplasmic reticulum, initiating CICR. When Ca^{2+} enters the cytosol, its free concentration can be elevated up to ten-fold from a resting level of ~100 nM to ~1 μM. As the cytosolic Ca^{2+}rises, it increases the probability of it binding to troponin C, leading to an axial shift in the tropomyosin positioning on actin. This shift partially exposes the myosin strong-binding sites on actin. A subsequent increase in myosin binding to the thin filament pushes tropomyosin into the open state, which unlatches multiple adjacent myosin-binding sites, leading to cooperative recruitment of myosin cross-bridges (figure 1.3).

Therefore, Ca^{2+}-based regulation depends on Ca^{2+}, myosin binding, and the coupling between troponin and tropomyosin[33]. The presence of an HCM-causing variant in any of the critical proteins in EC-coupling can lead to a disturbance in the dynamic relationship between the thick and thin filaments, thus reducing the affinity and coupling between them. Most commonly, HCM variants cause increased calcium sensitivity of the thin filament, making more myosin heads readily available to form acto-myosin crossbridges for a given level of cytosolic Ca^{2+}. This increased cross-bridge formation is one of several causes leading to elevated contractility and stiffness of the sarcomere[63,69].

1.2.4 Consequences on the transcriptome

The general dogma is that the HCM-causing genetic variants increase the Ca^{2+} sensitivity of the contractile element. This is posited to be due to an allosteric effect of these thin-filament structural changes on the Ca^{2+} binding affinity of the cTnC site II, which typically results from a reduced Ca^{2+} off rate constant (k_{off}). These

biophysical changes alone can impact the function of the heart by implementing changes to the transcriptome in intricate ways. These changes include but are not limited to[69]:

1. Alterations in contractile force (both magnitude and kinetics) which can act through the mechanosensitive properties of the myofilament (e.g., MAPK-mediated signalling pathways).
2. Changes in the cytosolic Ca^{2+} levels (amplitude and kinetics) can act indirectly on the transcriptome to induce hypertrophy (e.g., calcineurin-NFAT signalling pathway).
3. Modifications in metabolism due to increased cross bridge cycling which has been postulated to cause local depletion of ATP (impaired cellular energetics).

Due to these complex impacts on the transcriptome, it is critical to understand the subsequent changes implicated on the proteome.

1.2.5 Consequences on the proteome

While understanding the changes that occur on the transcriptomic level is crucial, the translational alterations are far more complex and more correlated to the observed HCM phenotype. The process of translating the mRNA to protein introduces great variability. So while humans are estimated to have about 21,000 protein encoding genes, alternative mRNA splicing and post-translational modifications (PTMs) may increase this number up to hundreds of thousands of proteins or protein fragments[70]. Such modifications play a vital role in modulating the function of many proteins, but this is not directly encoded by genes. Also, there are protein–protein interaction networks which are complexes formed by biochemical events or electrostatic forces that serve a distinct biological function as a complex. These interactions also cannot be inferred from the transcriptome[70,71].

As studied by the Ge research group at the University of Wisconsin-Madison[72], the molecular mechanisms by which sarcomeric protein variants lead to pathogenic cardiac remodelling, hypertrophy, and eventually heart failure, remain a conundrum. These studies were able to speculate on the occurrence of an overall organizational deviation in proteins responsible for the structural integrity of the thin and thick filaments. These studies also further confirmed that not all HCM variants manifest in a similar manner. Notably, one study by this group showed that uniform proteoform changes were present between the control and HCM groups, particularly in the phosphorylation of fundamental contractile proteins[72]. Many studies also demonstrate the heterogeneous nature of the proteomic landscape across different HCM patient samples which is likely due to considerable differences in the donor genome background. While the initial impact of the primary disease-causing variant may have unique features, the convergence of the HCM phenotype suggests common pathways that may be mediated by PTMs or alternative splicing to influence the function of sarcomeric proteins during hypertrophic remodeling[69]. Most studies involving translational analysis of an HCM model have shown the implication of a similar panel of proteins. These include major protein families involved in: contractility, the extracellular matrix, sarcomeric organization (Z-disc and cytoskeleton), and energy metabolism. Nevertheless, over the lifetime of the CM, and throughout the development of the disease, the precise mechanisms and complex signalling pathways that lead to the observed proteomic changes, in quantity, isoforms, and PTMs, are still not well understood[55,63,68,72].

Given these knowledge gaps, there is great importance in the molecular characterization of a wide range of HCM phenotypes to help define disease progression and prognosis based on the proteomic profile, not only in cardiomyocytes, but also in the various cell types involved in modifying cardiac function (e.g., fibroblasts, endothelial cells, and smooth muscle cells). This would aid in understanding the phenotypic manifestations and underlying dysfunctional signaling pathways, thus providing opportunities for novel targeted therapeutics.

1.2.6 Consequences on cardiac metabolism

One of the common downstream consequences that is believed to be central to HCM pathophysiology, is impaired cardiac energetics relative to the energy demand. Energetic defects have been long been recognized in genetic mouse models of HCM, as well as patient models with significant reductions in the energy reserve reflected by a decreased ratio of phosphocreatine (PCr) to ATP[47,73]. In patients with HCM, a lower PCr:ATP ratio is associated with the progression of hypertrophy and cardiac fibrosis. More recently, studies have shown a more detailed analysis of the dysregulation of specific enzymes and proteins involved in HCM cardiac metabolism. In particular, greatly reduced abundance of enzymes involved in fatty acid oxidation, which is evidence for a metabolic shift away from fatty acids as the primary fuel source, or a switch to the fetal gene program[73,74]. Also, a similar shift in substrate utilization has been shown in experimental models of cardiac hypertrophy. In the healthy heart, β-oxidation of fatty acids produces the majority of acetyl CoA that feeds into the TCA cycle which is used to eventually generate ATP. In conditions of myocardial stress, metabolic reprogramming of fuel utilization from free fatty acids to glycolysis occurs as an initial adaptive response to reduce the consumption of oxygen. But over time, this shift results in insufficient ATP production to meet the energetic demands of the heart, thus contributing to the pathogenesis of myocardial dysfunction and local energy depletion[75].

Moreover, the altered sarcomere contractility further provokes mitochondrial dysfunction, which increases reactive oxygen species (ROS) and leads to altered ion homeostasis and possibly, arrhythmias[76]. The fundamental premise is that high ATP utilization increases ADP, which will reduce the levels of NADH and NADPH, thereby triggering oxidative stress. In mitochondria, ADP accelerates ATP production via oxidation of NADH to NAD+. At the same time, Ca^{2+} stimulates the Krebs cycle (conversion of NAD+ to NADH) to match the ADP-mediated reduction in NADH, thereby maintaining the NADH/NAD+ balanced redox state. The HCM-causing mutation induces an increase in myofilament Ca^{2+} sensitivity which will enhance ATP utilization and increase ADP levels. The increase in ADP will

increase oxidation of both NADH and NADPH and disrupt the NADH/NAD+ balance. Additionally, as more Ca^{2+} will be bound to the sarcomeres, less Ca^{2+} will be available to stimulate the mitochondrial Krebs cycle and regenerate NADH. Through these mechanisms, impaired sarcomere energetics may thus provoke mitochondrial dysfunction, reduced ATP production, and increase ROS[74,76].

1.3 Modelling Hypertrophic Cardiomyopathy

1.3.1 Previous models of HCM and their limitations

Over the past 25-30 years, many models have been developed to recapitulate the human HCM genotype and facilitate the study of disease phenotype. Animal models have been developed as an invaluable research tool that has been utilized to confirm the causative gene defects in HCM and has allowed for extensive studies into the pathways involved in pathogenesis and the role of genetic and environmental modifying factors on clinical outcomes. The high degree of genetic homology (~98%) between humans and the common animal models of HCM, including mice and rabbits, allows for disease-causing variants to be investigated in a relevant model of cardiac physiology[77].

While genetically engineered mice have been the predominant animal model in HCM, other relevant non-mouse animal models have been successfully developed. For example, the R403Q mutation has been introduced into rabbits leading to the important development of an HCM rabbit model. This model has some advantages over the mouse model, as rabbits and humans have a more similar composition of sarcomere proteins, with rabbits predominantly expressing the β-MHC protein in the ventricles, as opposed to the α paralog in mice. Other similarities between rabbit and human hearts are the heart rate, making rabbits a more relevant model for arrhythmogenic studies, and the larger size of the heart, making the rabbit model easier for many physiological studies. The transgenic R403Q rabbit model reproduced the phenotype of HCM in humans, with rabbits exhibiting cardiac hypertrophy, myocyte disarray, interstitial fibrosis, and a significant increase in interventricular septal thickness and LV mass[77,78].

However, these animal models still have their limitations and drawbacks. 1) The cardiovascular system of each animal has evolved differently in order to meet the demands of that species. While blood pressure remains relatively constant across various laboratory animals and humans, there is tremendous variability regarding heart rate. 2) Despite the high level of genomic homology, the gene interactions, pathways, and manifestation of disease in model organisms are unrivaled to those of human. 3) Wide variations exist in the post-transcriptional processing of mRNA, thus generating different protein isoforms that are species-specific[79,80].

1.3.2 Human induced Pluripotent Stem Cells (hiPSCs) technology

In mammals the property of pluripotency is restricted to the oocyte, the zygote, early embryonic cells, and primordial germ cells. During early development, the human embryo possesses a population of pluripotential cells. These cells, through activation and transcriptional regulation of various signaling pathways, have the capacity to give rise to differentiated progeny representative of all three embryonic germ layers (i.e., endoderm, mesoderm, and ectoderm). Nevertheless, under certain conditions, pluripotential stem cells can be propagated immortally in vitro and still maintain the capacity for differentiation into a wide variety of somatic tissues[81].

The embryonic stem (ES) cells, which are derived from the inner cell mass of mammalian blastocysts, are able to grow indefinitely while maintaining their pluripotent characteristics. These properties have led to the conclusion that human ES cells might be useful to understand model diseases, screen effective and safe drugs, and possibly be utilized as a treatment option for patients of various diseases and injuries. However, the use of human embryos is a highly debated topic and is ethically controversial. In addition, it is challenging to generate patient- or disease-specific ES cells, which are required for effective assessment of disease phenotype and drug screening. One way to evade these issues is to induce a pluripotent status into somatic cells by direct reprogramming[81,82].

In 2007, Shinya Yamanaka et al. showed that induced pluripotent stem (iPS) cells can be generated from adult human fibroblasts by the retrovirus-mediated transfection of four transcription factors, specifically Oct3/4, Sox2, c-Myc, and Klf4[82]. These efforts have enabled the immortalized generation of hiPSCs from various adult human somatic cells, which have proven to be comparable to human ES cells[82].

Human induced Pluripotent Stem Cells (hiPSCs) exhibit unique properties that render them qualified as model systems for studying human diseases: 1) they are of human origin, which means they carry the human genome of the source cell; 2) they are pluripotent, which means, with proper activation/inhibition of specific signalling pathways, they can be differentiated into any of the human somatic cell types; and 3) they are stem cells, which means they can be expanded from a single cell into millions or even billions of cell progeny. iPSCs offer the unprecedented opportunity to generate cells that are genetically matched to individual patients. Furthermore, genome editing tools allow the introduction or correction of genetic variants for foundational studies of genetic disorders[82,83].

1.3.3 Using hiPSC-CMs to model HCM

Earlier disease models have greatly contributed to understanding HCM progression and have proved to be useful as a collective to advance towards better treatment options. However, due to HCM's intricate and diverse nature, most models have often fallen short to truly recapitulate HCM in vitro. Unlimited production of hPSC-CMs has facilitated deeper mechanistic studies, complementing the approaches from previous models[77,83] (figure 1.5).

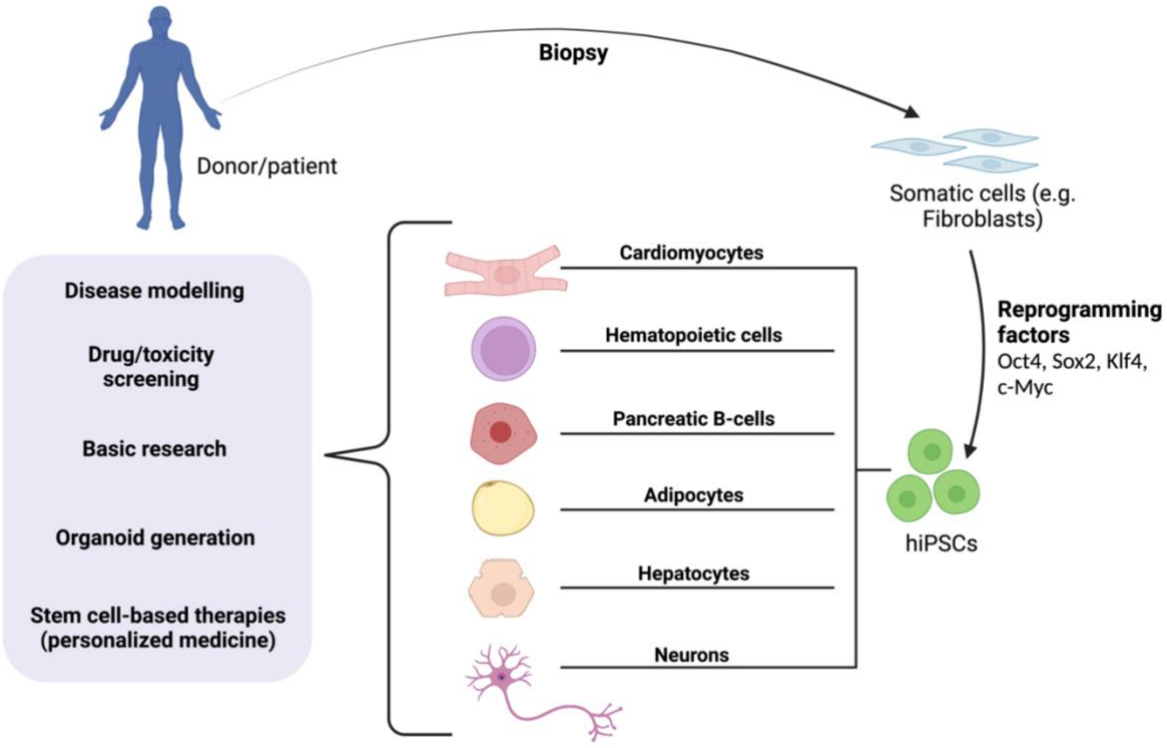

Figure 1. 5: The generation and use of induced pluripotent stem cells for various cell line generation, disease modeling, and precision medicine studies. *Created with BioRender.com.*

The differentiation of cardiomyocytes from human iPSCs can be achieved in vitro by modulating the signaling pathways involved in cardiac development. In a 2D monolayer cell culture, some small molecules could promote cardiac differentiation through a mesoderm lineage. Indirect activators, such as CHIR99021, and inhibitors, such as IWR, XAV, IWP2, all act on the key WNT signalling pathway (functions in cell fate determination during embryonic development)[84,85]. Appropriate timely application of these small molecules can push the hiPSCs into a cardiac progenitor fate, and eventually a monolayer of spontaneously beating hiPSC-CMs[85]. This protocol will be described in further detail in the Methods chapter of this thesis (Chapter 2).

1.4 HCM causing variants

As mentioned in sections 1.2-1.2.1, HCM is typically caused by a SNP in one of the core sarcomeric genes, this includes both thick and thin filament variants. Since the majority of HCM cases are caused by variants in the thick filament (~50%), most of the early studies were done on beta myosin heavy chain *(MYH7)* and myosin binding protein C *(MYBPC3)*[55,86]. The main inference from these studies is that overall, the clinical phenotypes do not seem to differ significantly between these two common HCM genes. Shortly after the characterization of thick filament mutations, the discovery of the involvement of many thin myofilament genes in HCM development paved a field shift to start exploring the mechanisms and pathogenetic variability among different sarcomeric variants[86].

However, HCM caused by variants in the thin myofilament proteins, exhibited a milder cardiac hypertrophy and an increased risk of systolic dysfunction[63,87]. The most common thin filament genes implicated in causing HCM are: Tropomyosin *(TPM1)*, cardiac alpha actin *(ACTC1),* cardiac troponin T *(TNNT2)*, and cardiac troponin I *(TNNI3)*[55,63]. *TNNT2* variants are the most prevalent in thin filament-caused HCM, in fact, 15-20% of all HCM cases are due to mutations in *TNNT2*[86]. Patients with *TNNT2* mutations generally exhibit mild or no ventricular hypertrophy yet demonstrate a high frequency of early sudden cardiac death. To understand the functional basis of these phenotypes, various *TNNT2* missense mutations must be induced and studied in human cell line models to take a deeper look into the molecular alterations[86–88].

The focus of this thesis is on two critical cardiac Troponin T *(TNNT2)* variants: the Isoleucine to Asparagine point mutation at amino acid residue 79 ($I79N^{+/-}$), and the Arginine to Cysteine point mutation at amino acid residue 278 ($R278C^{+/-}$). Due to the different mutation sites, $I79N^{+/-}$ and $R278C^{+/-}$ exhibit inconstant expressivity, even though both variants are in the same gene.

1.4.1 I79N$^{+/-}$ TNNT2

The clinical outcome of HCM patients is not only determined by the disease-causing mutation but is also greatly influenced by the variant location. As shown in figure 1.6, the *TNNT2* gene is composed of 17 exons, which encode for a 288 amino acid long protein[89]. The I79 site is located near the first helical complex which is speculated to structurally interact with actin and TPM. However, because that region of the protein is highly flexible, its structure and function are not well characterized[87,88] (figure 1.6A).

However, the replacement of the phylogenetically conserved, uncharged Isoleucine residue with the negatively charged Asparagine will undoubtedly carry consequences on the protein-protein interaction level, which is crucial for the stability of the sarcomere and crossbridge formation. The lack of structural insight complicates the process of understanding the biophysical consequences of this *TNNT2* variant. In 2003, the Knollmann group used transgenic mice expressing the I79N$^{+/-}$ mutant[88]. The results showed that the mice were particularly susceptible to ventricular tachycardias and arrhythmias that were coincident with an increased myofibrillar Ca^{2+} sensitivity, elevated force generation, and action potential triangulation[88]. A recent study has also recapitulated the same kinetic dysfunction results in hiPSC-CMs harbouring the I79N$^{+/-}$ variant[90].

1.4.2 R278C$^{+/-}$ TNNT2

The R278C$^{+/-}$ mutation is localized in the C- terminal domain of cTnT (figure 1.6B). Hence, the substitution of an uncharged cysteine (C) in place of the phylogenetically conserved, positively charged arginine (R) at residue 278 may weaken the interaction of cTnT with tropomyosin and thus reduce its binding affinity to the thin filament [91](figure 1.6B). The reduced coupling between the troponin complex and tropomyosin ultimately leads to a variety of contractility malfunctions ranging from slowed Ca^{2+} decay kinetics, to elevated myofilament tension generation (hypercontractility)[67,91]. Both of the described *TNNT2* variants share a common manifestation feature of directly or indirectly altering the thin filament Ca^{2+}

sensitivity, which in turn leads to progressive sarcomeric proteome remodelling through specific transcriptional signalling pathways. Most of the ongoing HCM-related research is clinical and functional-based inspection, which does not address the crucial underlying mechanisms that drive disease pathogenesis, especially on the proteomic level[87].

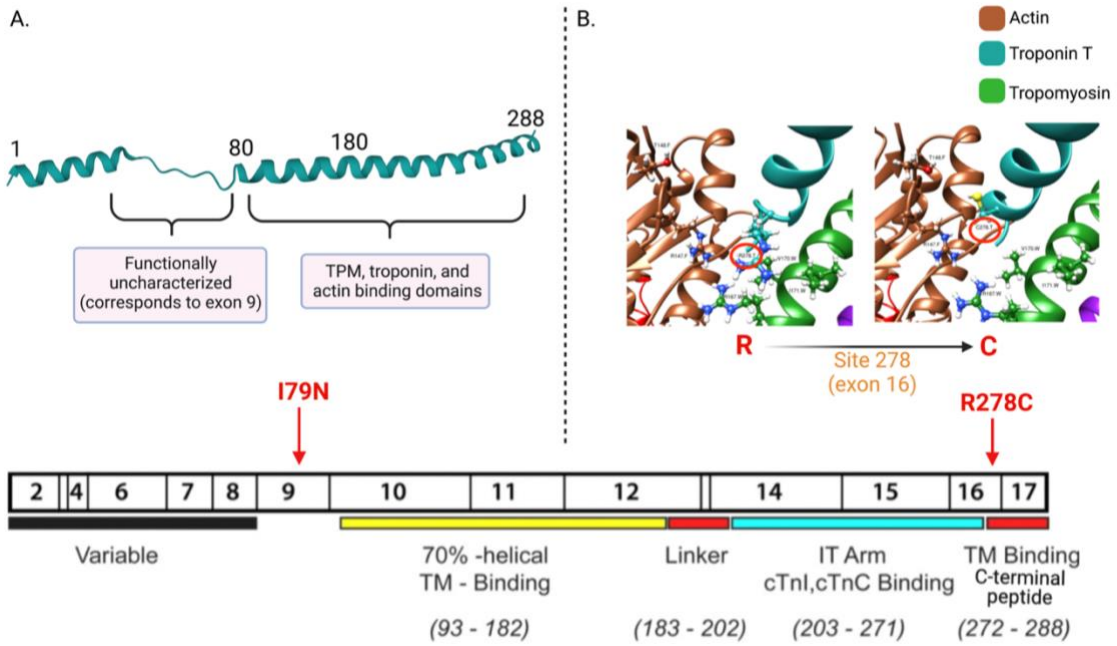

Figure 1. 6: Visualization of the troponin T secondary structure helices (288 aa) along with the corresponding exon distribution and location of the variants. The (R278C) mutation site is located near the C-terminal end of the functional domain where Tropomyosin (TM) binding takes place. The (I79N) mutation site is located near the first helical complex which remain functionally uncharacterized (adopted from Tardiff et al.[92]). *Created with BioRender.com.*

Accordingly, the current investigative approach is restricted by two important aspects that I will be addressing in this thesis: 1) proteomic profiling has been mainly conducted on animal models or patient-derived tissue samples. There is a lack of utilization of a proper human model that mirrors the in vivo pathogenic remodelling. Although data from HCM patients has been greatly impactful, it remains confined in its translational applicability. The hiPSC-CMs possess features that potentially render them as an excellent disease model system: they are of human origin, therefore carry human genomes so phylogenetic variation among orthologs is not an issue. Additionally, genome-editing tools offer the

unprecedented opportunity to introduce site-specific variants to hiPSC lines for disease modelling and characterization. 2) Most studies neglect to explore the course of remodelling in response to HCM-causing mutations over a sufficient period of time. The cardiomyocyte level of maturity is a critical factor that must be considered. The proteome profile must be assessed throughout the developmental process because protein expression is time- and condition-dependent, therefore, disease manifestation could present, clinically, at the early phase of development, or later on in adult stages[59].

1.5 The clinical complexity of HCM

It is now widely recognized that just knowledge of the variant type is not a reliable prognostic indicator for HCM[60]. Some variants previously thought to be associated with early onset HCM and SCA, were later found in individuals with a normal life span and very mild symptoms. Table 3 summarizes the clinical profiles for the leading common documented cases in genotype positive individuals. The most prominent symptoms shared across HCM patients are angina, atypical chest pain, and dyspnea[59]. The mechanisms underlying the convoluted variability in clinical expression and wide range of HCM phenotypes, shown in Table 3, are still not well understood. Therefore, it is crucial to explore the disease further at the proteoform level, while taking into consideration the impact of maturation and possible posttranslational modifications (PTMs). As shown in a recent review by Greenberg and Tardiff[60], there still is a lack of translational insights about HCM, as we have learned more about this progressive disorder, it is revealed that HCM is more intricate than generally appreciated. This complexity has limited our understanding of the molecular and cellular effectors that drive disease pathogenesis and frustrated the development of effective therapeutics.

In the past century, management of life expectancy in HCM patients has become relatively favorable. Approximately 60-70% of patients with HCM experience a normal life span without substantial morbidity[93]. In patients presenting with the pathogenic phenotype; atrial fibrillation, heart failure and stroke contribute to

morbidity later on during their lifespan[54,93]. Yet, carrying a heterozygous sarcomere gene mutation alone cannot fully explain HCM's pathological profile. The clinical course of the disease varies greatly in terms of expressivity, age penetrance, and clinical heterogeneity, even within family members carrying the same variant[94]. Thus, the primary defect is the sarcomeric mutation, but clinical expression is established by a complex network of genetic, epigenetic, and environmental factors[64,94].

Table 3: Clinical Features Characterstic of HCM [55,95,96–99]**.**

Clinical phenotype	Frequency in confirmed HCM cases
Chest pain	~ 85%
Dyspnoea	~ 80%
Asymmetric hypertrophy	~ 70%
Heart failure	~ 30%
Left ventricular outflow tract obstruction	~ 25%
Fainting (mostly during physical activity)	~ 25%
Microvascular modifications	~ 25%
Cardiac arrhythmias (e.g. Atrial fibrillation)	~ 20%
Sudden cardiac death	~ 1%

The primary and secondary effects of the mutations ultimately lead to the functional pathological phenotypes seen in HCM patients, such as myocardial hypertrophy and ventricular dysfunction[94]. Some cases present with microvascular ischemia. This can lead to cardiomyocyte energy depletion and apoptosis, which has adverse consequences in cellular remodeling with progressive myocyte loss and fibrous substitution in the myocardium. This is reflected clinically as patients present with histological phenotypes of myocyte disarray and myocardial fibrosis[64]. The reason why HCM is one of the leading causes of SCA is due to arrhythmogenesis. In HCM, arrhythmias are caused by both the primary mutation effects, such as disturbed calcium handling triggered by electrical afterdepolarization, as well as the secondary effects, such as cellular hypertrophy,

increasing the myocyte's automaticity in firing action potentials and myocardial fibrosis creating current disturbances and reentry[55,100].

1.6 Potential therapeutics for HCM

Until recently, treatment of HCM was based on using a combination of drugs to alleviate the secondary symptoms, without targeting the initial molecular insult. These include, β adrenergic receptor (β-AR) blockers, ACE inhibitors, and diuretics, all of which help ease the severity of the hypertension and angina, but do not provide any permanent resolution for the patient[101]. One heavily studied mechanism for HCM treatment is targeting the myosin-actin crossbridge formation.

Normally during relaxation, the head domains of the paired myosin molecules appear to adopt either a super relaxed state (SRX) conformation in which both ATP-binding domains are inhibited and unable to bind actin, or a disordered state (DRX) conformation in which one myosin head is available to hydrolyze ATP and interact with actin. This hypothetical model predicts that the fraction and balance of myosin in these conformations would influence both contractility, energetics and metabolic costs that enable life-long cardiac function[102]. Myosin heads undergo physiological shifts between the SRX conformation that maximizes energy conservation and the DRX conformation that increases the probability of cross-bridge formation with about a 10-fold increase in ATP consumption. Pathogenic variants in thick filament proteins have shown a destabilized SRX state and an increased proportion of myosin in the DRX conformation, which enhanced cardiomyocyte contractility, impaired relaxation and evoked hypertrophic remodeling with increased energetic stress[102].

A novel drug, Mavacamten, has been in clinical trials for the past 4 years. It has shown the most potential in targeting the hypercontractile (DRX) state of the CM and was approved by the FDA in April 2022. Mavacamten causes a dose-dependent reduction in the myosin ATPase rate, due to a reduction in the rate of actin-activated phosphate release. By reducing the rate of actin activated

phosphate release, Mavacamten slows down the transition of myosin cross-bridges into the strongly bound state, therefore, reducing the number of cross-bridges available to interact with the thin filament and favoring the myosin's SRX state. Hence, Mavacamten lessens force production, sarcomere contractility, and stiffness[103].

1.7 Mass Spectrometry Proteomics: Applications to heart diseases

Proteomics is a rising discipline that is becoming increasingly utilized for large-scale characterization of protein species within a biological system. Prior to the advancements in chemical and analytical platforms, western blots were the most common quantitative approach for proteins of interest.

Over the past 20 years, there has been an accelerating growth in the application of proteomics in cardiovascular biomedicine, predominantly, a notable shift towards Mass Spectrometry (MS)[104]. MS approaches have contributed to unique and powerful applications in cardiovascular biomedicine. To accurately grasp the biochemical basis of the combinatorial proteome changes that occur in HCM, mass spectrometry (MS)–based proteomics is becoming increasingly recognized as the primary tool for comprehensive analysis of purified proteoforms. One important type of MS is the top-down approach. In this method, intact protein samples are used to obtain various molecular information such as structure, function, and site-specific features. Protein inference is avoided due to the high accuracy and reproducibility of this technique[105]. Another branch of MS, called "bottom-up" proteomics, is a shotgun method that employs proteolytic digestion of proteins prior to MS analysis, resulting in protein identification in the sample through peptide-to-protein database searching and inference. Subsequently, proteoforms of interest can be fragmented by tandem (MS/MS) for sequence characterization and PTM localization[106,107].

It has become apparent that HCM is more complex in its molecular etiology and clinical presentation than generally perceived. This complexity has limited our understanding of the thin filament interactions that drive disease pathogenesis. It

is critical to study HCM at the proteomic level to gain valuable insights into its underlying molecular mechanisms that may affect cTnT isoforms and post-translational modifications (PTMs). The dynamic nature of the sarcomeric proteins' structures and how they are affected by HCM is not well understood. We postulate that the R278C and I79N variants of *TNNT2* contribute to rapid sarcomeric and thin filament proteome changes which eventually materialize as HCM[72].

1.8 Objectives

The cornerstone of this thesis is grounded on understanding the complex disease manifestation of HCM on an intricate molecular level using hiPSC-CMs. This work will offer a comprehensive examination of the dynamic nature of the cardiac proteome, and its alterations in response to the HCM-inducing *TNNT2* variants. Protein quantification using MS will provide us with a novel perception regarding the intrinsic mechanisms responsible for the clinical HCM phenotype. Previous research is limited in that the mutation effects were not directly translatable to the human situation since several other disease modifying factors, like PTMs and maturity levels, were not taken into consideration. However, this study will overcome this limitation by using hiPSC-CMs to examine more closely how HCM manifests at the proteomic micro-scale and address this manifestation temporally. This presents a future opportunity to identify new druggable targets and broad-spectrum treatments for this genetically challenging disease.

Null Hypothesis: *HCM-causing variants do not alter the proteomic profile of hiPSC-CMs relative to their isogenic controls.*

To refute this, the overall aims of this research are:

1. Determine the ramifications of the two multifarious *TNNT2* variants (I79N$^{+/-}$ and R278C$^{+/-}$) on the quantity of key protein groups in an hiPSC-CMs model using MS-proteomics.
2. Assess the effect of metabolic maturation media (MM) on the progression of the disease phenotype.
3. Examine how the *TNNT2* variants are altering vital signaling pathways by analyzing the PTM-profile implicated in HCM manifestation.

2 Chapter Two: Methods

2.1 Establishing and maintaining the hiPS cell lines

The primary model system used for this study was hiPSCs. To ensure the utilization of healthy cells with high differentiation efficiency, multiple quality control measures were implemented. First, the human iPSC lines (iPS IMR90-1) were obtained as frozen pellets from the Wicell Research Institute, Madison, WI. (https://www.wicell.org/). Cells were thawed at room temperature then seeded on a Geltrex-coated culture plates. The coating was done using a mixture of 0.5 mg Geltrex dissolved in DMEM/F-12/ 6-well plate. The seeding density was set around 100,000 cells cm^{-2} in mTeSR-plus medium (STEMCELL Technologies, Vancouver, BC). After this, the hiPSCs were passaged every 3-4 days using ReLeSR, the hiPSC-specific passaging reagent (STEMCELL Technologies). The medium was changed every other day, and cells were passaged according to their confluency, each passage was done at around 80%-90% confluency.

Through work done by our former lab member, Dr. Sanam Shafaatalab, CRISPR/Cas9 genome editing was used to create hiPSCs carrying the HCM-causing variants of interest[90]. Single-guide RNAs (sgRNAs) were designed to target the regions close to I79 *TNNT2* in one batch of cells, and R278 in another batch.

Therefore, using the WiCell hiPSCs, three cell lines were created; one line carrying the normal wild type *TNNT2* sequence (WT- isogenic control), one harboring the $I79N^{+/-}$ *TNNT2* variant, and one harboring the $R278C^{+/-}$ *TNNT2* variant. Table A.1 lists all of the reagents used to maintain these cell lines.

2.2 Differentiation of hiPSCs into beating CMs

Differentiation of hiPSCs to cardiomyocytes (hiPSC-CMs) employed a protocol published previously by Lian et al[108]. In brief, hiPSCs were maintained and passaged 3 times after thawing, and 3 days after the last passage, when the

monolayer of cells reached >90% confluency, the mTeSR plus medium was replaced with Roswell Park Memorial Institute (RPMI) 1640 basal medium (Thermo Fisher, Waltham, MA) plus B27 without insulin supplement (Thermo Fisher) containing 12 µM CHIR99021 (R&D Systems) for 24 h (day 0). This was followed by 5 mM IWP4 (Tocris) administered at day 3 for one day without medium change. At day 5, The medium was changed to RPMI 1640 plus B27- minus insulin, and subsequently by day 7, the medium was changed every 2–3 days to RPMI 1640 plus B27 complete supplement. Robust spontaneous beating of the monolayer was observed around day 12 after administration of CHIR99021[108]. A detailed illustrative timeline of this differentiation protocol is depicted in figure 2.1.

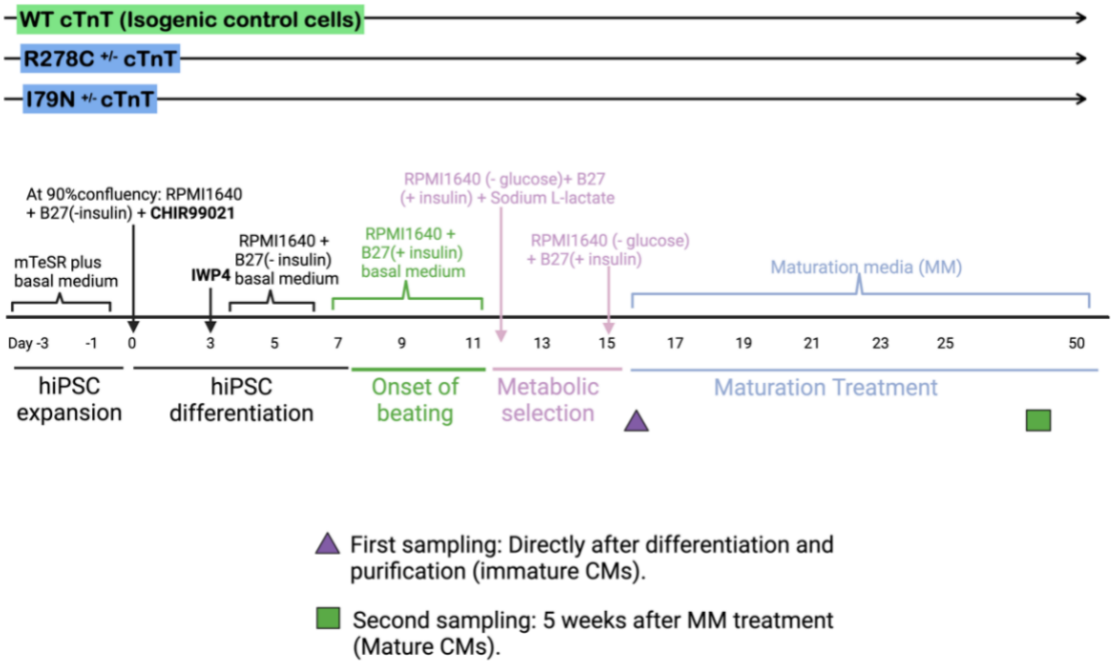

Figure 2.1: The experimental timeline for differentiation, hiPSC-CMs maturation, and sampling.

Following the detection of spontaneous beating, the newly differentiated hiPSC-CMs were subject to a 3-day purification process by glucose starvation and addition of lactate. The CMs were cultured with a purification-specific medium which consists of RPMI1640 without glucose, but with the addition of 5mM lactate. The study by Horikoshi et al, showed that iPSC-CMs cultured in lactate purification

medium for 7 days resulted in a significant increase in troponin T-positive cells from ~75% to 98%[109]. Cells were then re-plated for a second round purification prior to undergoing a chemically induced maturation phase (5 weeks) in special metabolic maturation media (MM) made mainly of free fatty acids[110]. This MM has been adopted from Feyen group[111], and was prepared according to set measurements listed in Table A.2. This MM mimics the adult CM's preference of utilizing fatty acids as the main metabolic substrate, which has been repeatedly shown to improve several aspects such as fatty acid metabolism, cellular structure, morphology, and lastly, enhanced gene expression of adult-like cardiac proteins.[109–111]

2.3 Protein isolation from hiPSC-Cardiomyocytes

In collaboration with the Lange research group at the BC Children's Hospital and Research Institute (BCCHR), the myocardial proteins were isolated from hiPSC-CM pellets (400k-500k cells) at different stages of maturity for all cell lines. The timely collection of the CMs was done using STEMdiff reagent from the CM dissociation kit (STEMCELL Technologies). STEMdiff was added to each well of hiPSC-CMs, and after incubation with its neutralizing agent, the cells detached from the Geltrex matrix and were pipetted up and down for a homogenous suspension. This was followed by centrifugation of the collected cells to obtain a pellet of hiPSC-CMs. The pellet was then resuspended in lysis buffer according to the number of cells. The cells were counted using the CellDrop automated cell counter (Froggabio, Ontario). The lysis buffer used contained 100 mM HEPES (pH= 8-8.5) + 20% SDS, and 75 µL of were added per~ 2 million cells. Cell lysates were then placed for 5 minutes in 95°C water bath, followed by 3 minutes on ice. To complete the lysis, the samples were sonicated twice for 30 seconds, and placed on ice between rounds. This was followed by treatment with benzonase (EMD Millipore-Sigma) at 37 °C for 30 min to fragment the chromatin.

After obtaining the CM lysate, each sample was reduced with 10 mM dithiothreitol (DTT) at 37 °C for 30 min, followed by alkylation with 50 mM Chloroacetamide (CAA) for 30 min in the dark. The alkylation was quenched in 50 mM DTT for 10 min at room temperature. To clean the lysates, high-resolution sample-preparation (SP3) technology was the purification approach used to isolate the proteins in the samples. This protocol is a paramagnetic bead–based approach for rapid and efficient processing of protein samples before proteomic analysis[112]. SP3 uses a hydrophilic interaction mechanism for the removal of interfering components (e.g., detergents, salts, buffers, acids, and solvents). The magnetic beads facilitate a wide range of nonselective protein binding that is enabled through the use of an ethanol-driven solvation layer on the surface of the beads. To each sample, hydrophilic and hydrophobic Sera-Mag Speed Beads (GE Life Sciences, Washington, US) were added in 1:1 ratio. Proteins were then bound to the beads with 100% ethanol (80% v/v) and washed twice with 90% ethanol.

As summarized in Figure 2.2, after binding of the proteins to the beads, the samples underwent an overnight enzymatic digestion with trypsin (1:50 w/w), followed by C18 matrix midi-column clean up and elution. The BioPure midi columns (Nest Group Inc.) were conditioned with 200 µL methanol, 200 µL 0.1% Formic Acid (FA), 60% Acetonitrile (ACN), and 200 µL 0.1% Trifluoroacetic Acid (TFA). Samples pH was adjusted to pH=3 – 4 using 10% TFA prior to loading the columns. Samples were sequentially eluted 3 times with 70 µL, 70 µL, and 50 µL 0.1% FA, 60% ACN. The eluate was collected into LoBind tubes and placed into a SpeedVac to remove the organic ACN. Lastly, the samples were re-suspended in 0.1% FA (ready for MS injection).

2.4 Protein detection and quantification using LC/MS

The total protein concentration for each of the purified samples was determined using Nanodrop. Mass spectrometric analyses were performed on Q Exactive HF Orbitrap mass spectrometer coupled with an Easy-nLC liquid chromatography system (Thermo Scientific). This intricate system detects the ionized peptides at

the specific time that they elute out of the LC column (retention time). This time is calculated as the period between injection to detection.

In the MS sample chamber (96-well plate), the samples were completely randomized across all conditions and biological replicates. A total of 1 µg peptide per sample was injected for analysis. The peptides were separated over a three-hour gradient consisting of Buffer A (0.1% FA in 2% acetonitrile) and 2%-80% Buffer B (0.1% FA in 95% acetonitrile) at a set flow rate of 300 nL/min. The computerized MS setup produces a pattern spectrum of masses based on the abundance and structure of the detected ionized molecules.

The raw mass-to-charge (M/Z) data acquired from the Q Exactive HF were searched with MaxQuant (MQ)-version 2.0.0.0 (Max Planck Institute, Germany), and Proteome discoverer software (Thermo Fisher Scientific, CA, USA), using the built-in search engine, and embedded standard DDA settings. The false discovery rate for protein and peptide searches was set at 1%. Digestion setting were set to trypsin. Oxidation (M) and Acetyl (N-term) were set as dynamic modifications. Carbamidomethyl (C) was set as fixed modification, and Phosphorylation (STY) was set as a variable modification. For the main comparative protein search, the human proteome database (FASTA) was downloaded from Uniprot (2022_06; 20,365 sequences) and used as the reference file. Common contaminants were embedded from MaxQuant. Peptide sequences that were labeled as “Potential contaminant/REV” were excluded from the final analysis.

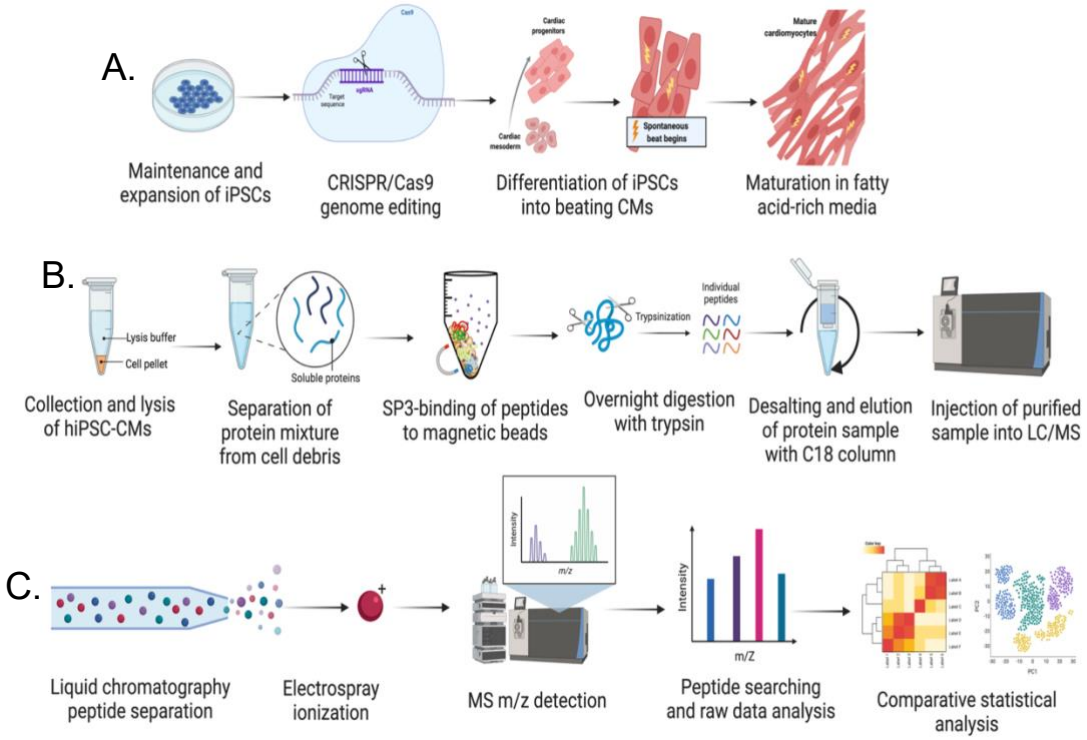

Figure 2.2: The workflow used for efficient hiPSC-CMs protein isolation and characterization. A) establishing and expanding the hiPSC-CM cell lines (control and variants). B) purification of the cytosolic proteins from the prepared cell pellet using high resolution SP3 protocol flowed by tryptic digestion. C) separation of the peptide mixture by LC column followed by electrospray ionization before entering the mass detector. MS spectrum raw data is then acquired for the eluting peptides at a given time (retention time). *Created with BioRender.com.*

2.5 Immunocytochemistry

To characterize the hiPSC-CMs 2D monolayers, confocal imaging was used to examine the viability, purity, and overall morphology of the CMs. At day 35, newly differentiated hiPSC-CMs from all three cell lines were replated onto 12 mm glass coverslips coated with Geltrex in a 24-well plate. ROCK inhibitor was added to the media and the CMs were left to attach for 5 days. The seeded cells were stained with 500 nM of MitoTracker DeepRed FM (Thermo Fisher), then fixed on the coverslips using 3% Paraformaldehyde (PFA).

The cells were then permeabilized by washing with PBS-Triton X. Troponin T primary antibody (Thermo Fisher) was used as a cardiac-specific marker to label the sarcomeric component of the CMs. It was added in 1:100 dilution factor[113] followed by 4 ^{o}C incubation overnight. Alexa Fluor488 goat anti-mouse (Thermo Fisher) was used as the secondary antibody. Lastly, the CMs were incubated with DAPI solution (1:50,000), followed by serial ethanol-based dehydration. The coverslips were mounted on glass slides using DEPEX mounting medium (Electron Microscopy Sciences) and stored to dry overnight. Fluorescent imaging was performed the following day on the mounted slides using the Leica Confocal SP8 system (BCCHR). Quantification and post-analysis of the images was done using the java-based ImageJ software (National Institute of Health, Version 1.1).

2.6 Statistical analysis

The generated raw data were filtered and transformed to $\log_2$ scale. This was followed by quantile normalization for all samples. The proteomic profile for both HCM variants was subject to comparative analysis against the isogenic control cell line. The protein groups file obtained from the DDA MQ search was used for all of the quantitative statistical analysis based on the detected intensities. All plots, visualizations and statistical comparisons were done using R (version 4.1.3) and Perseus (version 1.6.15.0) softwares based on the Student t-test of significance one-way ANOVA, and, when needed, post-hoc analysis.

3 Chapter Three: Results

3.1 Characterization and image-based quantification of the hiPSC-CMs

To assess purity of the cardiomyocytes, at least 150 nuclei were counted in four different regions of interest (ROIs), and the % nuclei staining positive with cTnT was calculated, the colocalization java plugin was used to quantify the double positive cells (DAPI+/cTnT+) relative to cTnT negative cells (DAPI+/cTnT-)[114] (Figure 3.1A). The morphology and structure were also compared across all three cell types on the single cell level (Figure 3.1B).

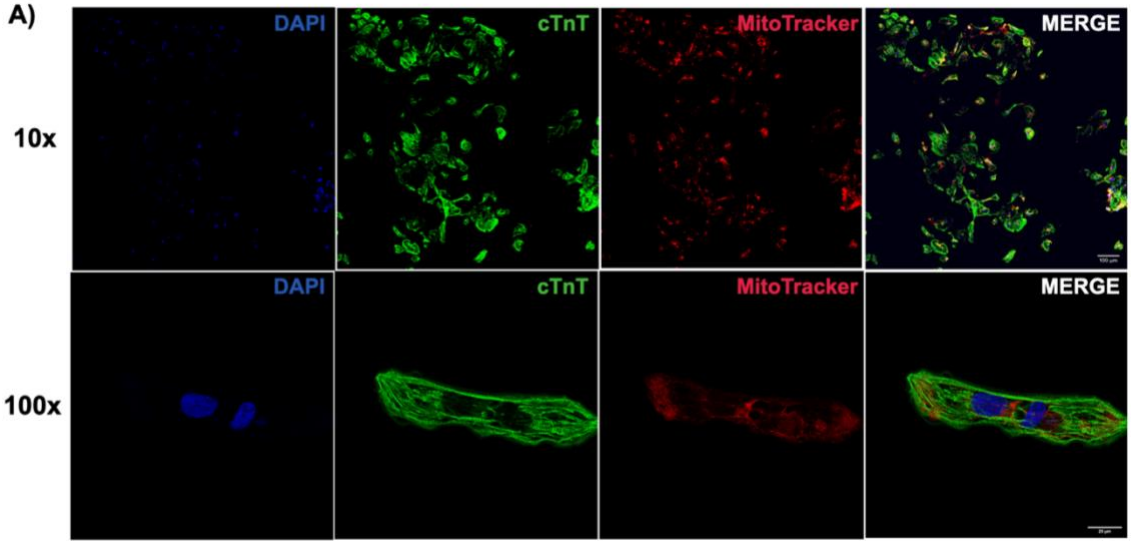

$$\%\ \text{CMs} = \frac{\#\text{DAPI+ \& cTnT+ cells}}{\#\text{DAPI+ \& cTnT}-\text{cells}} = \frac{141}{150} = \mathbf{94\%}$$

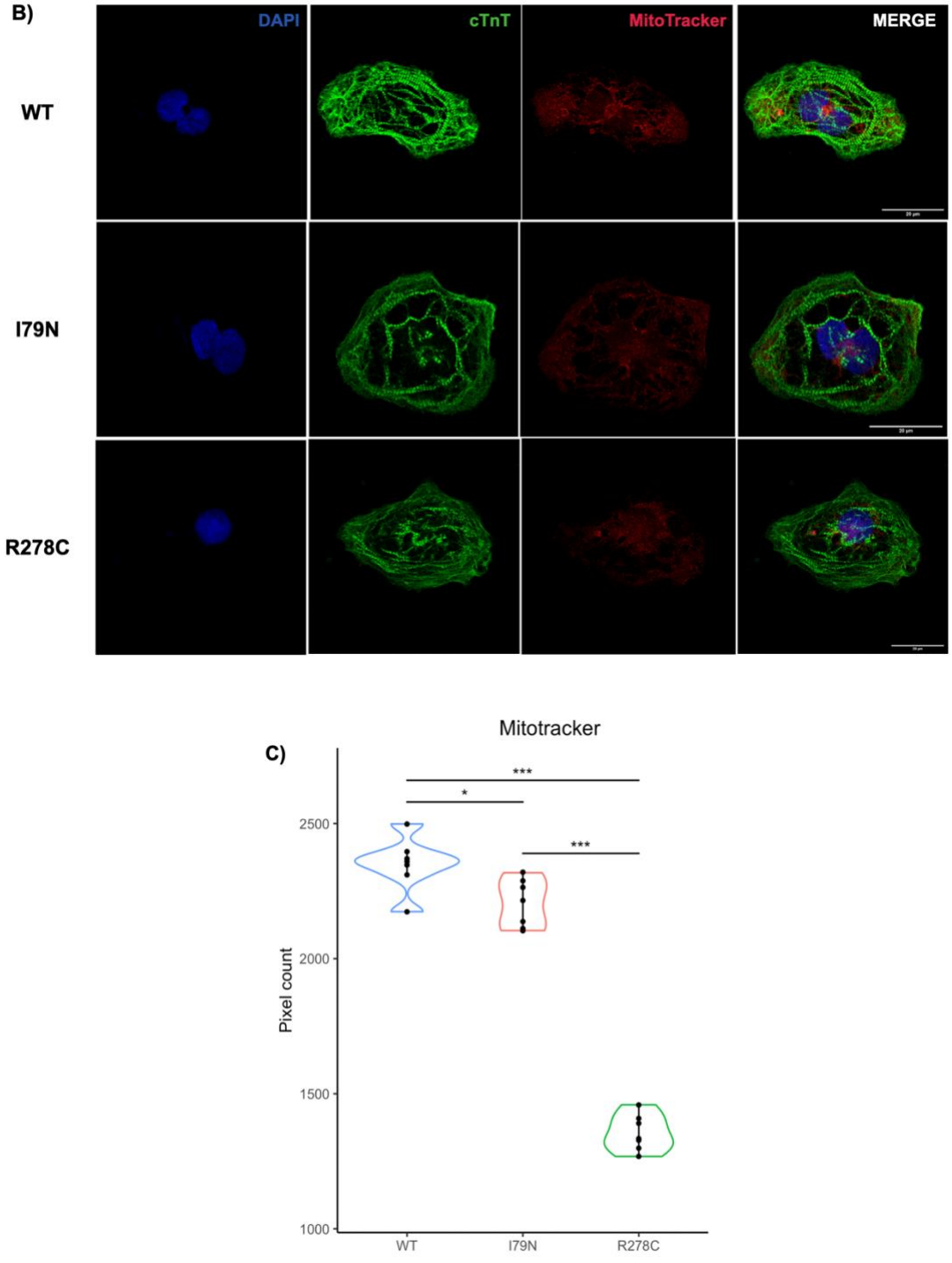

Figure 3.1: Immunocytochemistry images of hiPSC-CMs at day 35 of differentiation. A) Representative region of interest (ROI) to assess the purity of the WT 2D monolayer, top images captured at 10x. Bottom images captured at 100x. B) Morphological and structural comparisons across the three cell types (WT, I79N, and R278C) at 100x magnification. C) Pixel count for quantification of the Mitotracker cellular content across the 3 cell types (n=7). The hiPSC-CMs were stained with the cardiac-specific marker, troponin T (cTnT-green), MitoTracker (red), and DAPI (blue).

3.2 Proteomic profile of I79N$^{+/-}$ and R278C$^{+/-}$ hiPSC-CMs

To quantify the proteomic changes occurring in the HCM cell lines, we used bottom-up mass spectrometry to characterize the purified tryptic peptides. The detected mass spectra were plotted as a base peak chromatogram (BPC), which reflects the intensity across the entire range of masses being detected in that scan. Each peak reflects one peptide group, and the height of the peak represents the relative intensity or abundance of that peptide. As depicted in figure 3.2, the BPC for a representative sample (isogenic control), shows distinct peaks with the highest abundance peak at 100%. The data were collected over 90 minutes of retention time. For the three cell lines, ~ 4,900 protein groups were detected across all replicas, with and without MM.

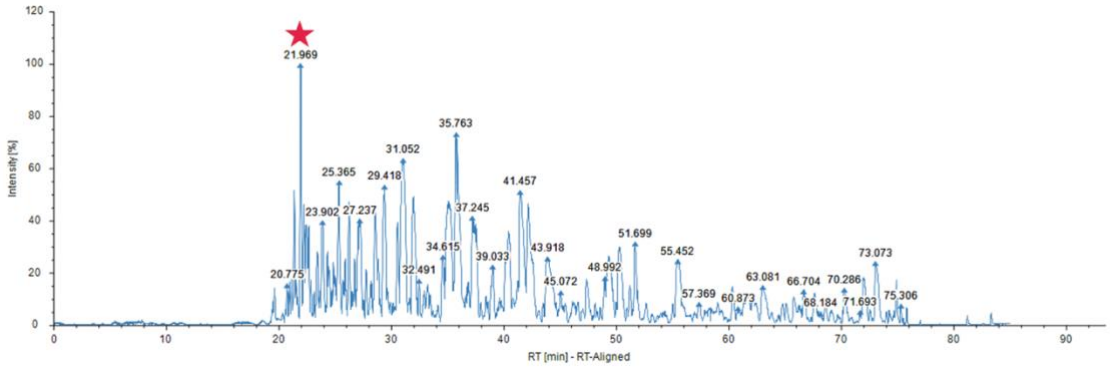

Figure 3.2: Example of the raw MS total isolated chromatogram (TIC). Each peak is represented as relative abundance to the peak with the highest intensity (labeled with red star).

3.2.1 WT (isogenic control cells) vs. I79N$^{+/-}$ *TNNT2* hiPSC-CMs

As stated in the first aim of this thesis, the main focus is to quantify the proteomic changes in a comparative manner to understand how the I79N$^{+/-}$ *TNNT2* variant is manifesting in the hiPSC-CMs relative to its isogenic control. To take a general look at the variation in proteins across the different cell lines, figure 3.3B shows a principal component analysis (PCA) that displays the overall changes occurring in each group and their respective replicates. A difference of 33.4% is recorded over the X-axis (PC1), and 19.7% over the Y-axis (PC2). A clear clustering pattern is

noted among samples of the same group. The intensity variation in the same protein can be visualized in a heat map based on Pearson correlation (figure 3.3A).

To explore the quantitative shifts amongst individual proteins, significance testing was used to determine which protein groups held the highest importance in HCM manifestation. The volcano plot in figure 3.4 shows a clear distinction between the WT and I79N$^{+/-}$ cells at a set false discovery rate (FDR) of 0.01.

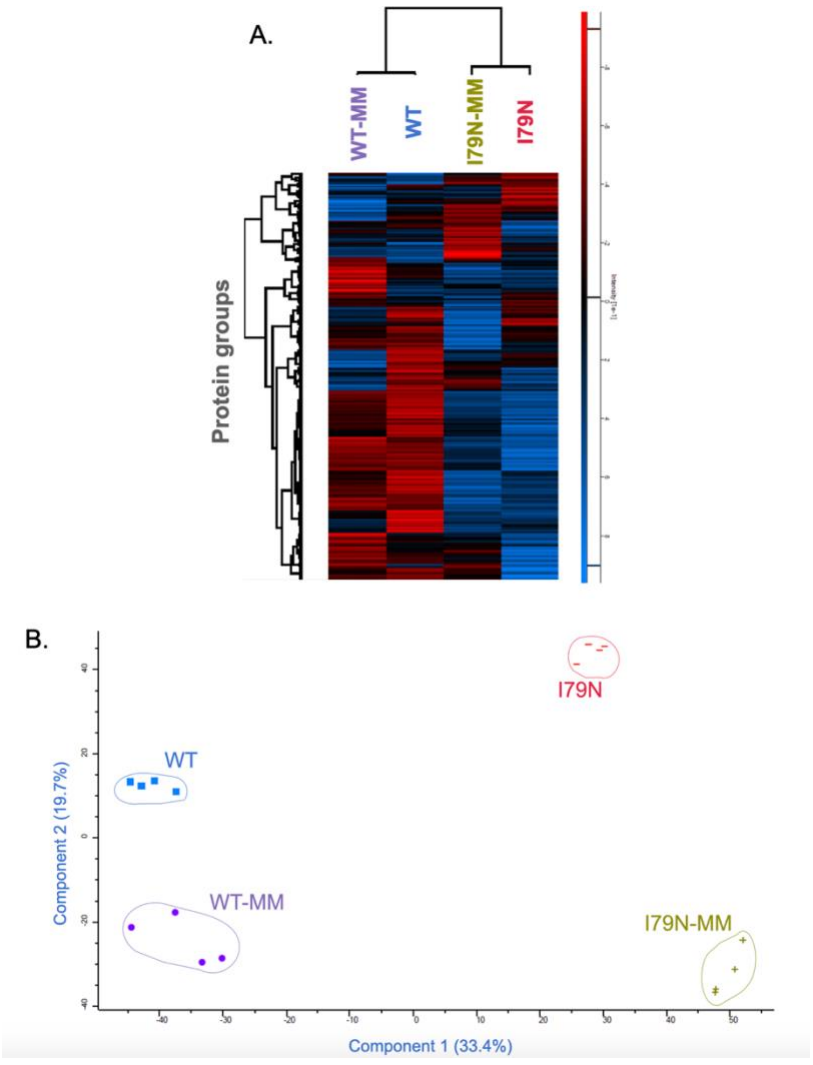

Figure 3.3: General comparison of the four cell lines (WT, WT_MM, I79N, I79N_MM). A) Hierarchal clustering of the groups based on the Pearson correlation. The heat map shows high intensity of proteins highlighted in blue, and a lower intensity of proteins highlighted in red. B) Principal component analysis of the 4 groups (n= 4 for each group). Clustering over the x-axis shows 33.4% variability (PC1), and 19.7% over the y-axis (PC2).

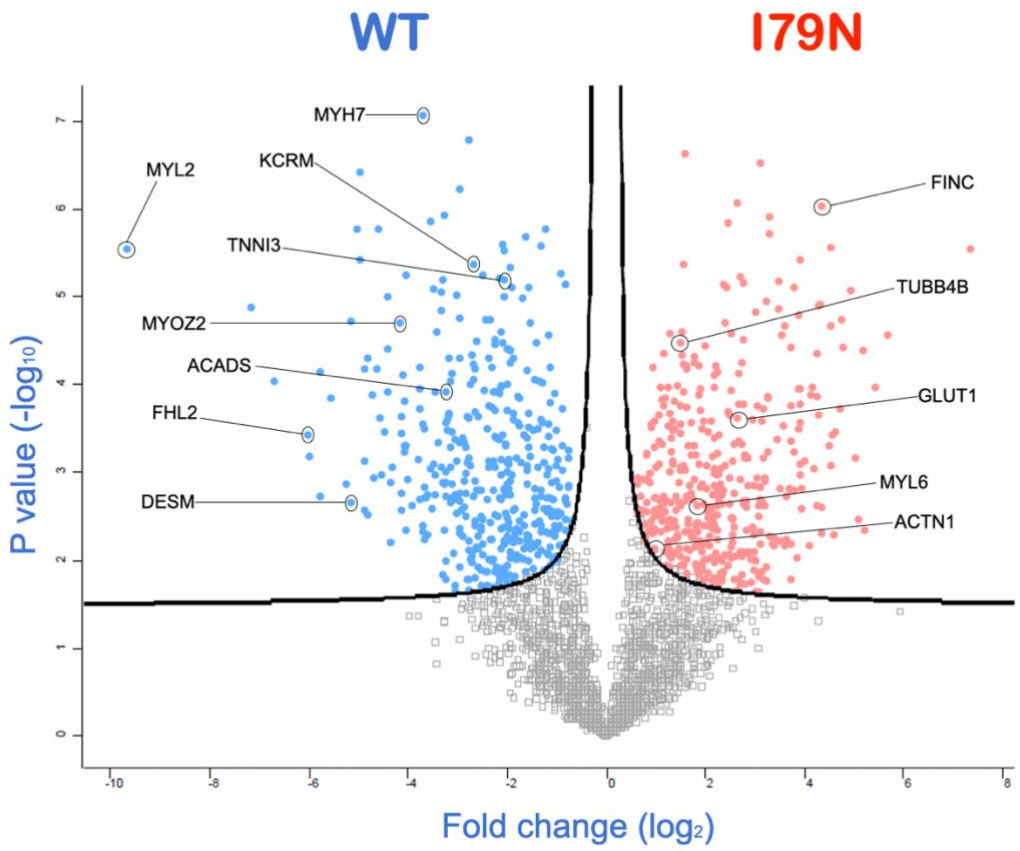

Figure 3.4: Fold change visualization of expression profile. Volcano plot comparison of WT vs. I79N on the protein level. The right side of the plot (red) reflects upregulated proteins in I79N hiPSC-CMs compared to WT, and the left side (blue) shows the proteins that were detected in higher quantity in the WT hiPSC-CMs relative to I79N hiPSC-CMs. FDR threshold was set to 0.01, and any data points beyond that were considered as statistically significant.

The proteins with the most relevance to the CM's contractility, structural integrity, organization, and metabolism, were selected for a closer comparative examination and significance testing. The first functional group shown in figure 3.5 comprises proteins involved in the organization of the sarcomere. A distinct difference in key sarcomeric proteins is seen between the WT and I79N$^{+/-}$ hiPSC-CMs. Figures 3.5-3.9 depict a panel of several functional groups, mainly proteins involved in: structural integrity of the Z-disc; stability of the microtubular network; remodelling response; metabolism; and energy production.

To understand the findings, a gene ontology (GO)- pathway enrichment analysis was conducted on the upregulated proteins detected in the I79N$^{+/-}$ hiPSC-CMs using Enrichr software[115]. Figure 3.20A summarizes the top search results in reference to KEGG, Elsevier, Jensen, and multiple other biological databases. Leading causes for the observed deviations include: primary familial HCM *(ClinVar, 2019)*, myogenesis *(MSigDB Hallmark, 2020)*, enhanced glucose import *(GO biological process, 2021)*, and increased glycolytic activity *(HumanCyc, 2016)*.

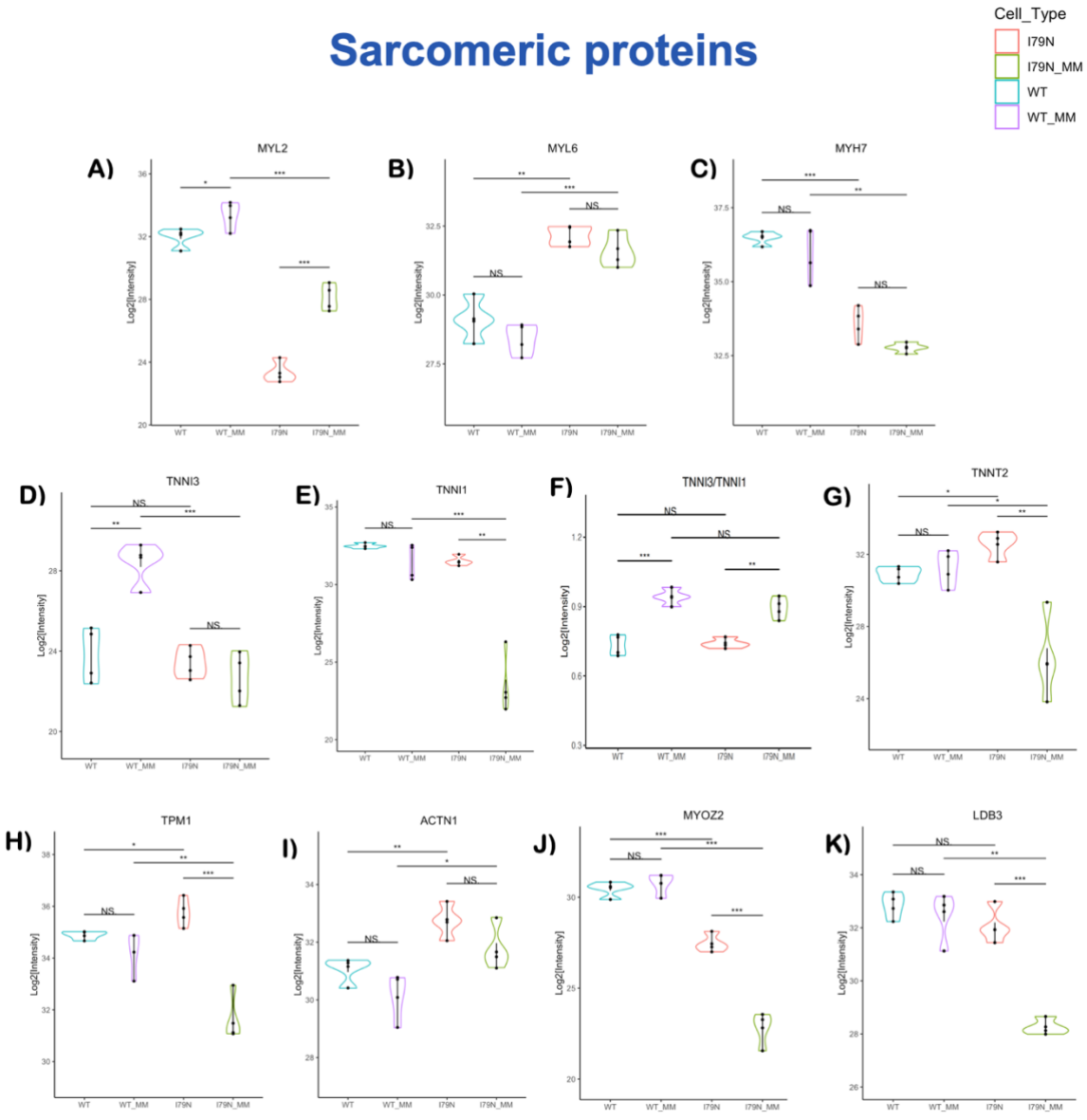

Figure 3.5: Protein level comparisons for the sarcomeric functional group in WT vs. I79N cells. Violin plot representations of individual proteins that exhibited significant changes across the four cell groups. Selected proteins include: A) MYL2 (myosin regulatory light chain-ventricular isoform), B) MYL6 (myosin regulatory light chain 6), C) MYH7 (beta myosin heavy chain), D) TNNI3 (Troponin I- cardiac isoform), E) TNNI1 (Troponin I-slow skeletal isoform), F) TNNI3/TNNI1 intensity ratio, G) TNNT2 (Troponin T), H) TPM1 (Tropomyosin), I) ACTN1 (alpha-actinin), J) MYOZ2 (Myozenin-2), and K) LDB3 (LIM-domain binding protein 3). *P-value<0.05, **P-value<0.01, ***P-value<0.001

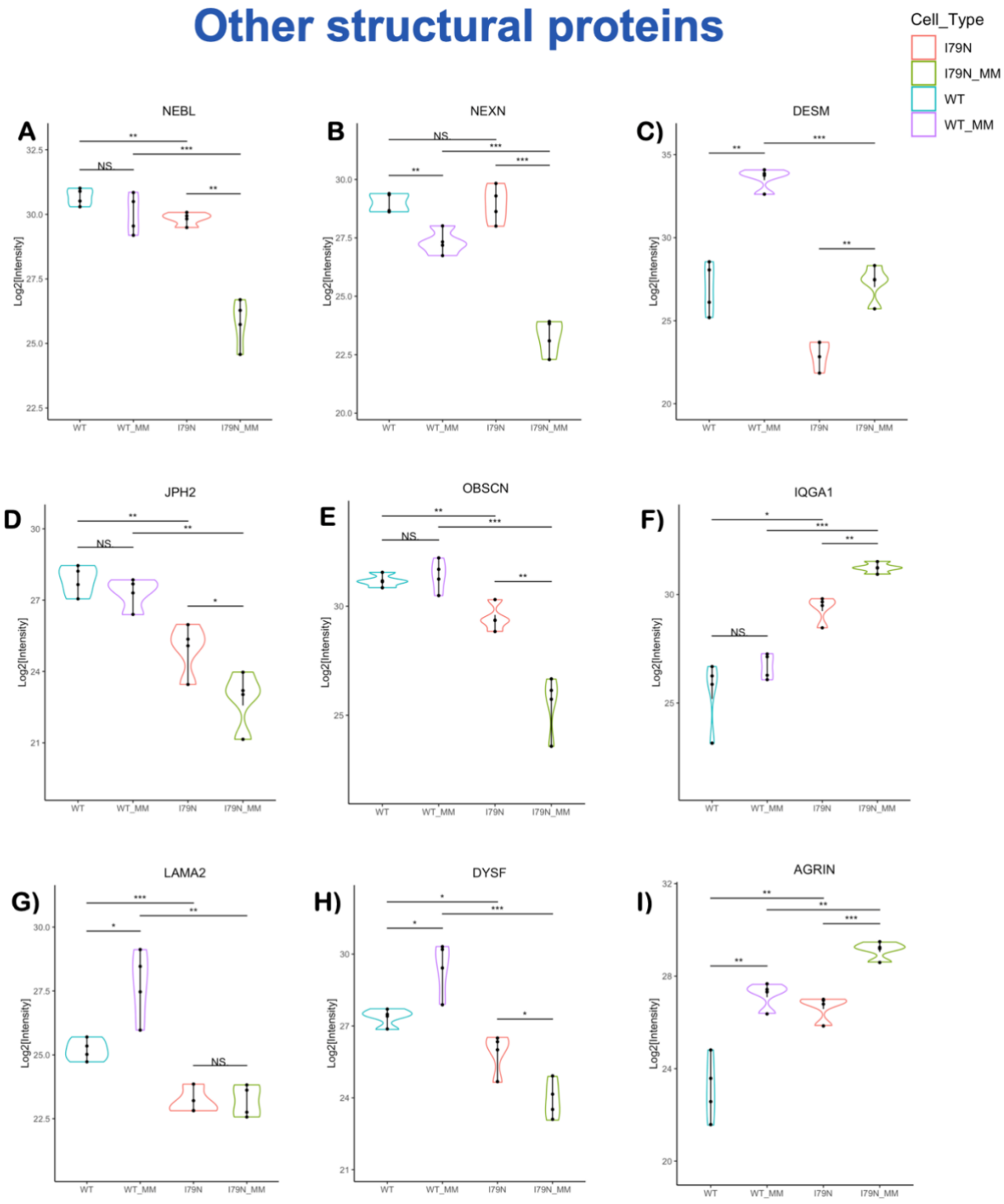

Figure 3.6: Protein level comparisons for the structural functional group in WT vs. I79N cells. Violin plot representations of individual proteins that exhibited significant changes across the four cell groups. Selected proteins include: A) NEBL (Nebulette), B) NEXN (Nexilin), C) DESM (Desmin), D) JPH2 (Junctophilin-2), E) OBSCN (Obscurin), F) IQGA1 (Ras GTPase-activating-like protein), G) LAMA2 (Laminin), H) DYSF (Dysferlin), and I) AGRIN (Agrin). *P-value<0.05, **P-value<0.01, ***P-value<0.001.

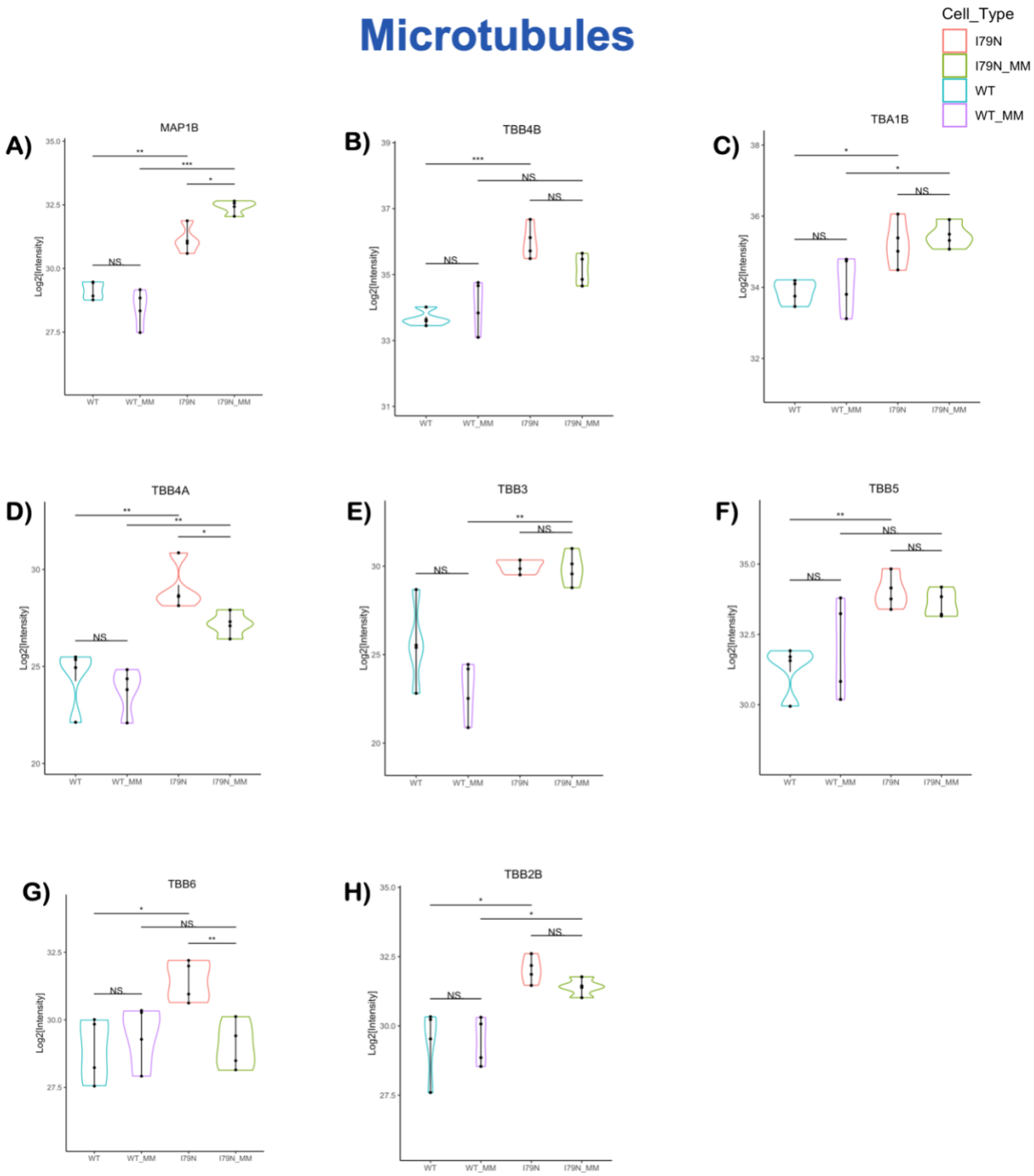

Figure 3.7: Protein level comparisons for the microtubular network functional group in WT vs. I79N cells. Violin plot representations of individual proteins that exhibited significant changes across the four cell groups. Selected proteins include: A) MAP1B (Microtubule-associated protein1B), B) TBB4B (Tubulin beta-4B chain), C) TBA1B (Tubulin alpha-1B chain), D) TBB4A (Tubulin beta-4A chain), E) TBB3 (Tubulin beta-3 chain), F) TBB5 (Tubulin beta-5 chain), G) TBB6 (Tubulin beta-6 chain), and H) TBB2B (Tubulin beta-2B chain). *P-value<0.05, **P-value<0.01, ***P-value<0.001.

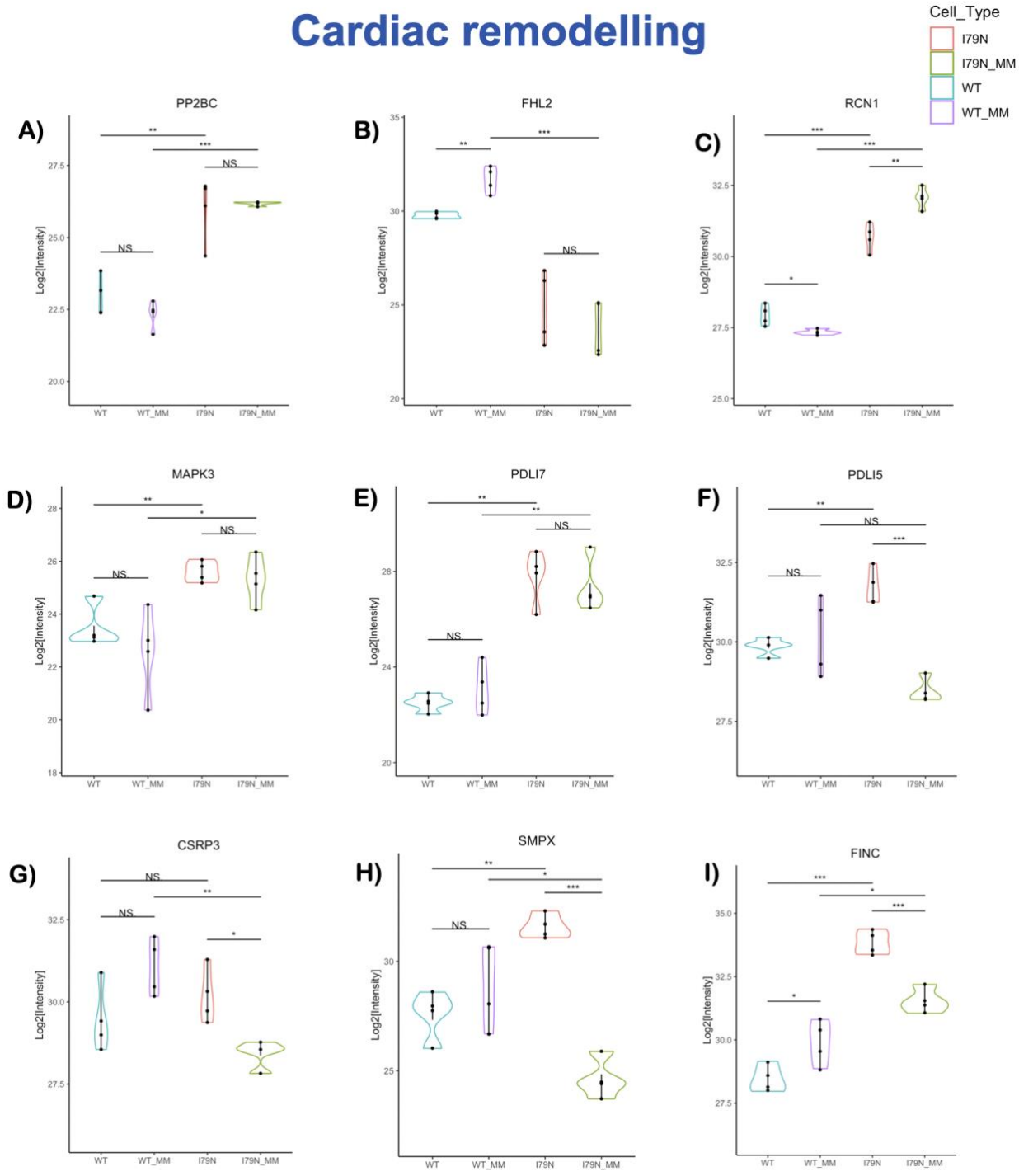

Figure 3.8: Protein level comparisons for the cardiac remodelling functional group in WT vs. I79N cells. Violin plot representations of individual proteins that exhibited significant changes across the four cell groups. Selected proteins include: A) PP2BC (Serine/threonine-protein phosphatase 2B), B) FHL2 (Four and a half LIM domains), C) RCN1 (Reticulocalbin), D) MAPK3 (MAP kinase-activated protein kinase 3), E) PDLI7 (PDZ and LIM domain protein 7), F) PDLI5 (PDZ and LIM domain protein 5), G) CSRP3 (Cysteine and glycine-rich protein 3), H) SMPX (Small muscular protein), and I) FINC (Fibronectin). *P-value<0.05, **P-value<0.01, ***P-value<0.001.

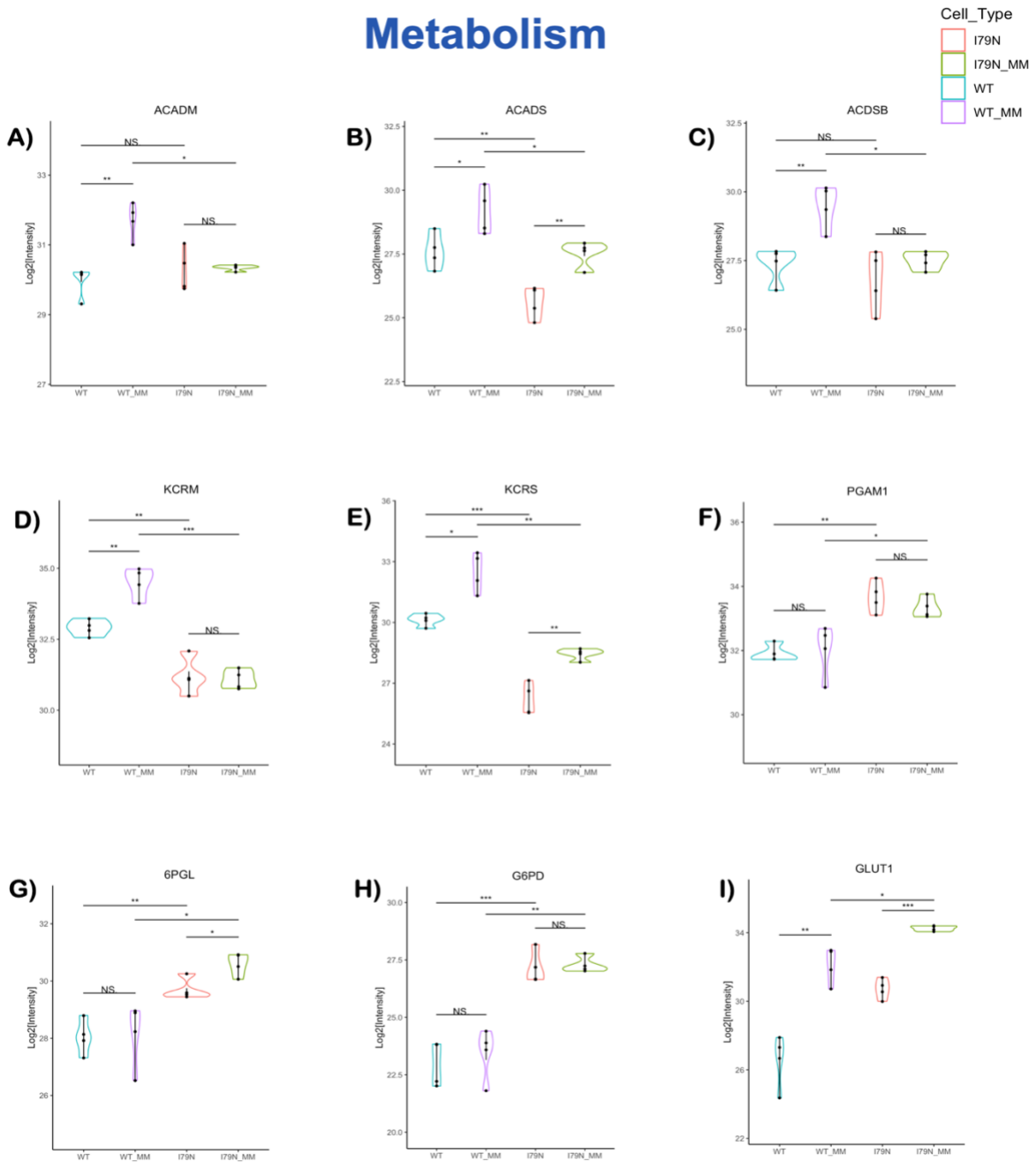

Figure 3.9: Protein level comparisons for the metabolism (fatty acid oxidation and glycolysis) production functional group in WT vs. I79N cells. Violin plot representations of individual proteins that exhibited significant changes across the four cell groups. Selected proteins include: A) ACADM (Medium-chain specific acyl-CoA dehydrogenase), B) ACADS (Short-chain specific acyl-CoA dehydrogenase), C) ACDSB (Short/branched chain specific acyl-CoA dehydrogenase), D) KCRM (Creatine kinase M-type), E) KCRS (Creatine kinase S-type), F) PGAM1 (Phosphoglycerate mutase 1), G) 6PGL (6-phosphogluconolactonase), H) G6PD (Glucose-6-phosphate 1-dehydrogenase), and I) GLUT1 (Facilitated glucose transporter member 1). *P-value<0.05, **P-value<0.01, ***P-value<0.001.

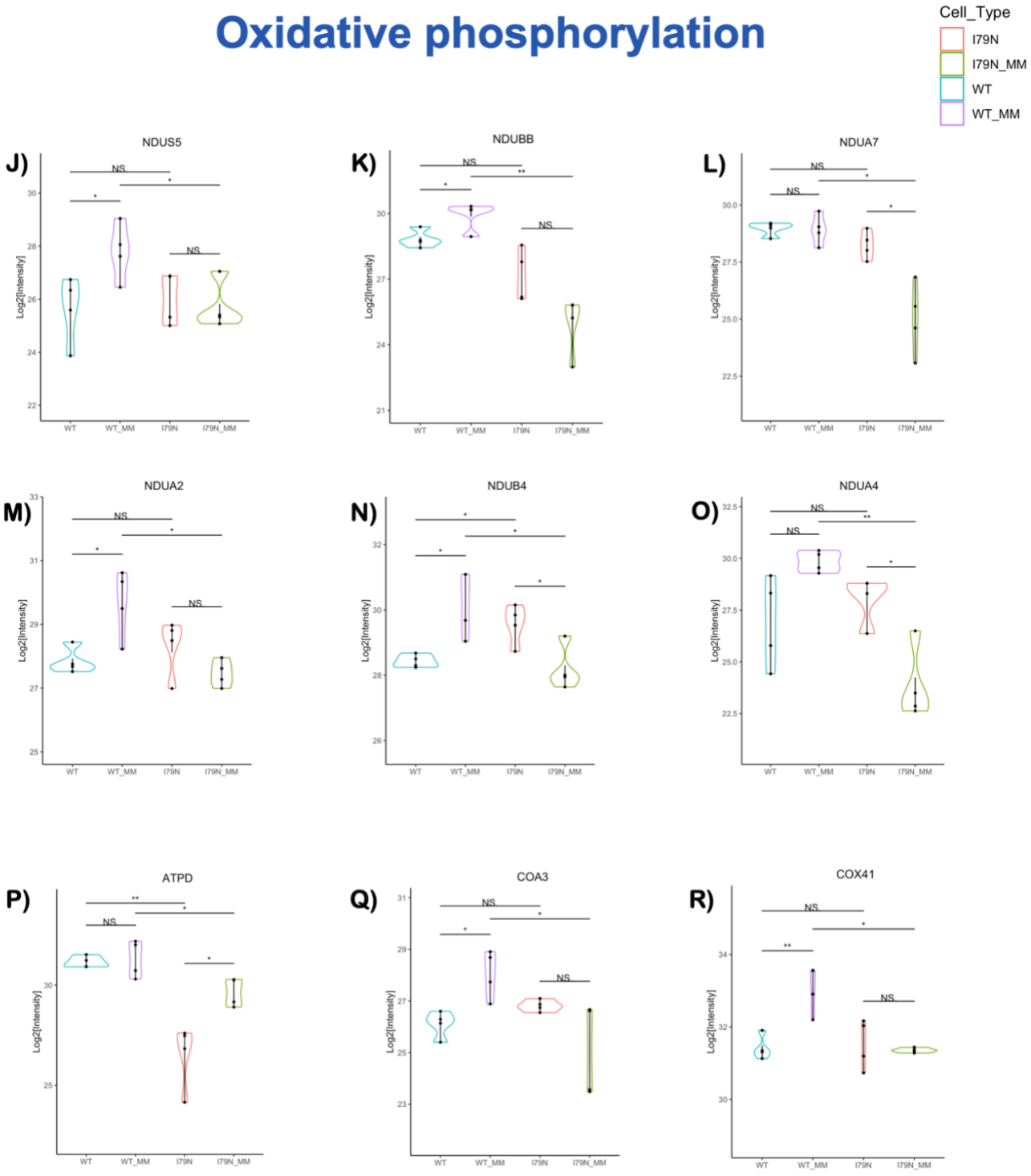

Figure 3.9: Protein level comparisons for the metabolism (fatty acid oxidation and glycolysis) production functional group in WT vs. I79N cells. Violin plot representations of individual proteins that exhibited significant changes across the four cell groups. Selected proteins include: J-O) Cytochrome c oxidase subunits-NDUs (NADH-Ubiquinone Oxidoreductase subunits), P) ATPD (ATP synthase), Q) COA3 (Cytochrome c oxidase assembly factor 3), and R) COX41 (Cytochrome c oxidase subunit 4). *P-value<0.05, **P-value<0.01, ***P-value<0.001.

3.2.2 WT (isogenic control cells) vs. R278C$^{+/-}$ *TNNT2* hiPSC-CMs

For the second part of the first aim of this thesis, the same methods were applied to quantify the proteomic changes in a comparative manner to understand how the R278C$^{+/-}$ *TNNT2* variant is manifested in the hiPSC-CMs relative to its isogenic control. To take a general look at the variation in proteins across the samples, figure 3.11B shows a principal component analysis (PCA) that displays the overall changes occurring in each group and their respective replicates. A difference of 23.3% is recorded over the X-axis (PC1), and 20.1% over the Y-axis (PC2). A clear clustering pattern is noted among samples of the same group. The intensity variation in the same protein can be visualized in a heat map based on the Pearson correlation coefficient (figure 3.11A).

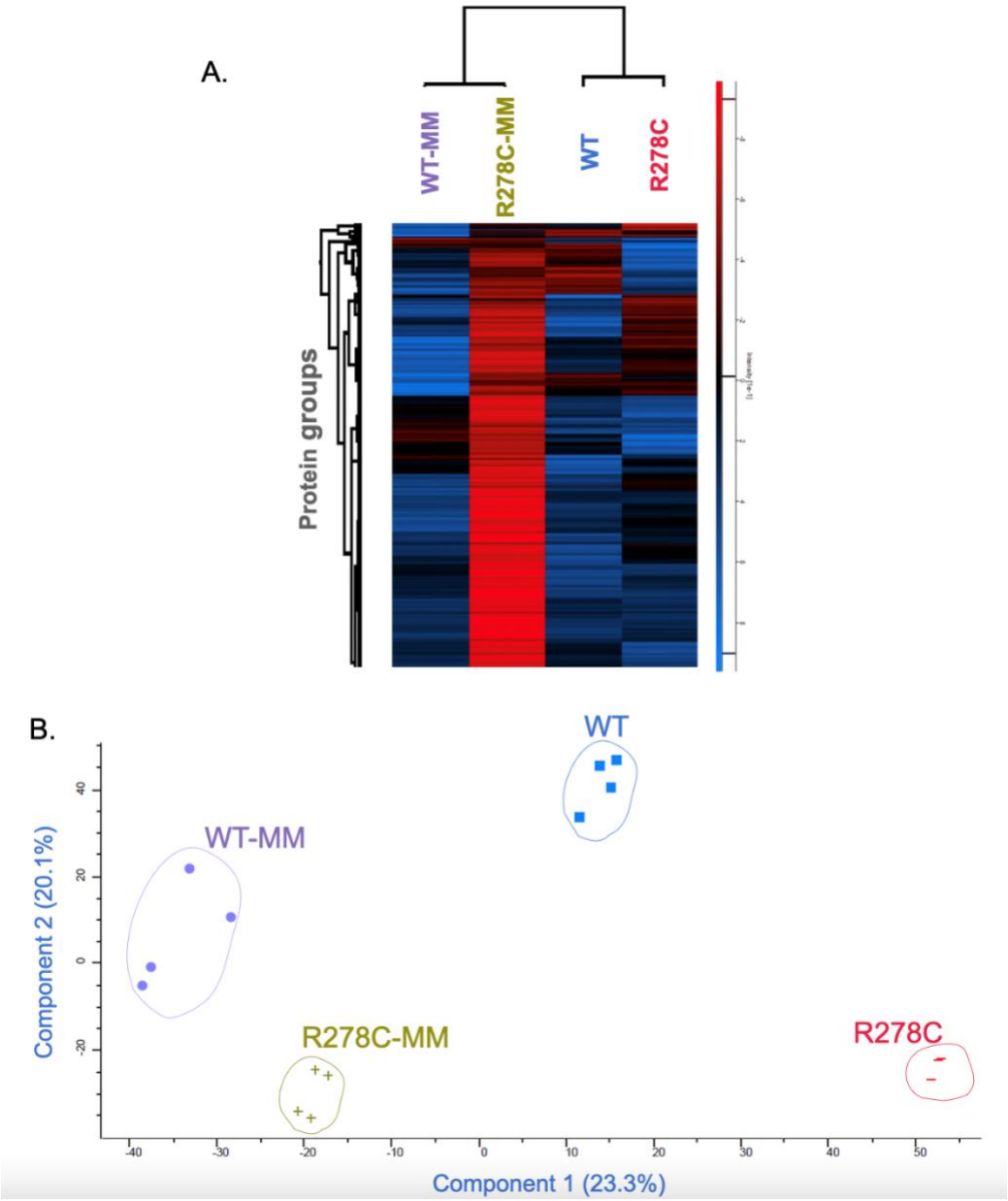

Figure 3.10: General comparison of the four cell lines (WT n=4, WT_MM n=4, R278C n=3, R278C_MM n=4). A) Hierarchal clustering of the groups based on Pearson's correlation. The heat map shows high intensity of proteins highlighted in blue, and a lower intensity of proteins highlighted in red. B) Principal component analysis of the four groups. Clustering over the x-axis shows 23.3% variability (PC1), and 20.1% over the y-axis (PC2).

To explore the quantitative shifts amongst individual proteins, significance testing was used to determine which protein groups held the highest importance in HCM manifestation. The volcano plot in figure 3.12 shows a clear distinction between the WT and R278C$^{+/-}$ hiPSC-CM cells at a set false discovery rate (FDR) of 0.01.

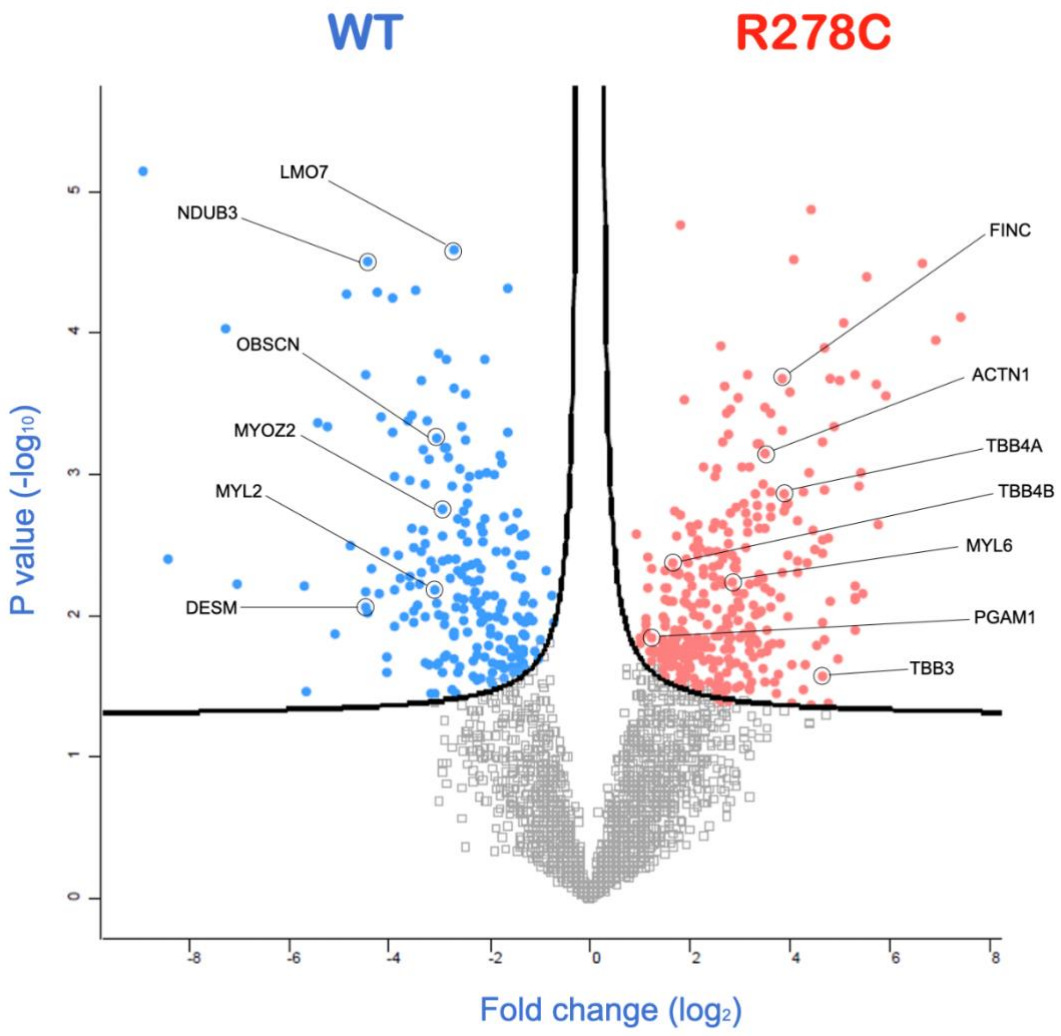

Figure 3.11: Fold change visualization of expression profile. Volcano plot comparison of WT vs. R278C on the protein level. Right side of the plot (red) reflects upregulated proteins in R278C hiPSC-CMs, and the left side (blue) shows the proteins that were detected in higher quantity in the WT hiPSC-CMs. FDR threshold was set to 0.01, and any data points beyond that were considered as statistically significant.

The proteins with the most relevance to the CM's contractility, structural integrity, organization, and metabolism, were selected for a closer comparative examination and significance testing. The first functional group shown in figure 3.13 is comprised of proteins involved in the organization of the sarcomere. A distinct difference in eleven key sarcomeric proteins is seen between the WT and R278C$^{+/-}$ hiPSC-CMs. Figures 3.13-3.17 depict a wide panel of several functional groups,

mainly proteins involved in; structural integrity of the Z-disc, stability of the microtubular network, remodelling response, metabolism, and energy production.

To understand the findings, a gene ontology (GO)- pathway enrichment analysis was conducted on the upregulated proteins detected in the R278C$^{+/-}$ hiPSC-CMs using Enrichr software[115]. Figure 3.20B summarizes the top search results reference to KEGG, Elsevier, Jensen, and multiple other biological databases. Leading causes for the observed deviations include: HCM *(KEGG, 2021)*, sarcomere disorganization *(Elsevier Pathway Collection, 2021)*, enhanced actin-myosin filament sliding *(GO biological process, 2021)*, and cardiomyopathy *(Jensen, 2020)*.

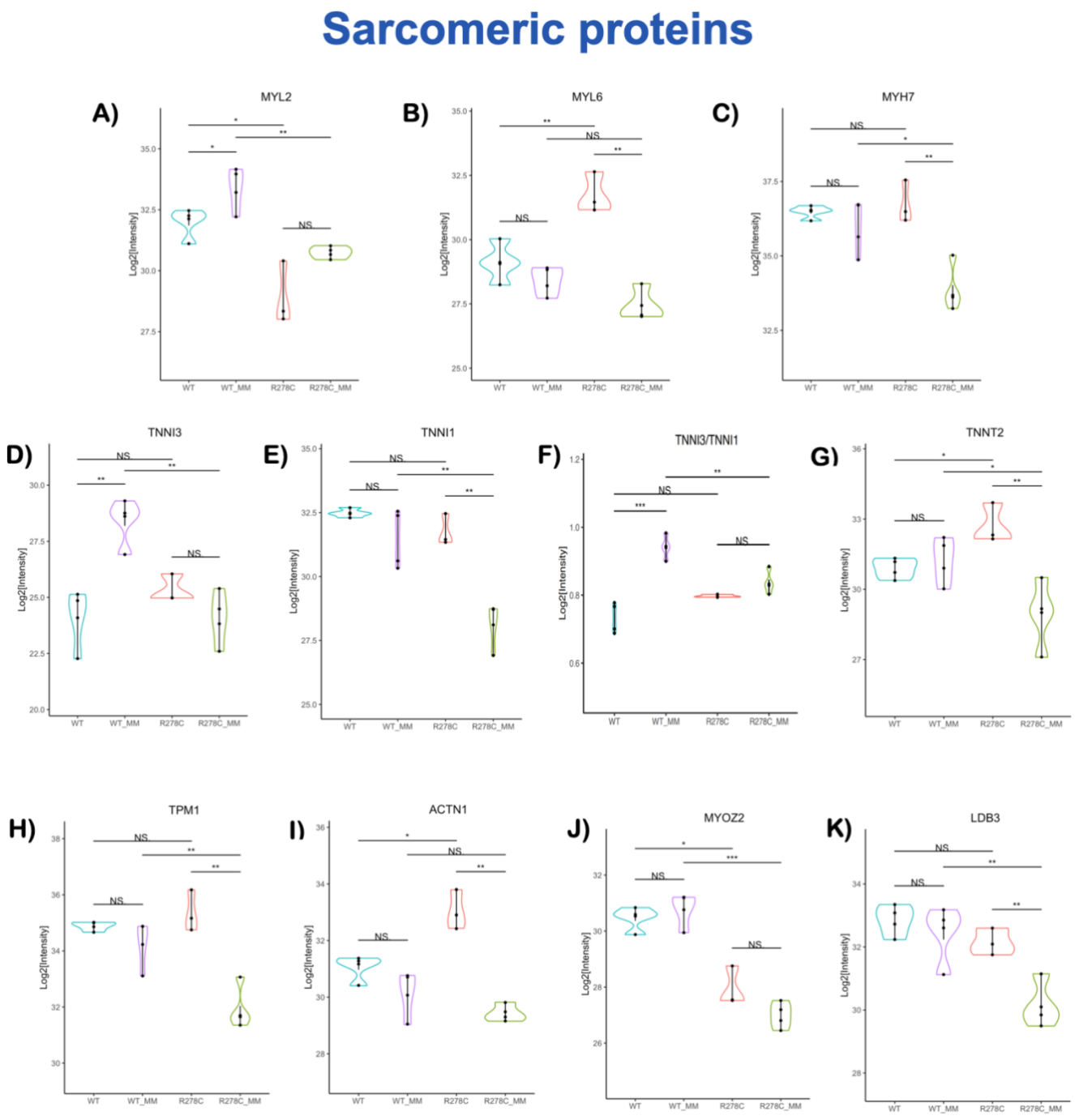

Figure 3.12: Protein level comparisons for the sarcomeric functional group in WT vs. R278C cells. Violin plot representations of individual proteins that exhibited significant changes across the four cell groups. Selected proteins include: A) MYL2 (myosin regulatory light chain-ventricular isoform), B) MYL6 (myosin regulatory light chain 6), C) MYH7 (beta myosin heavy chain), D) TNNI3 (Troponin I- cardiac isoform, E) TNNI1 (Troponin I-slow skeletal isoform), F) TNNI3/TNNI1 intensity ratio, G) TNNT2 (Troponin T), H) TPM1 (Tropomyosin), I) ACTN1 (alpha-actinin), J) MYOZ2 (Myozenin-2), and K) LDB3 (LIM-domain binding protein 3). *P-value<0.05, **P-value<0.01, ***P-value<0.001

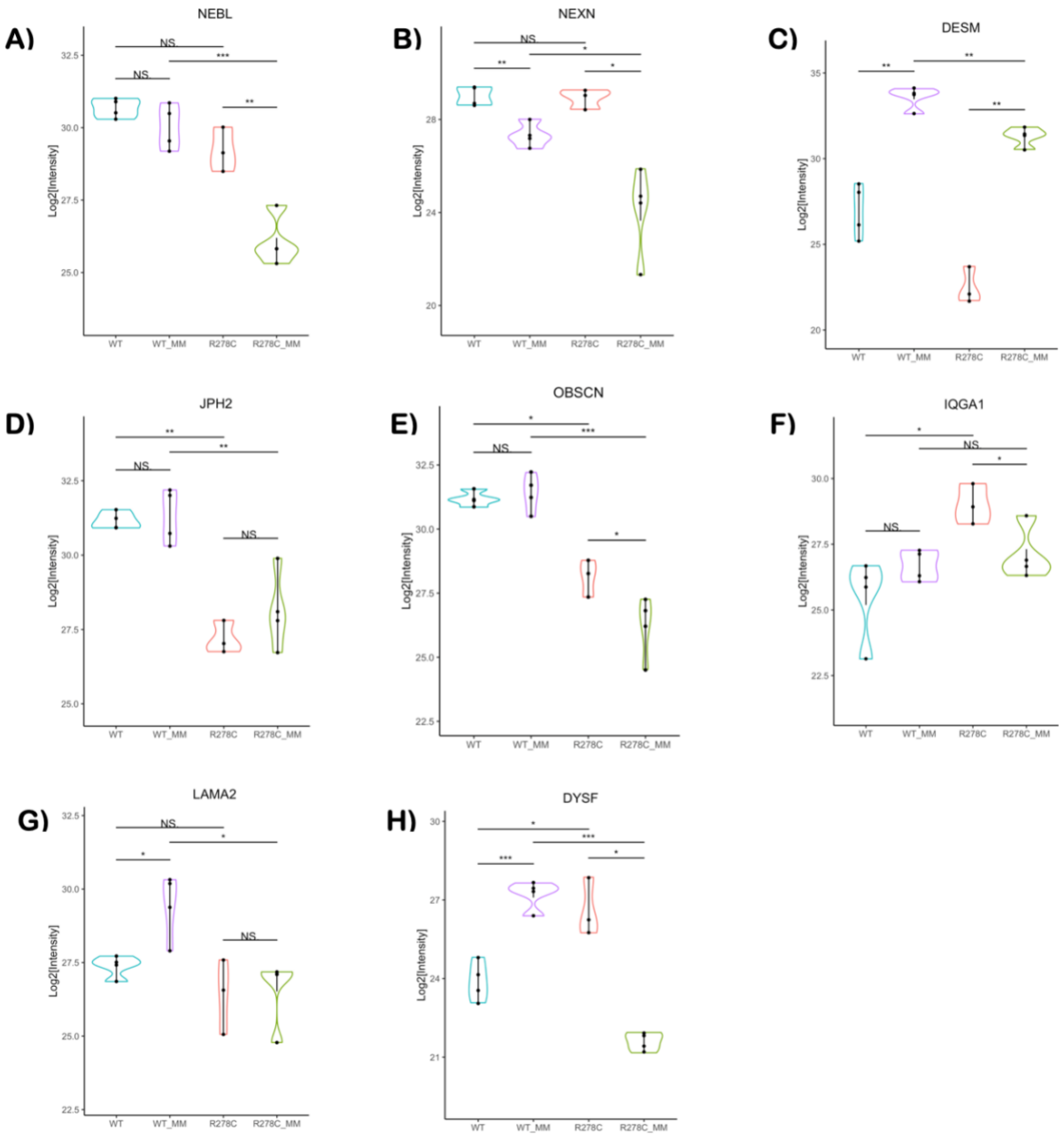

Figure 3.13: Protein level comparisons for the structural functional group in WT vs. R278C cells. Violin plot representations of individual proteins that exhibited significant changes across the four cell groups. Selected proteins include: A) NEBL (Nebulette), B) NEXN (Nexilin), C) DESM (Desmin), D) JPH2 (Junctophilin-2), E) OBSCN (Obscurin), F) IQGA1 (Ras GTPase-activating-like protein), G) LAMA2 (Laminin), and H) DYSF (Dysferlin). *P-value<0.05, **P-value<0.01, ***P-value<0.001.

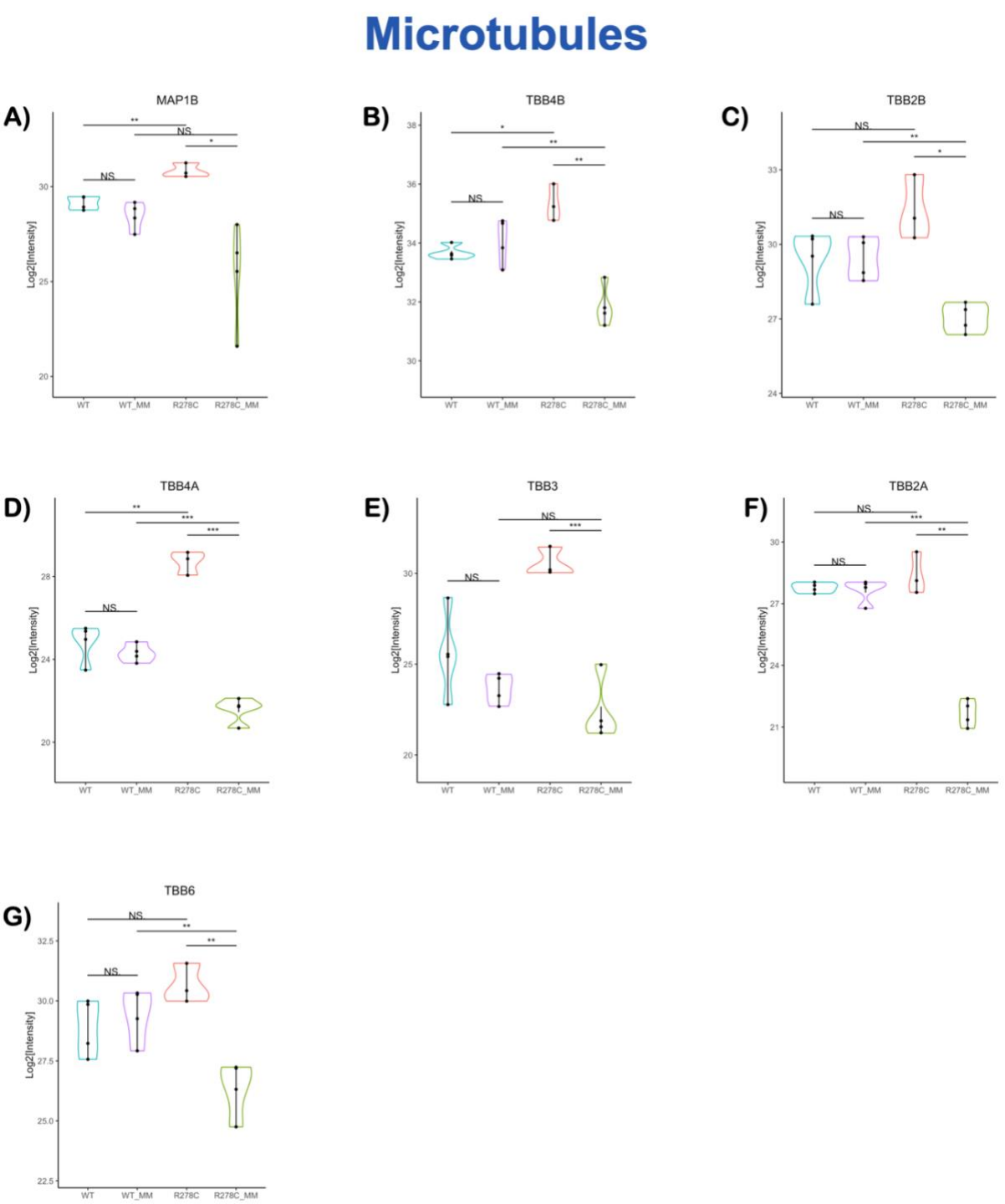

Figure 3.14: Protein level comparisons for the microtubular network functional group in WT vs. R278C cells. Violin plot representations of individual proteins that exhibited significant changes across the four cell groups. Selected proteins include: A) MAP1B (Microtubule-associated protein1B), B) TBB4B (Tubulin beta-4B chain), C) TBB2B (Tubulin beta-2B chain), D) TBB4A (Tubulin beta-4A chain), E) TBB3 (Tubulin beta-3 chain), F) TBB2A (Tubulin beta-2A chain), and G) TBB6 (Tubulin beta-6 chain). *P-value<0.05, **P-value<0.01, ***P-value<0.001.

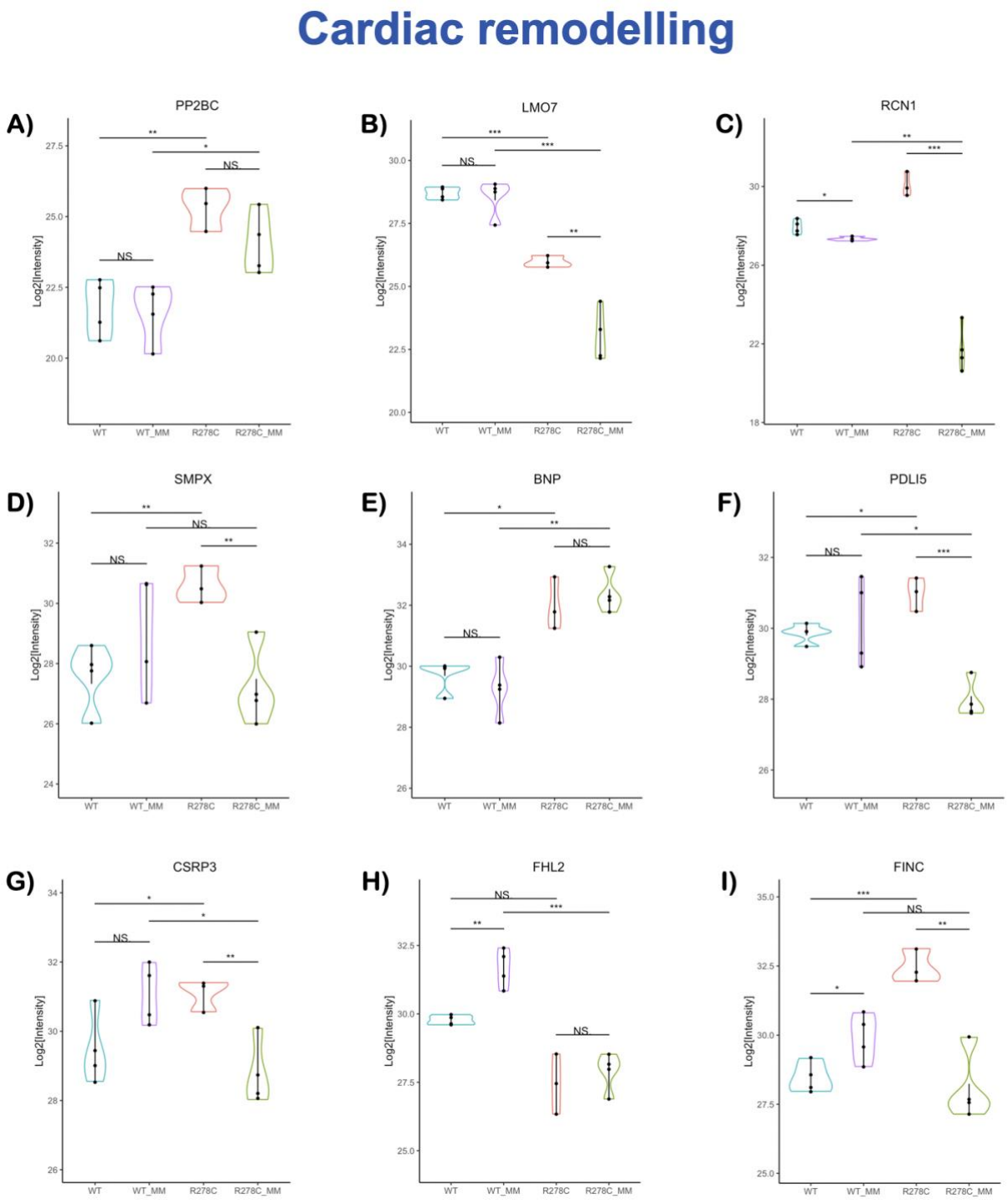

Figure 3.15: Protein level comparisons for the cardiac remodelling functional group in WT vs. R278C cells. Violin plot representations of individual proteins that exhibited significant changes across the four cell groups. Selected proteins include: A) PP2BC (Serine/threonine-protein phosphatase 2B), B) LMO7 (LIM domain only protein 7), C) RCN1 (Reticulocalbin), D) SMPX (Small muscular protein), E) BNP (Natriuretic peptide B), F) PDLI5 (PDZ and LIM domain protein 5), G) CSRP3 (Cysteine and glycine-rich protein 3), H) FHL2 (Four and a half LIM domains), and I) FINC (Fibronectin),. *P-value<0.05, **P-value<0.01, ***P-value<0.001.

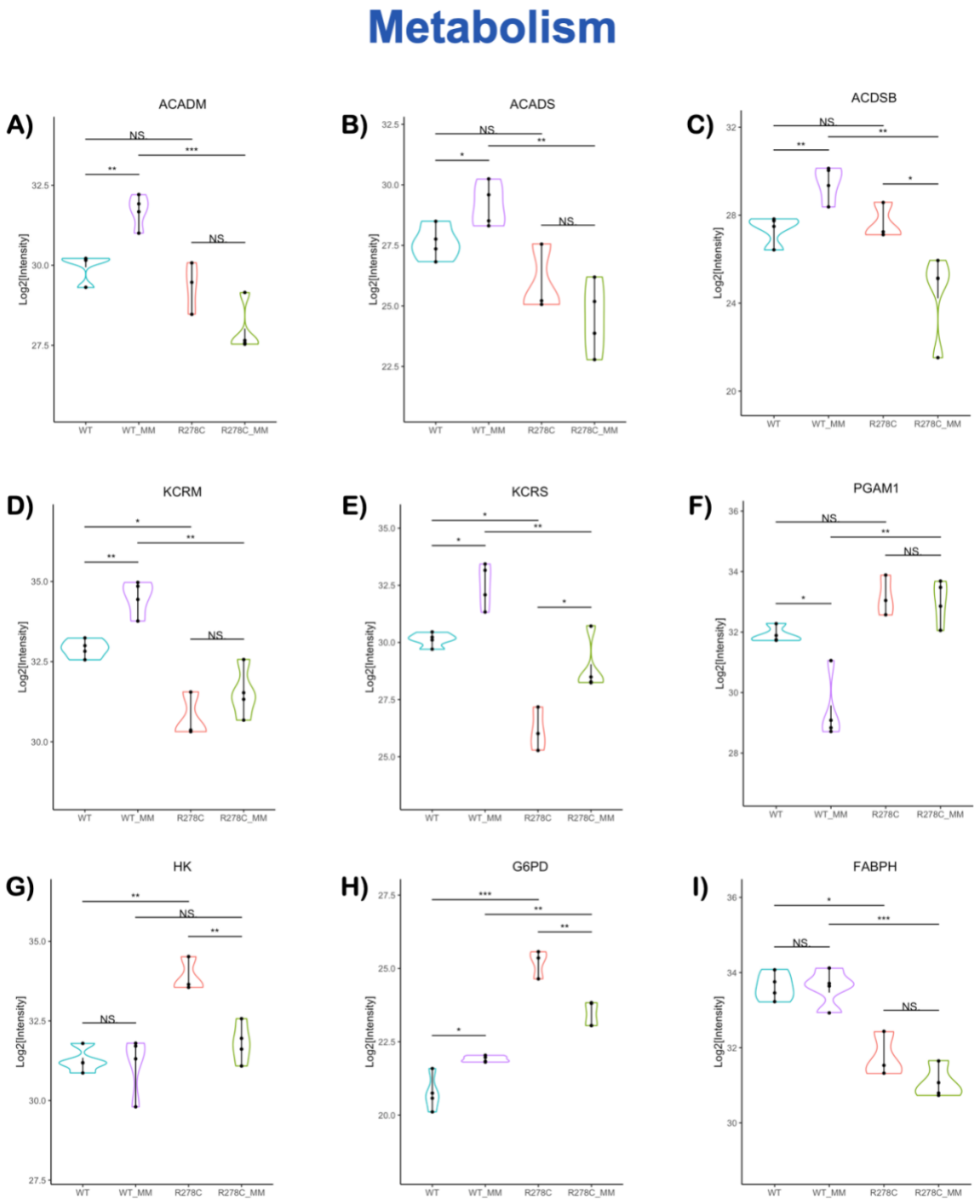

Figure 3.16A: Protein level comparisons for the metabolism (fatty acid oxidation and glycolysis) functional group in WT vs. R278C cells. Violin plot representations of individual proteins that exhibited significant changes across the four cell groups. Selected proteins include: A) ACADM (Medium-chain specific acyl-CoA dehydrogenase), B) ACADS (Short-chain specific acyl-CoA dehydrogenase), C) ACDSB (Short/branched chain specific acyl-CoA dehydrogenase), D) KCRM (Creatine kinase M-type), E) KCRS (Creatine kinase S-type), F) PGAM1 (Phosphoglycerate mutase 1), G) HK (Hexokinase), H) G6PD (Glucose-6-phosphate 1-dehydrogenase), and I) FABPH (Fatty acid-binding protein, heart). *P-value<0.05, **P-value<0.01, ***P-value<0.001.

Oxidative phosphorylation

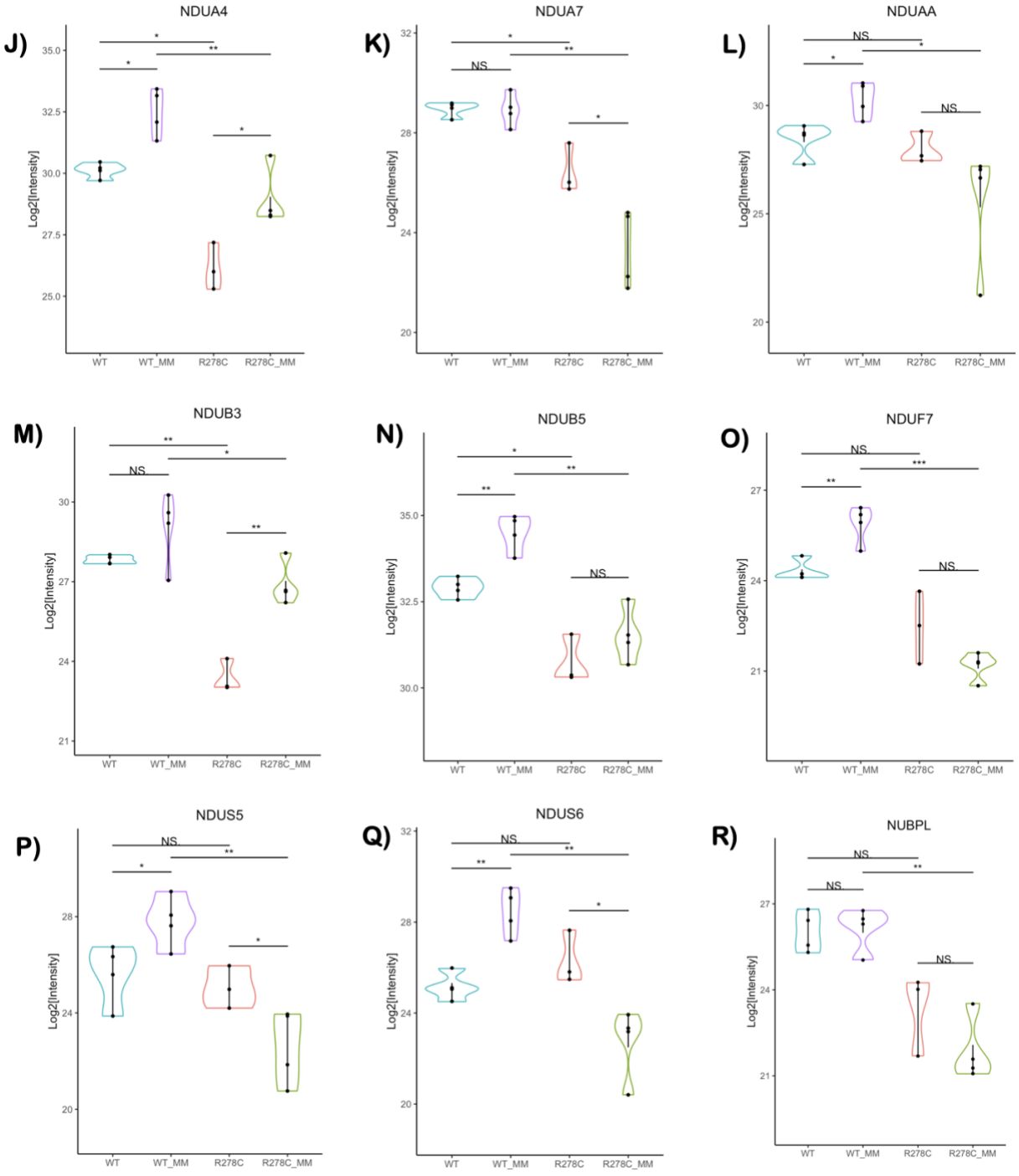

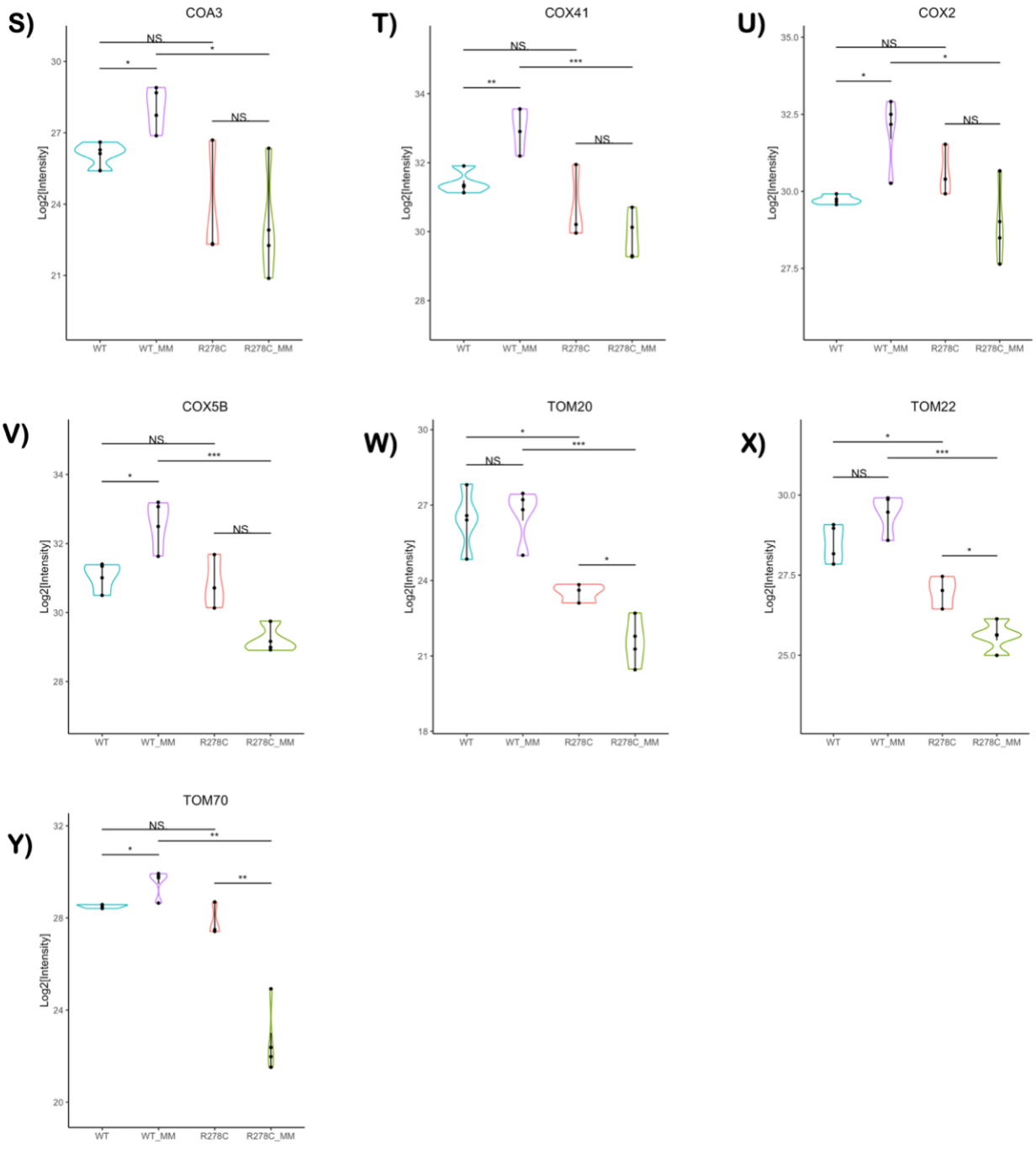

Figure 3.17B: Protein level comparisons for the metabolic/energy production functional group in WT vs. R278C cells. Violin plot representations of individual proteins that exhibited significant changes across the four cell groups. Selected proteins include: J-R) Cytochrome c oxidase subunits-NDUs (NADH-Ubiquinone Oxidoreductase subunits), S) COA3 (Cytochrome c oxidase assembly factor 3), T) COX41 (Cytochrome c oxidase subunit 4), U) COX2 (Cytochrome c oxidase subunit 2), V) COX5B (Cytochrome c oxidase subunit 5B, W) TOM20 (Mitochondrial import receptor subunit TOM20), X) TOM22 (Mitochondrial import receptor subunit TOM22), and Y) TOM70 (Mitochondrial import receptor subunit TOM70). *P-value<0.05, **P-value<0.01, ***P-value<0.001.

3.2.3 I79N$^{+/-}$ vs. R278C$^{+/-}$ *TNNT2* hiPSC-CMs

As mentioned in section 1.4, the phenotypic outcome of an HCM-causing variant is determined, at least in part, by the location of the molecular insult. Therefore, despite the clear overlap in key features, it is hypothesized that some variation will still rise between the I79N$^{+/-}$ and R278C$^{+/-}$ cells, even though both mutations are in the same gene *TNNT2*. As presented is figure 3.19, a prominent difference is noted between the two variants. The clustering behaviour (figure 3.19A) reflects an overall difference in protein expression profile, and the volcano plot (figure 3.19B) further distinguishes the manifestation mechanisms between the I79N$^{+/-}$ and R278C$^{+/-}$ cells.

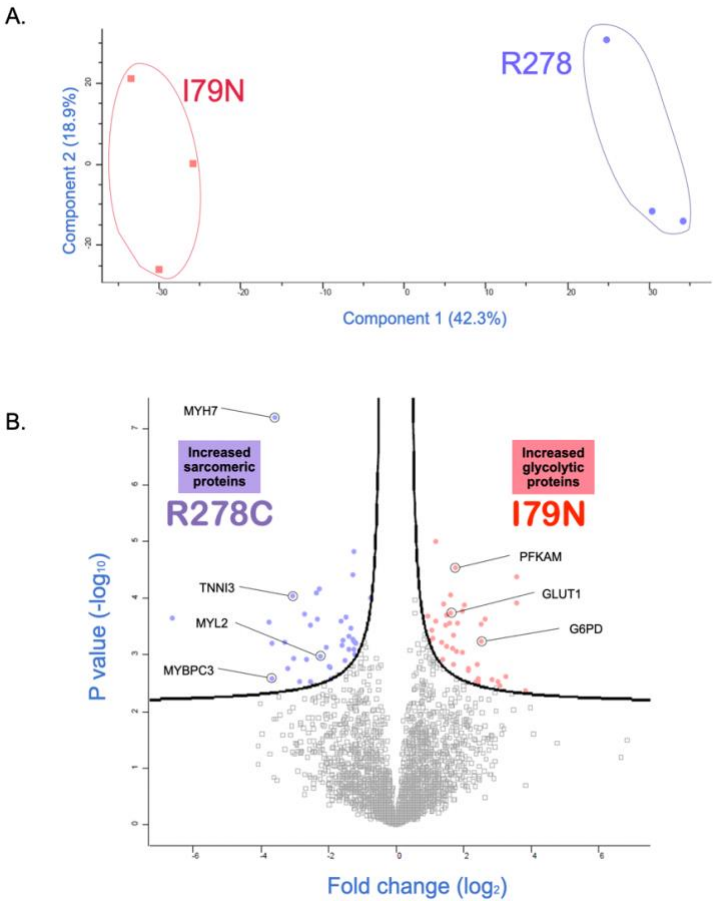

Figure 3.18: General comparison of the two HCM-causing variants (I79N and R278C). A) Principal component analysis of the two groups (n=3 for each cell line). Clustering over the x-axis shows 42.3% variability (PC1), and 18.9% over the y-axis (PC2). B) Fold change visualization of expression profile. Volcano plot comparison of I79N vs. R278C on the protein level. Right side of the plot (red) reflects upregulated proteins in I79N hiPSC-CMs, and the left side (purple) shows the

proteins that were detected in higher quantity in the I79N hiPSC-CMs. FDR threshold was set to 0.01, and any data points beyond that were considered as statistically significant.

Figure 3.19: Gene ontology (GO) and pathway enrichment analysis for the over-expressed proteins in each variant cell line. The most significantly- upregulated proteins in the A) I79N CMs (212 protein groups), and B) R278C CMs (198 protein groups), were selected for GO analysis. The top relevant cross searches are displayed as bar-plots reflecting the magnitude of association to each ontology.

3.3 Post-translational modifications (PTMs) related to HCM progression in I79N$^{+/-}$ and R278C$^{+/-}$ hiPSC-CMs

As described in section 1.5, one of the main mechanisms involved in HCM manifestation, is through disrupting the regulation of certain signaling pathways by altering the phosphorylation profile. Depending on the protein and its function, the phosphorylation could be stimulatory or inhibitory. Furthermore, two different phosphorylation sites on the same protein could have opposite regulatory effects[116].

3.3.1 Activation of cardiac remodelling signalling via phosphorylation and dephosphorylation of key proteins

The phospho-peptides detected by MS were analyzed in each variant and compared to the isogenic control samples. Across all samples, 895 phosphorylation sites were detected. After data filtering at a set FDR value of 0.05, 167 sites were selected for further analysis. The differential phosphosite quantitative profile of 6 different proteins was plotted against the fold change in phosphorylation relative to the WT samples. The ratio was calculated based on the following equation:

$$\frac{[\textbf{Mean of total protein intensity}]\textbf{WT} - [\textbf{mean of phosphosite intensity}]\textbf{WT}}{[\textbf{Mean of total protein intensity}]\textbf{MT} - [\textbf{mean of phosphosite intensity}]\textbf{MT}}$$

As shown in figure 3.21, the variants exhibit a significant increase in phosphorylation of 3 phosphosites corresponding to *MYBPC3-Ser284*, *MYL2-Ser15*, and *HSPB1-Ser15*. While a relative decrease in phosphorylation is detected in *NEXN-Ser80*, *NFATC2-Ser179*, and *CTNA3- Ser637*.

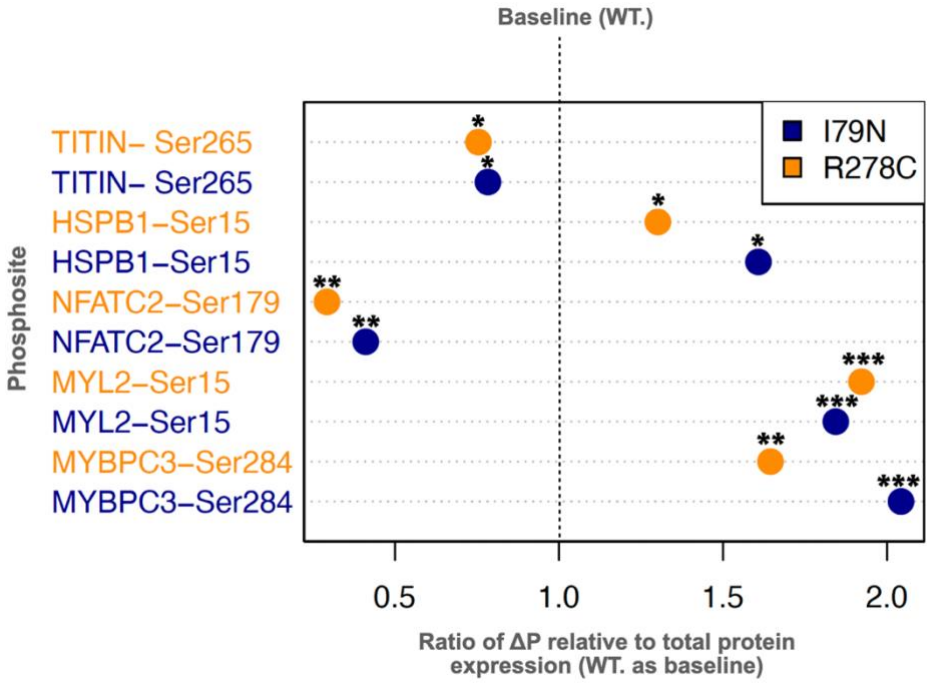

Figure 3.20: Comparative overview of the phosphorylation profile of 6 selected phosphosites in I79N (navy) vs. R278C (orange) hiPSC-CMs. Dot plot representation of the phosphorylation change relative to the total protein expression. WT phosphorylation was used as the baseline to study the trends in the described phosphosites.

4 Chapter Four: Discussion

4.1 Characterization of the hiPSC-CMs

To characterize the hiPSC-CM culture, immunocytochemistry was performed on newly differentiated cardiomyocytes (day 35 post differentiation). As shown in figure 3.1A, the purity was assessed using a regular colocalization counting method, in which double positive cells (DAPI+/cTnT+) were quantified relative to only DAPI positive cells (DAPI+/cTnT-). The percent of CMs across four different ROIs was found to be ~94%. This provides evidence that the used purification protocol is reproducible and able to generate cultures highly populated with CMs relative to all other cell types (e.g. fibroblasts, myofibroblasts, endothelial cells).

Furthermore, the mitochondrial content was quantified and compared across the 3 cell lines (Figure 3.1B, 3.1C). The results show that the R278C-harbouring hiPSC-CMs have a significantly lower mitochondrial content relative to the I79N and WT CMs. This correlates with the proteomic discoveries regarding decreased mitochondrial function and energy production as will be discussed in section 4.2.

4.2 Proteomic profile of I79N$^{+/-}$ and R278C$^{+/-}$ hiPSC-CMs

Due to its highly flexible nature, most regions of cTnT remain not well understood (figure 1.6A). As mentioned in section 1.4.1, the I79 site is located in an uncharacterized region, which is speculated to be involved in the dynamic interaction between actin and TPM. The simulation data for R278C (figure 1.6B), suggest that the charge repulsion between the positively charged native R278 and the local environment might be necessary for its normal function and for the molecular movement that is propagated along the thin filament in response to the Ca^{2+} binding. Moreover, the I79 and R278 equivalent sites have been proven to be phylogenetically conserved over 400 million years of evolution[90]. Consequently, both mutation sites are crucial for the optimum function of troponin T, and any variation in the amino acid nature will result in mechanical alterations to contractility and subsequently, the translational profile of the cardiac cell.

Therefore, exploring the effect of a point mutation in sites 79 and 278 might be the steppingstone to deduce and characterize the normal function of those two cTnT hypervariable regions. In the following sections, an in-depth discussion of the consequences of these variants on the proteome will be presented. Proteins of interest were categorized according to their functional groups which include: sarcomeric, structural, microtubular, cardiac remodeling, metabolism, and energy production- related proteins.

4.2.1 Sarcomeric proteins

Myosin

Sarcomeres are comprised of an array of proteins, organized in a very stringent crystalline structure. Despite the vast similarity in the sarcomeric protein network among different striated muscles (e.g., skeletal versus cardiac muscle), there is still a high degree of molecular variability due to the existence of multiple paralogs of each component. Moreover, the distinctive function of each muscle type is dictated by the differential expression of protein isoforms[117]. For example, in cardiac muscle, two main cardiac-specific myosin II isoforms are expressed: alpha myosin heavy chain (αM-II) *MYH6* and beta myosin heavy chain (βM-II) *MYH7*. β-myosin is expressed chiefly in the left ventricle and interventricular septum, while α-myosin is primarily expressed in the atrium. The distinct myosin paralog expression is linked to their activities, because physiologically, the atria twitch contraction must be very fast to complete the ventricular filling before the start of the much longer ventricular systole[118]. Therefore, the α-myosin has fast twitch mechanics response to excitation-contraction coupling, while β-myosin has more of a slow but powerful stroke[118].

Myosin light chain-2 (*MYL2*/MLC-2) is a major sarcomeric protein in the mammalian cardiac muscle, it is also referred to as the regulatory light chain (RLC) of the contractile unit. As shown in figure 2, the RLCs are located in the neck region of the myosin complex (S1). MYL2 plays an important role in embryonic heart muscle structure and function, its phosphorylation regulates cardiac myosin cycling kinetics, rotation, and contractility[117]. Figures 3.5A and 3.13A reflect the expression levels of MYL2 in I79N$^{+/-}$ and R278C$^{+/-}$ hiPSCs, respectively, compared to the isogenic control cells. A significant decrease in MYL2 expression levels has been recorded in both *TNNT2* variants and the metabolically matured CMs. This deviation could be attributed to the increased myofilament calcium sensitivity instigated by the HCM-causing variants. The “sticky” myofibrils result in prolonged crossbridge formation, which in turn may result in a disrupted need for regulation by MYL2, leading to a negative response of decreased expression in the variants.

One non-sarcomeric light chain paralog, MYL6, was detected with a significant fold change compared to the wildtype CMs. It plays an important role in force generation for cellular movement and was found to be higher in both cell lines harboring the HCM variants (Figures 3.5B and 3.13B).

The muscle thick filaments' main motor protein group is called the myosin heavy chain (MYH). Most species develop a large number of temporally and spatially controlled muscle MYH paralogs. This implies that diverse MYH isoform features are required for determining particular contractility qualities. The enzymatic activity of the ATPase in the myosin head is responsible for the fueling of the myosin power stroke. This process converts chemical energy to mechanical energy, and propels the shortening of the by driving actin filaments towards the M-line[119]. The main heavy chain isoform in the adult heart is MYH7, which was found to be significantly lower in the I79N CMs (figure 3.5C). The cells in metabolic maturation media (I79N-MM), were also showing a similar trend of decreased MYH7 expression.

As for R278C (figure 3.13C), the cells in regular RPMI medium showed no significant difference in MYH7 expression compared to the wild type CMs. However, the cells in metabolic maturation media (R278C-MM), show an exacerbated decrease in MYH7 expression level compared to their isogenic controls. This reduction in protein level might be related to the fetal gene program switch, which is a common phenomenon observed in most cardiomyopathies. Essentially, a common response of the cardiac cells to mechanical or metabolic stress is the suppression of the adult gene program, resulting in the predominance of the fetal gene program. This transition has been extensively studied in heart failure, DCM, and HCM, all of which have shown a significant downregulation of the post-natal MYH7 isoform[120].

The Troponin complex and Tropomyosin

As shown in figure 1.2 (section 1.1.1), The troponin/tropomyosin complex is composed of *TNNC1* (cardiac troponin C), which is the calcium-sensing unit of the complex, *TNNI1* (cardiac troponin I), which is the inhibitory component, and

TNNT2 (cardiac troponin T), which anchors the troponin complex to *TPM* (tropomyosin 1). Since the variants of interest are in *TNNT2*, there are quantitative consequences on this complex. Physiologically, troponin I undergoes a prominent paralog switch from *TNNI1* to *TNNI3* as the cells transition into adult-like cardiomyocytes. As shown in figures 3.5D and 3.13D, the expression levels of TNNI3 have increased as expected in the control cells cultured in MM (WT-MM). However, the CMs harboring the HCM variants are showing a significant decrease in this paralog, even with MM, which further corroborates the switch to fetal gene program principle.

Moreover, *TNNT2* and *TPM* are showing a similar trend in both variants. As shown in figures 3.5 E,F and 3.13 E,F, there is a significant increase in these proteins in the CMs cultured in regular RPMI medium. However, the effect of MM altered this profile in both cell lines and caused a notable downregulation in *TNNT2* and *TPM* expression. This downregulation has been reported in previous HCM studies, the main speculation is that the proposed increase in myofilament Ca^{+2} sensitivity promotes an early upregulation of the whole troponin/TPM complex initiated by troponin C to accommodate the high demand for cross-bridging. However, with prolonged culturing of the hiPSC-CMs in MM, over-stimulation of the troponin/TPM complex will create a negative desensitization effect which will counteract the hypercontractility by downregulating the expression of these protein groups[72].

The Z-disc

The Z-disc (figure 1.2) is a protein-rich structure that acts to tether the thin filament in the sarcomeres. Proteins of the Z-disc are integral for maintaining the architectural integrity of the sarcomere. They also enable it to function as a mechanical signalling centre[121]. Numerous proteins interact in the Z-disc to facilitate force transduction and intracellular signalling in cardiac muscle. In this study, many proteomic alterations were found to be directly or indirectly associated with Z-disc disorganization and myofibrillar disarray. This is shown in figures 3.5G-I and 3.13 G-I, where both HCM-causing variants (I79N and R278C) are showing

prominent Z-disc modifications in a similar fashion. α-actinin is a major protein found in the Z-disc and is involved in the crosslinking of actin filaments. It also interacts with titin to form a scaffold for large protein complexes[121]. During the pathogenic manifestation of cardiomyopathies, such as HCM, an upregulation of α-actinin is expected due to the increased mechanical stiffness of the CM. In figures 3.5G and 3.13G, the expression levels of alpha-actinin1 (*ACTN1*) are showing a significant increase compared to the isogenic control cells. On the other hand, protein groups responsible for the structural integrity and stability of the Z-disc, such as *MYOZ2* (Myozenin2) and *LDB3* (LIM-domain binding protein 3*)*[121] (Figures 3.5 H,I and 3.13 H,I), were significantly downregulated, especially in the matured variants, which indicates a further exacerbation of the Z-disc inflexibility and disorganization.

4.2.2 Structural proteins

It is crucial to examine the non-sarcomeric proteins that participate in conserving the cardiomyocyte's contractility and structural integrity. The protein level intensity of various structural/calcium handling proteins is shown in figures 3.6 (A-I) and 3.14 (A-I). Significant alterations of relevant proteins were selected, for example, desmin (DESM), a key structural intermediate filament, is greatly reduced in the variant cell lines[122]. Normally, desmin levels increase drastically with development, however, despite culturing the HCM-harboring CMs in MM, desmin levels did not rise to the expected levels as the WT-MM cells (figures 3.6C and 3.14C). This deviation is a strong indication of structural disorganization and remodelling taking place in the hiPSCs with the *TNNT2* variants.

Moreover, other structural components that function in sarcomeric protein crosslinking and assembly are showing a consistent decline in protein quantity in the HCM cell lines relative to the isogenic control CMs. Examples of such proteins are shown in figures 3.6 and 3.14, which include *NEBL* (Nebulette)- functionally links sarcomeric actin to the desmin intermediate filaments in the sarcomeres[123], *NEXN* (Nexilin)- has an essential role in the maintenance of Z line and sarcomere

integrity[124], *JPH2* (Junctophilin2)- provides a structural bridge between the plasma membrane and the sarcoplasmic reticulum and is required for normal excitation-contraction coupling in cardiomyocytes[125] , *OBSCN* (Obscurin)- highly involved in involved in the assembly of myosin into sarcomeric A bands[126], *LAMA2* (Laminin)- interacts with the extracellular matrix to mediate the attachment, migration and organization of CMs into tissues during embryonic development, and *DYSF* (dysferlin)- plays a role in the sarcolemma repair mechanism in cardiomyocytes that permits the repair of membranes disrupted by mechanical stress. Based on that, the significant decrease discovered in these protein groups could be a strong indication for some underlying serious structural remodelling transpiring.

4.2.3 Microtubules

As explained in section 1.1.2, the highly organized CMs are saturated with dense non-sarcomeric cytoskeletal networks that consist of β-actin, ɣ-actin, intermediate filaments, and microtubules. Collectively, the microtubules and intermediate filaments form a crosslinked scaffold, which is responsible for the transport of intracellular cargo, transmission of mechanical signals, shaping of membrane systems, and organization of myofibrils and various organelles. In a pathological state, microtubules are extensively altered as part of adaptive cardiac remodeling, which has diverse consequences on the structure and function of the cardiomyocyte [24]. For example, in end-stage heart failure and HCM patients, the density of the microtubular network increases, with a supplementary decrease in sarcomeric protein density [24,127].

The microtubular complex consists mainly of a variety of α- and β-tubulins, however, there are other interacting protein groups, such as MAP1B (microtubule-associated protein 1B), that facilitate the polymerization, tyrosination, and stabilization of the network. Evidence for this stabilization and increased stiffness is provided in figures 3.7 and 3.15, where MAP1B, alpha tubulins, and beta tubulins are overexpressed in both variant cell lines. This increase is representative of elevated tubulin polymerization and stabilization, which is an early pathological

adaptive response in cardiomyopathies that induces stiffness and cellular remodelling [24,127]. One interesting observation is that the R278C-harboring hiPSC-CMs exhibited an opposite trend when matured (figure 3.15). The R278C-MM cells are expressing a decreased amount of tubulins and MAPs relative to the CMs in regular RPMI medium. As shown in a study by Schuldt et al using patient cardiac samples, the main speculation is that variant location defines the degree of myofilament dysfunction, and in contrast to I79N, the R278C *TNNT2* variant has been shown to variable effects on calcium sensitivity depending on the mutant protein dose. In some cases, the cells display a reduced thin-filament binding affinity to the troponin complex, which alters the mechanical signalling and contractility properties of the CM, thus destabilizing the non-sarcomeric cytoskeletal network [67].

4.2.4 Cardiac remodelling proteins

Several pathways and factors have been revealed repeatedly to induce hypertrophy that is most consistent with a concentric remodelling response. As mentioned in section 1.1.8, one such pathway is facilitated by the calmodulin-activated protein phosphatase calcineurin (PP2B). Calcineurin is activated by elevations in cytosolic calcium, which enables binding to its downstream effector, the nuclear factor of activated T cells (NFAT). NFAT is usually in a phosphorylated state and sequestered in the cytoplasm, but then can translocate to the nucleus after dephosphorylation by calcineurin. Activation of the calcineurin-NFAT pathway leads to a significant increase in heart muscle size[128]. Inhibition of this signaling, such as in calcineurin-Nfatc2−/− knockout mice, has been shown to notably reduce pathological hypertrophy[129].

Various other pathways appear to be anti-remodelling or cardioprotective, working to counteract pathologic changes in the cardiac muscle. Atrial natriuretic peptide (ANP) and B-type natriuretic peptide (BNP) are re-expressed in the adult heart in response to stress stimulation. They have been shown to signal locally in the cardiac myocyte where they can antagonize hypertrophy[130].

In this study, several cardiac remodelling components have been detected with a significant change in the hiPSC-CMs expressing the HCM-causing variants (figures 3.8 and 3.16). Both *TNNT2* variant cell lines exhibit a significant increase in calcineurin- *PP2BC* (figures 3.8A and 3.16A), but only R278C showed a significant upregulation in *BNP* expression (figure 3.16E). Crucial proteins in this functional group include: *FHL2* (Four and a half LIM domains)- negatively regulates the calcineurin/NFAT signaling pathway in cardiomyocytes[63,121], *LMO7* (LIM domain only protein 7)- important in counteracting the pathological fibrotic response through negative feedback regulation of TGF-β signaling and ECM deposition[131], and *CSRP3* (Cysteine and glycine-rich protein 3)- plays a crucial and role in the organization of cytosolic structures in cardiomyocytes, acts as a scaffold protein that promotes the assembly of interacting proteins at Z-line structures, and contributes to the maintenance of muscle cell integrity through an actin-based mechanism[132]. All of the above-mentioned components are displaying a significant quantitative decrease in both I79N and R278C hiPSC-CMs, which provides further evidence for the loss of structural integrity and sarcomeric disorganization (figures 3.8 and 3.16).

On the other hand, a notable increase was detected in groups responsible for the structural remodelling response, these include proteins such as: *RCN1* (reticulocalbin)- a novel marker thar functions as a negative modulator of cardiomyocyte hypertrophy, its expression has been shown to be up-regulated under conditions of induced cardiac hypertrophy[133], *PDLIM* (PDZ and LIM domain protein)- plays a role in the regulation of cardiomyocyte expansion, its overexpression has been hypothesized to promote the development of cardiac hypertrophy[72], *MAPK3* (MAP kinase-activated protein kinase 3)- in mechanical overload, MAPK3 is activated by extracellular signals, causing it to translocate to the nucleus, phosphorylate targets, and initiate transcription. Overactivation of the MAPK3 pathway has been directly linked to causing hypertrophy[134], and *FINC* (Fibronectin)- promotes adhesion and motility of CMs, and has been shown to

highly contribute to pathological cardiomyocyte hypertrophy in vitro and in vivo studies.[135] (figures 3.8 and 3.16).

4.2.5 Metabolism & energy production proteins

From a metabolic standpoint, other significant expression differences were discovered in key glycolysis and energy production-related proteins. Such proteins include SLC2A1 and HK2, which are crucial for the functionality of glycolysis. *SLC2A1* or *GLUT1* (Solute carrier family 2, facilitated glucose transporter member 1) is one of the main transporters that brings in extracellular glucose for metabolic use[136]. HK2 (*Hexokinase*) facilitates the first step of glycolysis in which a phosphate is added to glucose to ensure its fate into the pathway[137]. We speculate that the hiPSC-CMs harboring a *TNNT2* variant undergo a switch to the fetal metabolic program, which heavily depends on glycolysis for ATP generation. It has been shown in many studies that in failing and hypertrophic hearts, the switch to the fetal metabolic gene profile is done by downregulating adult gene transcripts rather than by upregulating the fetal genes[138]. The main source of energy in the post-natal cardiac muscle relies on the metabolism of fatty acids. Key proteins involved in this oxidative pathway include short, medium, and long- chain specific acyl-CoA dehydrogenases[47]. These enzymes are responsible for catalyzing the first step of mitochondrial beta-oxidation, which leads to the breakdown of fatty acids into acetyl-CoA thus allowing for the production of energy from fats[50].

In this study, several glycolysis-related proteins were detected in higher quantities relative to the major proteins involved in fatty acid oxidation. The data reflect a significant down-regulation in the β-oxidation pathway. For example, HK2, GLUT1, G6PD, and PGAM1 were all increased in the I79N and R278C samples relative to their isogenic control cells (figures 3.9F-I and 3.17F-G). However, major fatty-acid metabolism proteins, such as ACADS, ACADM, and ACADSB, and FABPH were significantly down-regulated in the HCM-variants (figures 3.9A-C and 3.17A-C). This provides further evidence for the manifestation of the switch to the fetal gene program.

Another major metabolic hallmark of cardiac pathology is a notable reduction of *CKMT* (KCRS, mitochondrial creatine kinase) / *CK* (KCRM, creatine kinase) ratios in pre-hypertrophic patients. This decrease is a direct reflection of impaired energetics and inefficient ATP utilization in failing and hypertrophic hearts[139]. Similarly, as mentioned in section 1.2.6, the HCM-related impaired sarcomere energetics may provoke mitochondrial dysfunction, reduced ATP production, and increased ROS generation. All these indices are directly related to a potential pathogenic decline in the rate of electron transport chain, leading to lower amounts of respiratory complex proteins and mitochondrial protective proteins[140].

As displayed in figures 3.9D-E and 3.17D-E, KCRM (creatine kinase) and KCRS (mitochondrial creatine kinase) are both significantly decreased in both I79N and R278C cell lines. Moreover, the results show strong evidence for reduced mitochondrial content and energy production through the electron transport chain. Most of the crucial respiratory chain peptides are significantly decreased, these include NDUs, which are mitochondrial NADH dehydrogenases that constitute a major part of complex I in the electron transport chain. Expression of cytochrome c oxidase subunits, e.g. COX41, were also down-regulated in the HCM-harboring hiPSC-CMs (figures 3.9J-R and 3.17J-V).

Lastly, the results in the R278C hiPSC-CMs demonstrate some additional evidence of mitochondrial dysfunction due to a significant decrease in the expression of TOM 20,22,and 70 (figure 3.17W-Y). This reduction is related to mitochondrial abnormalities that are speculated to be associated with elevated reactive oxygen species (ROS) and reduced antioxidant defenses[140].

4.3 Post-translational modifications (PTMs) related to HCM progression in I79N$^{+/-}$ and R278C$^{+/-}$ hiPSC-CMs

To provide further evidence for contractility changes within the proteomic findings, the phosphorylation profile alterations among WT, I79N and R278C hiPSC-CMs were quantified using MS. Cardiac contractility is regulated by numerous factors including sarcomeric proteins phosphorylation. As mentioned in section 1.6, during relaxation, two myosin heads pack together to form an interacting-heads motif (IHM). In relaxed healthy cardiac muscle, myosin heads are in the super-relaxed (SRX) state with low ATP consumption and a disordered relaxed (DRX) state with swaying free heads that can sway, hydrolyze ATP at rates ~10x higher than in the SRX state, and increase the probability of its binding to actin. However, in pathological conditions like HCM, the IHM state of myosin is disturbed. The populations of myosin in the SRX and DRX states were found to be decreased and increased, respectively resulting in increased contractility, decreased relaxation, and increased ATP consumption. It has been hypothesized that myosin binding protein-C (MyBPC3) and myosin regulatory light chain (MYL2) phosphorylation may promote the DRX state by recruitment of sequestered IHM heads[117,141,142]. Evidence for the favored transition to the DRX state is shown in figure 3.21, there is an increased number of phosphorylated peptides in *MYBPC3* and *MYL2* at sites Ser284 and Ser15, respectively.

Other crucial proteins that undergo regulatory phosphorylation include NFATC2 (nuclear factor of activated T-cells). As mentioned in section 1.1.8 of this thesis, many studies show evidence of calcineurin- NFAT signaling activation in pathological cardiac hypertrophy and heart failure through the NFAT translocation into the nucleus, which in turn activates a pro-hypertrophic/pro-growth gene program[143]. As shown in figure 3.21, NFATC2 phosphorylation at Ser179 is decreased several fold relative to the WT CMs.

On the other hand, HSPB1 (heat shock protein1), also known as *HSP27*, has an established function of preventing stress-induced protein aggregation and myocardial damage. In this study, there is an observed increase in HSPB1 phosphorylation in both variants at site Ser15 (figure 3.21). In a recent study by the Hamdani group (2020), they showed that phosphorylation of HSP27 was increased in HCM hearts in an effort to protect the CMs from apoptosis effectors, oxidative stress, and ischemia[144,145]. Moreover, HSP27 is abundant in cardiac cells, and commonly localized to the Z-disk regions of the sarcomere for its involvement in the protection of titin[145].

Based on that, modulation of stiffness has been shown to be directly related to phosphorylation of titin at various sites[145]. Overall, most of the detected titin phosphosites in this study had a lower intensity in the HCM cell lines than their control. Particularly, phosphorylation at site Ser265 (figure 3.21), was significantly decreased in the I79N and R278C CMs. The location of this site is in the Z-disc portion of titin that anchors it to the sarcomere, it is speculated that this regulatory phosphorylation acts to facilitate the spring anchoring and lowers passive force generation in response to changes in stretch. Therefore, reduced phosphorylation in this region of titin could be reflective of regulatory changes occurring in response to mechanical stress[145,146].

4.4 Conclusions, limitations, and future directions

This thesis provides a novel perspective regarding the translational changes that occur on the proteomic level in an in vitro model of hiPSC-CMs harboring HCM-causing variants. The use of hiPSCs allowed for the generation of a stable, robust, and reproducible model of cardiomyocytes (CMs). Based on the presented data, the hiPSC-CMs proteome is dramatically impacted by the generation of point mutations resulting in I79N$^{+/-}$ and R278C$^{+/-}$ *TNNT2* variants which likely have profound consequences resulting in the disease phenotype. The hiPSC-CMs along with the genome-editing tools demonstrate the effectiveness of this technology for modeling sarcomeric mutations linked with HCM, identifying the pathogenic

remodelling factors and, potentially, developing therapeutic agents for treatment of HCM based on the novel markers identified. We propose a new therapeutic strategy for thin-filament variants by targeting key calcium buffering proteins in an effort to ameliorate the clinical phenotype. The suggested mechanism is to increase the phosphorylation of Troponin I (cTnI) and Phospholamban (PLN), due to their strong involvement in accelerating cardiac relaxation, as well as counteracting the increased myofilament calcium sensitivity. Building on previous studies done at our lab[90], the increased calcium sensitivity and reduced k_{off} are postulated to be the main mechanisms responsible for the initiation of hypertrophic remodelling signals and post-translational modifications in response to hypercontractility. By increasing the phosphorylation of cTnI and PLN, it would decrease the calcium binding affinity of Troponin C and increase the calcium reuptake into the SR by SERCA due to the removal of PLN inhibition from SERCA. We speculate that this targeted decrease in myofilament calcium affinity would be a crucial start-point attempt to increase calcium cycling back into the SR, which would improve the relaxation dynamics of the CMs, counter the diastolic dysfunction, amend the hypercontractility, decrease the stimulation of the mechanosensitive pathways, and eventually lead to improved energetics, sarcomeric organization, structural integrity, and overall cardiac contractility.

This study was an effort to uncover the molecular proteomic alterations on a broad scale using an unbiased approach. Despite that, several limitations arose that could be improved in future experiments. Firstly, the protein purification protocol is based on a magnetic bead-based solvation layer that captures mostly hydrophilic proteins or soluble portions of proteins. This presents a limitation in studying hydrophobic or membrane-bound proteins (e.g. ion channels). Therefore, we should explore new detergents that are able to extract and purify these proteins without interfering with the MS intensity detection. An alternative way would be to transition into the top-down field of mass spectrometry. This approach, which doesn’t require tryptic digestion, allows for intact protein ions to be introduced into the gas phase, undergo fragmentation and analysis in the mass spectrometer. The

raw data can then be used to deduce the complete primary structure of the protein, including transmembrane domains[147].

Another limitation to the label-free bottom-up approach is the detection capacity of PTMs, predominantly, phosphorylation. Setting phosphorylation as a variable PTM in the raw data analysis does provide some valuable information about the more abundant peptides, however, other smaller, low abundance proteins' PTMs will not be detected. For example, even though TNNI3 phosphorylation of serine residues 23 and 24 is known to increase cardiomyocyte relaxation by increasing the Ca^{2+} off rate constant from TNNC1[19], phosphorylation at this site could not be detected in these MS proteomic profiles. Therefore, a PTM-specific enrichment step should be added to the protein isolation protocol. Whether it is an antibody-based affinity enrichment, or ionic interaction-based enrichment, it will provide us with more information regarding other important modifications involved in oxidative stress such as S-glutathionylation or oxidation[18,148]. Moreover, even though the hiPSC-CMs went through a metabolic maturation process, they are still not fully mature, a combination of complex approaches must be utilized in an effort to recapitulate the full profile of adult cardiomyocytes. Lastly, the focus of this project is entirely at the cardiomyocyte level, whereas the progression of HCM has been well documented to involve modifications beyond just the cardiomyocyte. Therefore, 3D bioprinting of cardiac tissues with hiPSC-derived CMs, fibroblasts, and endothelial cells can provide the insights necessary to allow us to draw solid conclusions about the tissue-level pathophysiology.

In conclusion, we aim to build on this work by improving the MS protocol, widening our analysis capacity, exploring more HCM-causing variants, enhancing the maturity of our model, studying the pathogenesis in other cardiac cells, and possibly, developing a drug targeted for thin-filament variants.

References

1. Litviňuková, M. *et al.* Cells of the adult human heart. *Nature* **588**, 466–472 (2020).
2. Doll, S. *et al.* Region and cell-type resolved quantitative proteomic map of the human heart. *Nat Commun* **8**, 1469 (2017).
3. Kléber, A. G. & Rudy, Y. Basic Mechanisms of Cardiac Impulse Propagation and Associated Arrhythmias. *Physiological Reviews* **84**, 431–488 (2004).
4. Pappano, A. J. & Wier, W. G. *Cardiovascular Physiology - E-Book*. (Elsevier Health Sciences, 2018).
5. Kartha, C. C. Structure and Function of Cardiomyocyte. in *Cardiomyocytes in Health and Disease* (ed. Kartha, C. C.) 3–12 (Springer International Publishing, 2021). doi:10.1007/978-3-030-85536-9_1.
6. Woodcock, E. A. & Matkovich, S. J. Cardiomyocytes structure, function and associated pathologies. *The International Journal of Biochemistry & Cell Biology* **37**, 1746–1751 (2005).
7. Stienen, G. J. M. Cardiac Disorders and Pathophysiology of Sarcomeric Proteins. *Physiological Reviews* **99**, 381–426 (2019).
8. Crocini, C. & Gotthardt, M. Cardiac sarcomere mechanics in health and disease. *Biophys Rev* **13**, 637–652 (2021).
9. Reiser, P. J., Portman, M. A., Ning, X. H. & Schomisch Moravec, C. Human cardiac myosin heavy chain isoforms in fetal and failing adult atria and ventricles. *Am J Physiol Heart Circ Physiol* **280**, H1814-1820 (2001).
10. Hartman, M. A. & Spudich, J. A. The myosin superfamily at a glance. *J Cell Sci* **125**, 1627–1632 (2012).

11. Pope, B., Hoh, J. F. & Weeds, A. The ATPase activities of rat cardiac myosin isoenzymes. *FEBS Lett* **118**, 205–208 (1980).

12. Gupta, M. P. Factors controlling cardiac myosin-isoform shift during hypertrophy and heart failure. *J Mol Cell Cardiol* **43**, 388–403 (2007).

13. Markandran, K., Poh, J. W., Ferenczi, M. A. & Cheung, C. Regulatory Light Chains in Cardiac Development and Disease. *Int J Mol Sci* **22**, 4351 (2021).

14. Sitbon, Y. H., Yadav, S., Kazmierczak, K. & Szczesna-Cordary, D. Insights into myosin regulatory and essential light chains: a focus on their roles in cardiac and skeletal muscle function, development and disease. *J Muscle Res Cell Motil* **41**, 313–327 (2020).

15. Muthu, P. *et al.* Structural and functional aspects of the myosin essential light chain in cardiac muscle contraction. *FASEB J* **25**, 4394–4405 (2011).

16. Flashman, E., Redwood, C., Moolman-Smook, J. & Watkins, H. Cardiac Myosin Binding Protein C. *Circulation Research* **94**, 1279–1289 (2004).

17. Powers, J. D., Malingen, S. A., Regnier, M. & Daniel, T. L. The Sliding Filament Theory Since Andrew Huxley: Multiscale and Multidisciplinary Muscle Research. *Annu Rev Biophys* **50**, 373–400 (2021).

18. Rosas, P. C. & Solaro, R. J. Implications of S-glutathionylation of sarcomere proteins in cardiac disorders, therapies, and diagnosis. *Frontiers in Cardiovascular Medicine* **9**, (2023).

19. Solís, C. & Solaro, R. J. Novel insights into sarcomere regulatory systems control of cardiac thin filament activation. *J Gen Physiol* **153**, e202012777 (2021).

20. LeWinter, M. M. & Granzier, H. Cardiac Titin. *Circulation* **121**, 2137–2145 (2010).

21. Bang, M.-L. *et al.* The Complete Gene Sequence of Titin, Expression of an Unusual ≈700-kDa Titin Isoform, and Its Interaction With Obscurin Identify a Novel Z-Line to I-Band Linking System. *Circulation Research* **89**, 1065–1072 (2001).

22. Kötter, S., Andresen, C. & Krüger, M. Titin: central player of hypertrophic signaling and sarcomeric protein quality control. *Biological Chemistry* **395**, 1341–1352 (2014).

23. Neagoe, C. *et al.* Titin Isoform Switch in Ischemic Human Heart Disease. *Circulation* **106**, 1333–1341 (2002).

24. Caporizzo, M. A., Chen, C. Y. & Prosser, B. L. Cardiac microtubules in health and heart disease. *Exp Biol Med (Maywood)* **244**, 1255–1272 (2019).

25. Kerr, J. P. *et al.* Detyrosinated microtubules modulate mechanotransduction in heart and skeletal muscle. *Nat Commun* **6**, 8526 (2015).

26. Cleary, J. M. & Hancock, W. O. Molecular mechanisms underlying microtubule growth dynamics. *Current Biology* **31**, R560–R573 (2021).

27. Walker, C. A. & Spinale, F. G. The structure and function of the cardiac myocyte: A review of fundamental concepts. *The Journal of Thoracic and Cardiovascular Surgery* **118**, 375–382 (1999).

28. Lockhart, M., Wirrig, E., Phelps, A. & Wessels, A. Extracellular Matrix and Heart Development. *Birth Defects Res A Clin Mol Teratol* **91**, 535–550 (2011).

29. Zhao, Q., Sun, Q., Zhou, L., Liu, K. & Jiao, K. Complex Regulation of Mitochondrial Function During Cardiac Development. *Journal of the American Heart Association* **8**, e012731 (2019).

30. Li, A., Gao, M., Jiang, W., Qin, Y. & Gong, G. Mitochondrial Dynamics in Adult Cardiomyocytes and Heart Diseases. *Frontiers in Cell and Developmental Biology* **8**, (2020).

31. Doenst, T., Nguyen, T. D. & Abel, E. D. Cardiac metabolism in heart failure: implications beyond ATP production. *Circ Res* **113**, 709–724 (2013).

32. Brette, F. & Orchard, C. T-Tubule Function in Mammalian Cardiac Myocytes. *Circulation Research* **92**, 1182–1192 (2003).

33. Eisner, D. A., Caldwell, J. L., Kistamás, K. & Trafford, A. W. Calcium and Excitation-Contraction Coupling in the Heart. *Circ Res* **121**, 181–195 (2017).

34. Kossmann, C. E. & Fawcett, D. W. The Sarcoplasmic Reticulum of Skeletal and Cardiac Muscle. *Circulation* **24**, 336–348 (1961).

35. Fearnley, C. J., Roderick, H. L. & Bootman, M. D. Calcium Signaling in Cardiac Myocytes. *Cold Spring Harb Perspect Biol* **3**, a004242 (2011).

36. Kuo, I. Y. & Ehrlich, B. E. Signaling in Muscle Contraction. *Cold Spring Harbor Perspectives in Biology* **7**, (2015).

37. Solís, C., Kim, G. H., Moutsoglou, M. E. & Robinson, J. M. Ca2+ and Myosin Cycle States Work as Allosteric Effectors of Troponin Activation. *Biophysical Journal* **115**, 1762–1769 (2018).

38. Lyon, R. C., Zanella, F., Omens, J. H. & Sheikh, F. Mechanotransduction in cardiac hypertrophy and failure. *Circ Res* **116**, 1462–1476 (2015).

39. Heineke, J. *et al.* Attenuation of cardiac remodeling after myocardial infarction by muscle LIM protein-calcineurin signaling at the sarcomeric Z-disc. *Proceedings of the National Academy of Sciences* **102**, 1655–1660 (2005).

40. Crabtree, G. R. & Olson, E. N. NFAT Signaling: Choreographing the Social Lives of Cells. *Cell* **109**, S67–S79 (2002).

41. Frey, N. *et al.* Mice lacking calsarcin-1 are sensitized to calcineurin signaling and show accelerated cardiomyopathy in response to pathological biomechanical stress. *Nat Med* **10**, 1336–1343 (2004).

42. Granzier, H. L. & Labeit, S. The Giant Protein Titin: A Major Player in Myocardial Mechanics, Signaling, and Disease. *Circulation Research* **94**, 284–295 (2004).

43. Hoshijima, M. Mechanical stress-strain sensors embedded in cardiac cytoskeleton: Z disk, titin, and associated structures. *Am J Physiol Heart Circ Physiol* **290**, H1313–H1325 (2006).

44. Krüger, M. & Linke, W. A. Titin-based mechanical signalling in normal and failing myocardium. *Journal of Molecular and Cellular Cardiology* **46**, 490–498 (2009).

45. Kolwicz, S. C., Purohit, S. & Tian, R. Cardiac Metabolism and Its Interactions with Contraction, Growth, and Survival of the Cardiomyocte. *Circ Res* **113**, 10.1161/CIRCRESAHA.113.302095 (2013).

46. Piquereau, J. & Ventura-Clapier, R. Maturation of Cardiac Energy Metabolism During Perinatal Development. *Frontiers in Physiology* **9**, (2018).

47. Lopaschuk, G. D. & Jaswal, J. S. Energy Metabolic Phenotype of the Cardiomyocyte During Development, Differentiation, and Postnatal Maturation. *Journal of Cardiovascular Pharmacology* **56**, 130–140 (2010).

48. Makinde, A.-O., Kantor, P. F. & Lopaschuk, G. D. Maturation of fatty acid and carbohydrate metabolism in the newborn heart. in *Molecular and Cellular Effects of Nutrition on Disease Processes* (eds. Pierce, G. N., Izumi, T., Rupp, H. & Grynberg, A.) 49–56 (Springer US, 1998). doi:10.1007/978-1-4615-5763-0_6.

49. Lopaschuk, G. D., Karwi, Q. G., Tian, R., Wende, A. R. & Abel, E. D. Cardiac Energy Metabolism in Heart Failure. *Circulation Research* **128**, 1487–1513 (2021).

50. Ritterhoff, J. & Tian, R. Metabolism in cardiomyopathy: every substrate matters. *Cardiovascular Research* **113**, 411–421 (2017).

51. Goodwin, G. W. & Taegtmeyer, H. Improved energy homeostasis of the heart in the metabolic state of exercise. *American Journal of Physiology-Heart and Circulatory Physiology* **279**, H1490–H1501 (2000).

52. Wentz, A. E. *et al.* Adaptation of Myocardial Substrate Metabolism to a Ketogenic Nutrient Environment*. *Journal of Biological Chemistry* **285**, 24447–24456 (2010).

53. Watkins, H., Ashrafian, H. & Redwood, C. Inherited Cardiomyopathies. *New England Journal of Medicine* **364**, 1643–1656 (2011).

54. Maron, B. J. *et al.* Contemporary Definitions and Classification of the Cardiomyopathies. *Circulation* **113**, 1807–1816 (2006).

55. Marian, A. J. & Braunwald, E. Hypertrophic Cardiomyopathy. *Circulation Research* **121**, 749–770 (2017).

56. Sisakian, H. Cardiomyopathies: Evolution of pathogenesis concepts and potential for new therapies. *World J Cardiol* **6**, 478–494 (2014).

57. Greaves, S. C., Roche, A. H., Neutze, J. M., Whitlock, R. M. & Veale, A. M. Inheritance of hypertrophic cardiomyopathy: a cross sectional and M mode echocardiographic study of 50 families. *Heart* **58**, 259–266 (1987).

58. Geisterfer-Lowrance, A. A. T. *et al.* A molecular basis for familial hypertrophic cardiomyopathy: A β cardiac myosin heavy chain gene missense mutation. *Cell* **62**, 999–1006 (1990).

59. Van Driest, S. L. *et al.* Prevalence and spectrum of thin filament mutations in an outpatient referral population with hypertrophic cardiomyopathy. *Circulation* **108**, 445–451 (2003).

60. Greenberg, M. J. & Tardiff, J. C. Complexity in genetic cardiomyopathies and new approaches for mechanism-based precision medicine. *Journal of General Physiology* **153**, e202012662 (2021).

61. Auton, A. *et al.* A global reference for human genetic variation. *Nature* **526**, 68–74 (2015).

62. Wheeler, D. A. *et al.* The complete genome of an individual by massively parallel DNA sequencing. *Nature* **452**, 872–876 (2008).

63. Marian, A. j. Molecular Genetic Basis of Hypertrophic Cardiomyopathy. *Circulation Research* **128**, 1533–1553 (2021).

64. Wolf, C. M. Hypertrophic cardiomyopathy: genetics and clinical perspectives. *Cardiovasc Diagn Ther* **9**, S388–S415 (2019).

65. Marian, A. J. Hypertrophic cardiomyopathy: from genetics to treatment. *European Journal of Clinical Investigation* **40**, 360–369 (2010).

66. Bonne, G., Carrier, L., Richard, P., Hainque, B. & Schwartz, K. Familial Hypertrophic Cardiomyopathy. *Circulation Research* **83**, 580–593 (1998).

67. Schuldt, M. *et al.* Mutation location of HCM-causing troponin T mutations defines the degree of myofilament dysfunction in human cardiomyocytes. *J Mol Cell Cardiol* **150**, 77–90 (2021).

68. Marston, S. B. How Do Mutations in Contractile Proteins Cause the Primary Familial Cardiomyopathies? *J. of Cardiovasc. Trans. Res.* **4**, 245–255 (2011).

69. Chou, C. & Chin, M. T. Pathogenic Mechanisms of Hypertrophic Cardiomyopathy beyond Sarcomere Dysfunction. *International Journal of Molecular Sciences* **22**, 8933 (2021).

70. Aebersold, R. *et al.* How many human proteoforms are there? *Nat Chem Biol* **14**, 206–214 (2018).

71. Cho, W. C. S. Proteomics Technologies and Challenges. *Genomics Proteomics Bioinformatics* **5**, 77–85 (2007).

72. Tucholski, T. *et al.* Distinct hypertrophic cardiomyopathy genotypes result in convergent sarcomeric proteoform profiles revealed by top-down proteomics. *Proceedings of the National Academy of Sciences* **117**, 24691–24700 (2020).

73. van der Velden, J. *et al.* Metabolic changes in hypertrophic cardiomyopathies: scientific update from the Working Group of Myocardial Function of the European Society of Cardiology. *Cardiovasc Res* **114**, 1273–1280 (2018).

74. Crilley, J. G. *et al.* Hypertrophic cardiomyopathy due to sarcomeric gene mutations is characterized by impaired energy metabolism irrespective of the degree of hypertrophy. *Journal of the American College of Cardiology* **41**, 1776–1782 (2003).

75. Kolwicz, S. C. & Tian, R. Glucose metabolism and cardiac hypertrophy. *Cardiovasc Res* **90**, 194–201 (2011).

76. Balaban, R. S. Cardiac Energy Metabolism Homeostasis: Role of Cytosolic Calcium. **34**, 1259–1271 (2002).

77. Shephard, R. & Semsarian, C. Role of Animal Models in HCM Research. *J. of Cardiovasc. Trans. Res.* **2**, 471–482 (2009).

78. Mosqueira, D., Smith, J. G. W., Bhagwan, J. R. & Denning, C. Modeling Hypertrophic Cardiomyopathy: Mechanistic Insights and Pharmacological Intervention. *Trends in Molecular Medicine* **25**, 775–790 (2019).

79. Vakrou, S. *et al.* Differences in molecular phenotype in mouse and human hypertrophic cardiomyopathy. *Sci Rep* **11**, 13163 (2021).

80. Doncheva, N. T. *et al.* Human pathways in animal models: possibilities and limitations. *Nucleic Acids Research* **49**, 1859–1871 (2021).

81. Reubinoff, B. E., Pera, M. F., Fong, C.-Y., Trounson, A. & Bongso, A. Embryonic stem cell lines from human blastocysts: somatic differentiation in vitro. *Nat Biotechnol* **18**, 399–404 (2000).

82. Takahashi, K. *et al.* Induction of Pluripotent Stem Cells from Adult Human Fibroblasts by Defined Factors. *Cell* **131**, 861–872 (2007).

83. Musunuru, K. *et al.* Induced Pluripotent Stem Cells for Cardiovascular Disease Modeling and Precision Medicine: A Scientific Statement From the American Heart Association. *Circulation: Genomic and Precision Medicine* **11**, e000043 (2018).

84. Li, J., Feng, X. & Wei, X. Modeling hypertrophic cardiomyopathy with human cardiomyocytes derived from induced pluripotent stem cells. *Stem Cell Research & Therapy* **13**, 232 (2022).

85. Lian, X. *et al.* Directed cardiomyocyte differentiation from human pluripotent stem cells by modulating Wnt/β-catenin signaling under fully defined conditions. *Nat Protoc* **8**, 162–175 (2013).

86. Akhtar, M. & Elliott, P. The genetics of hypertrophic cardiomyopathy. *Glob Cardiol Sci Pract* **2018**, 36.

87. Tardiff, J. C. *et al.* Cardiac troponin T mutations result in allele-specific phenotypes in a mouse model for hypertrophic cardiomyopathy. *J Clin Invest* **104**, 469–481 (1999).

88. Knollmann, B. C. *et al.* Familial hypertrophic cardiomyopathy-linked mutant troponin T causes stress-induced ventricular tachycardia and Ca2+-dependent action potential remodeling. *Circ Res* **92**, 428–436 (2003).

89. Wei, B. & Jin, J.-P. Troponin T Isoforms and Posttranscriptional Modifications: Evolution, Regulation and Function. *Arch Biochem Biophys* **505**, 144–154 (2011).

90. Shafaattalab, S. *et al.* Mechanisms of Arrhythmogenicity of Hypertrophic Cardiomyopathy-Associated Troponin T (TNNT2) Variant I79N. *Frontiers in Cell and Developmental Biology* **9**, (2021).

91. Hernandez, O. M. *et al.* F110I and R278C Troponin T Mutations That Cause Familial Hypertrophic Cardiomyopathy Affect Muscle Contraction in Transgenic Mice and Reconstituted Human Cardiac Fibers *. *Journal of Biological Chemistry* **280**, 37183–37194 (2005).

92. Tardiff, J. C., Robbins, J., Seidman, C. & Watkins, H. Thin Filament Mutations. *Circulation Research* **108**, 765–782 (2011).

93. Maron, M. S. *et al.* Contemporary Natural History and Management of Nonobstructive Hypertrophic Cardiomyopathy. *Journal of the American College of Cardiology* **67**, 1399–1409 (2016).

94. Rangaraju, A., Calambur, N. & Nallari, P. Epidemiological and clinical analyses of hypertrophic cardiomyopathy. *J Med Sci Res* **3**, 9–16 (2015).

95. Díez-López, C. & Salazar-Mendiguchía, J. Clinical presentations of hypertrophic cardiomyopathy and implications for therapy. *Glob Cardiol Sci Pract* **2018**, 19.

96. Weissler-Snir, A. *et al.* Hypertrophic Cardiomyopathy–Related Sudden Cardiac Death in Young People in Ontario. *Circulation* **140**, 1706–1716 (2019).

97. Elliott, P. M. *et al.* Left ventricular outflow tract obstruction and sudden death risk in patients with hypertrophic cardiomyopathy. *European Heart Journal* **27**, 1933–1941 (2006).

98. Zaiser, E. *et al.* Patient experiences with hypertrophic cardiomyopathy: a conceptual model of symptoms and impacts on quality of life. *Journal of Patient-Reported Outcomes* **4**, 102 (2020).

99. Moon, I. *et al.* Trends of the prevalence and incidence of hypertrophic cardiomyopathy in Korea: A nationwide population-based cohort study. *PLOS ONE* **15**, e0227012 (2020).

100. Wolf, C. M. & Berul, C. I. Molecular Mechanisms of Inherited Arrhythmias. *Curr Genomics* **9**, 160–168 (2008).

101. Goldspink, P. H., Warren, C. M., Kitajewski, J., Wolska, B. M. & Solaro, R. J. A Perspective on Personalized Therapies in Hypertrophic Cardiomyopathy. *J Cardiovasc Pharmacol* **77**, 317–322 (2021).

102. Toepfer, C. N. *et al.* Myosin Sequestration Regulates Sarcomere Function, Cardiomyocyte Energetics, and Metabolism, Informing the Pathogenesis of Hypertrophic Cardiomyopathy. *Circulation* **141**, 828–842 (2020).

103. Olivotto, I. *et al.* Mavacamten for treatment of symptomatic obstructive hypertrophic cardiomyopathy (EXPLORER-HCM): a randomised, double-blind, placebo-controlled, phase 3 trial. *Lancet* **396**, 759–769 (2020).

104. Lam, M. P. Y., Ping, P. & Murphy, E. Proteomics Research in Cardiovascular Medicine and Biomarker Discovery. *J Am Coll Cardiol* **68**, 2819–2830 (2016).

105. Toby, T. K. *et al.* A comprehensive pipeline for translational top-down proteomics from a single blood draw. *Nat Protoc* **14**, 119–152 (2019).

106. Mesaros, C. & Blair, I. A. Mass spectrometry-based approaches to targeted quantitative proteomics in cardiovascular disease. *Clinical Proteomics* **13**, 20 (2016).

107. Cai, W. *et al.* An Unbiased Proteomics Method to Assess the Maturation of Human Pluripotent Stem Cell-Derived Cardiomyocytes. *Circ Res* **125**, 936–953 (2019).

108. Lian, X. *et al.* Robust cardiomyocyte differentiation from human pluripotent stem cells via temporal modulation of canonical Wnt signaling. *Proceedings of the National Academy of Sciences* **109**, E1848–E1857 (2012).

109. Horikoshi, Y. *et al.* Fatty Acid-Treated Induced Pluripotent Stem Cell-Derived Human Cardiomyocytes Exhibit Adult Cardiomyocyte-Like Energy Metabolism Phenotypes. *Cells* **8**, 1095 (2019).

110. Yang, X. *et al.* Fatty Acids Enhance the Maturation of Cardiomyocytes Derived from Human Pluripotent Stem Cells. *Stem Cell Reports* **13**, 657–668 (2019).

111. M. Feyen, D. A. *et al.* Metabolic Maturation Media Improve Physiological Function of Human iPSC-Derived Cardiomyocytes. *Cell Rep* **32**, 107925 (2020).

112. Hughes, C. S. *et al.* Single-pot, solid-phase-enhanced sample preparation for proteomics experiments. *Nat Protoc* **14**, 68–85 (2019).

113. Park, S.-J. *et al.* Dual stem cell therapy synergistically improves cardiac function and vascular regeneration following myocardial infarction. *Nat Commun* **10**, 3123 (2019).

114. Stauffer, W., Sheng, H. & Lim, H. N. EzColocalization: An ImageJ plugin for visualizing and measuring colocalization in cells and organisms. *Sci Rep* **8**, 15764 (2018).

115. Chen, E. Y. *et al.* Enrichr: interactive and collaborative HTML5 gene list enrichment analysis tool. *BMC Bioinformatics* **14**, 128 (2013).

116. Salazar, C. & Höfer, T. Multisite protein phosphorylation – from molecular mechanisms to kinetic models. *The FEBS Journal* **276**, 3177–3198 (2009).

117. Sheikh, F., Lyon, R. C. & Chen, J. Functions of Myosin Light Chain-2 (MYL2) In Cardiac Muscle and Disease. *Gene* **569**, 14–20 (2015).

118. Walklate, J. *et al.* Alpha and beta myosin isoforms and human atrial and ventricular contraction. *Cell. Mol. Life Sci.* **78**, 7309–7337 (2021).

119. Homburger, J. R. *et al.* Multidimensional structure-function relationships in human β-cardiac myosin from population-scale genetic variation. *Proceedings of the National Academy of Sciences* **113**, 6701–6706 (2016).

120. Taegtmeyer, H., Sen, S. & Vela, D. Return to the fetal gene program. *Annals of the New York Academy of Sciences* **1188**, 191–198 (2010).

121. Wadmore, K., Azad, A. J. & Gehmlich, K. The Role of Z-disc Proteins in Myopathy and Cardiomyopathy. *Int J Mol Sci* **22**, 3058 (2021).

122. Coats, C. J. *et al.* Proteomic Analysis of the Myocardium in Hypertrophic Obstructive Cardiomyopathy. *Circulation: Genomic and Precision Medicine* **11**, e001974 (2018).

123. Perrot, A. *et al.* Mutations in NEBL encoding the cardiac Z-disk protein nebulette are associated with various cardiomyopathies. *Arch Med Sci* **12**, 263–278 (2016).

124. Wang, H. *et al.* Mutations in NEXN, a Z-disc gene, are associated with hypertrophic cardiomyopathy. *Am J Hum Genet* **87**, 687–693 (2010).

125. Beavers, D. L., Landstrom, A. P., Chiang, D. Y. & Wehrens, X. H. T. Emerging roles of junctophilin-2 in the heart and implications for cardiac diseases. *Cardiovascular Research* **103**, 198–205 (2014).

126. Marston, S. Obscurin variants and inherited cardiomyopathies. *Biophys Rev* **9**, 239–243 (2017).

127. Zile, M. R. *et al.* Cardiocyte cytoskeleton in patients with left ventricular pressure overload hypertrophy. *Journal of the American College of Cardiology* **37**, 1080–1084 (2001).

128. Kehat, I. & Molkentin, J. D. Molecular pathways underlying cardiac remodeling during pathophysiologic stimulation. *Circulation* **122**, 10.1161/CIRCULATIONAHA.110.942268 (2010).

129. Wilkins, B. J. *et al.* Targeted Disruption of NFATc3, but Not NFATc4, Reveals an Intrinsic Defect in Calcineurin-Mediated Cardiac Hypertrophic Growth. *Mol Cell Biol* **22**, 7603–7613 (2002).

130. Cambronero, F. *et al.* Biomarkers of pathophysiology in hypertrophic cardiomyopathy: implications for clinical management and prognosis. *European Heart Journal* **30**, 139–151 (2009).

131. Xie, Y. *et al.* LMO7 Is a Negative Feedback Regulator of Transforming Growth Factor β Signaling and Fibrosis. *Circulation* **139**, 679–693 (2019).

132. Vafiadaki, E., Arvanitis, D. A. & Sanoudou, D. Muscle Lim Protein: master regulator of cardiac and skeletal muscle function. *Gene* **566**, 1–7 (2015).

133. Kramann, N., Hasenfuß, G. & Seidler, T. B-RAF and its novel negative regulator reticulocalbin 1 (RCN1) modulates cardiomyocyte hypertrophy. *Cardiovascular Research* **102**, 88–96 (2014).

134. ROSE, B. A., FORCE, T. & WANG, Y. Mitogen-Activated Protein Kinase Signaling in the Heart: Angels Versus Demons in a Heart-Breaking Tale. *Physiol Rev* **90**, 10.1152/physrev.00054.2009 (2010).

135. Konstandin, M. H. *et al.* Fibronectin contributes to pathological cardiac hypertrophy but not physiological growth. *Basic Res Cardiol* **108**, 375 (2013).

136. Shao, D. & Tian, R. Glucose Transporters in Cardiac Metabolism and Hypertrophy. *Compr Physiol* **6**, 331–351 (2015).

137. Liang, Q., Donthi, R. V., Kralik, P. M. & Epstein, P. N. Elevated hexokinase increases cardiac glycolysis in transgenic mice. *Cardiovascular Research* **53**, 423–430 (2002).

138. Razeghi, P. *et al.* Metabolic gene expression in fetal and failing human heart. *Circulation* **104**, 2923–2931 (2001).

139. Vakrou, S. & Abraham, M. R. Hypertrophic cardiomyopathy: a heart in need of an energy bar? *Frontiers in Physiology* **5**, (2014).

140. Ranjbarvaziri, S. *et al.* Altered Cardiac Energetics and Mitochondrial Dysfunction in Hypertrophic Cardiomyopathy. *Circulation* **144**, 1714–1731 (2021).

141. Schmid, M. & Toepfer, C. N. Cardiac myosin super relaxation (SRX): a perspective on fundamental biology, human disease and therapeutics. *Biology Open* **10**, bio057646 (2021).

142. Barefield, D. & Sadayappan, S. Phosphorylation and function of cardiac myosin binding protein-C in health and disease. *J Mol Cell Cardiol* **48**, 866–875 (2010).

143. Molkentin, J. D. Calcineurin–NFAT signaling regulates the cardiac hypertrophic response in coordination with the MAPKs. *Cardiovascular Research* **63**, 467–475 (2004).

144. Collier, M. P. *et al.* HspB1 phosphorylation regulates its intramolecular dynamics and mechanosensitive molecular chaperone interaction with filamin C. *Sci Adv* **5**, eaav8421 (2019).

145. Herwig, M. *et al.* Modulation of Titin-Based Stiffness in Hypertrophic Cardiomyopathy via Protein Kinase D. *Frontiers in Physiology* **11**, (2020).

146. Hamdani, N., Herwig, M. & Linke, W. A. Tampering with springs: phosphorylation of titin affecting the mechanical function of cardiomyocytes. *Biophys Rev* **9**, 225–237 (2017).

147. Karr, U., Simonian, M. & Whitelegge, J. P. Integral membrane proteins: bottom-up, top-down and structural proteomics. *Expert Rev Proteomics* **14**, 715–723 (2017).

148. Zhao, Y. & Jensen, O. N. Modification-specific proteomics: Strategies for characterization of post-translational modifications using enrichment techniques. *Proteomics* **9**, 4632–4641 (2009).

Appendix A: List of Used Reagents

Table A.1: List of Used Chemical Reagents.

Product name	Company	Used for
Acetonitrile (ACN)	Thermo Fisher	Organic solvent in elution buffer
B27 supplement with insulin	Thermo Fisher	Medium supplement
B27 supplement without insulin	Thermo Fisher	Medium supplement
Benzonase	Sigma Aldrich	Endonuclease to degrade DNA and RNA
C18 matrix- midi prep columns	BioPure, Nest Group	Peptide desalting
CHIR99021	R&D Systems	Small molecule, acts as a WNT pathway activator
Chloroacetamide (CAA)	Sigma Aldrich	Alkylating agent
Dithiothreitol (DTT)	Thermo Fisher	Reducing agent
Dulbecco's Modified Eagle Medium (DMEM F12)	Thermo Fisher	Basal medium
Formic acid (FA)	Thermo Fisher	Mobile phase solvent in elution buffer
Geltrex	Thermo Fisher	Culture plate coating
HEPES	Thermo Fisher	Buffering agent
IWP4	Tocris	Small molecule, acts as a WNT pathway inhibitor
LC/MS-grade water	Thermo Fisher	-
Magnetic beads	Sera-mag, Cytiva (GE life sciences)	For protein binding, isolation, and purification
MitoTracker Deep Red FM	Thermo Fisher	Mitochondrial fluorescent dye
mTeSR-plus medium	STEMCELL technologies	Maintenance & expansion of hiPSCs
Paraformaldehyde (PFA)		Cell fixative
ProLong Gold Antifade Mountant with DAPI	Thermo Fisher	Mounting media with DNA stain to label the nucleus

ReLeSR	STEMCELL technologies	iPSCs passaging reagent
Roswell Park Memorial Institute (RPMI) 1640 basal medium	Thermo Fisher	Maintenance of hiPSC-CMs
Sodium dodecyl sulfate (SDS)	Sigma Aldrich	Detergent (denaturation agent)
Sodium L-Lactate	Sigma Aldrich	Medium supplement
STEMdiff	STEMCELL technologies	Cardiomyocyte dissociation
Trifluoroacetic acid (TFA)	Thermo Fisher	pH adjustment + elution
Troponin T primary antibody	Thermo Fisher	Monoclonal antibody that binds Troponin T specifically
Trypsin	VWR	Proteolytic digestion

Table A.2: Measurements Used of Specific Reagents Formulating the Maturation Media (MM).

Reagent's name	Manufacturer	Final concentration	Amount added
DMEM (-glu)	Thermo Fisher Scientific	-	500 mL
Glucose	Sigma Aldrich	3 mM	0.27024 g
L-lactate	Sigma Aldrich	10 mM	0.5603 g
Creatine monohydrate	Sigma Aldrich	5 mM	0.37287 g
Taurine	Sigma Aldrich	2 mM	0.12515 g
L-carnitine	Sigma Aldrich	2 mM	0.19766 g
Ascorbic acid	Sigma Aldrich	0.5 mM	0.072385 g
AlbuMax	Thermo Fisher Scientific	0.5% (w/v)	2.5 g
Non-essential amino acids (NEAA)	Thermo Fisher Scientific	1%	5 mL
B27 +insulin	Thermo Fisher Scientific	2%	10 mL
Knock out serum replacement (KOSR)	Thermo Fisher Scientific	1%	5 mL
Vitamin B12 (10mM)	Sigma Aldrich	3.69 µM	184.45 µL
Biotin (1mM)	Sigma Aldrich	0.82 µM	410 µL